The Department of Geodesy and Geoinformatics

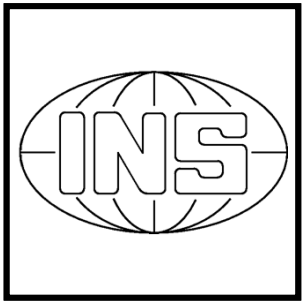

Stuttgart University

2010

editing and layout:
volker walter, friedhelm krumm, martin metzner, wolfgang schöller

Dear friends and colleagues,

It is our great pleasure to present to you this annual report on the 2010[1] activities and academic highlights of the Department of Geodesy & Geoinformatics of the University of Stuttgart. The Department consists of the four institutes:

- Institute of Geodesy (GIS),
- Institute for Photogrammetry (ifp),
- Institute of Navigation (INS),
- Institute for Engineering Geodesy (IIGS, formerly IAGB),

and is part of the Faculty of Aerospace Engineering and Geodesy.

On April 1st Prof. Dr. Ing. habil. Volker Schwieger accepted the chair of a Professor for Engineering Geodesy and Geodetic Measurements and became head of the Institute for Applications of Geodesy to Engineering (IAGB). As the institute covers a broad area in research and teaching it was renamed into Institute for Engineering Geodesy Stuttgart (IIGS) in September 2010.

Research

This annual report documents our research contributions in many diverse fields of Geodesy & Geoinformatics: from satellite and physical geodesy through navigation, remote sensing, engineering surveying and telematics to photogrammetry, geographical information systems and location based services. Detailed information on projects and research output can be found in the following individual institutes' sections.

Teaching

Our new BSc programme *Geodesy & Geoinformatics* is currently in its second year of operation. The Diploma progamme is slowly being phased out. Total enrolment, in both the BSc and the Diploma programmes, is stable at about 125 students. In 2010 we have graduated 12 Diploma students. Please visit our redesigned website *www.geodaesie.uni-stuttgart.de* for additional information on the programme.

In its 5th year of existence, our international MSc programme *Geomatics Engineering* (GEOENGINE) has a stable enrolment of 15 students. We attract the GEOENGINE student population from such diverse countries as China, Taiwan, Iran, Pakistan, Nepal, Nigeria, Ghana, Ethiopia and Palestine. Please visit *www.geoengine.uni-stuttgart.de* for more information.

Beyond these two core curricula, the institutes are involved in a host of other programmes around campus.

[1] A version with colour graphics is downloadable from
http://www.ifp.uni-stuttgart.de/publications/jahresberichte/jahresbericht.html

Awards and scholarships

We want to express our gratitude to our friends and sponsors, most notably

- ▷ Verein Freunde des Studienganges Geodäsie und Geoinformatik an der Universität Stuttgart e.V. (F2GeoS),
- ▷ Microsoft company Vexcel Imaging GmbH,
- ▷ Ingenieur-Gesellschaft für Interfaces mbH (IGI),
- ▷ DVW Landesverein Baden-Württemberg,

who support our programmes and our students with scholarships, awards and travel support.

Below is the list of the recipients of the 2010 awards and scholarships. The criterion for all prizes is academic performance; for some prizes GPA-based, for other prizes based on thesis work. Congratulations to all recipients! We take particular pride that one of our students, Mr. Lorenz, received the Diploma Thesis Award from the Friends of the University, an award for which he stood in direct competition with theses from the Aerospace Engineering Programme.

Award	**Recipient**	**Sponsor**	**Programme**
Karl-Ramsayer Preis	Katrin Bentel	Department of Geodesy & Geoinformatics	Geodesy & Geoinformatics
Harbert-Buchpreis	Katrin Bentel Junyi Tao	DVW	Geodesy & Geoinformatics
Diploma Thesis Award	Katrin Bentel	F2GeoS	Geodesy & Geoinformatics
Vordiplompreis F2GeoS	Stephan Laatsch	F2GeoS	Geodesy & Geoinformatics
MS Photogrammetry Vexcel Imaging Scholarship	Yuxing Li	MS Photogrammetry Vexcel Imaging	GeoEngine
IGI Scholarship	Zhou Cao	IGI mbH	GeoEngine
matching funds	M. Omidalizarandi Qinyu Yang Lin Wang	DAAD	GeoEngine
Diploma Thesis Award	Christof Lorenz	Friends of the University of Stuttgart	All university, one per faculty

Nico Sneeuw
Associate Dean (Academic)
sneeuw@gis.uni-stuttgart.de

Institute for Engineering Geodesy

Geschwister-Scholl-Str. 24D, D-70174 Stuttgart,
Tel.: +49 711 685 84041, Fax: +49 711 685 84044
e-mail: Sekretariat@ingeo.uni-stuttgart.de or
firstname.secondname@ingeo.uni-stuttgart.de
url: http://www.uni-stuttgart.de/ingeo/

Head of Institute

Prof. Dr.-Ing. Habil. Volker Schwieger since April 2010
Prof. Dr.-Ing. Ewald Krämer, (Provisional Director) until March 2010
Dr.-Ing. Martin Metzner, Akad. Oberrat

Secretary

Elke Rawe

Emeritus

Prof. Dr.-Ing. Dr.sc.techn.h.c. Dr.h.c. Klaus Linkwitz

Scientific Staff

Dipl.-Ing. Alexander Beetz	Sensor Integration
Dipl.-Ing. Jacek Frank (since 01.05.2010)	Quality Assurance
Dipl.-Ing. Ralf Laufer	Information Quality
Dipl.-Ing. Annette Scheider (since March 2010)	Engineering Geodesy
MSc Rainer Schützle	Information Quality
Dipl.-Ing. Jürgen Schweitzer	Construction Process
Dipl.-Ing. Li Zhang	Construction Process
Dipl.-Ing. Bimin Zheng	Kinematic Positioning
M.Sc. Shenghua Chen (since September 2010)	Kinematic positioning
M.Sc. Zhenzhong Su (since February 2010)	Sensor Integration

Technical Staff

Martin Knihs
Lars Plate
Doris Reichert
Mathias Stange

External teaching staff

Dr.-Ing. Max Mayer - Landesamt für Flurneuordnung
Dipl.-Ing. Thomas Meyer - Landratsamt Ludwigsburg - Fachbereich Vermessung

General View

On the 1st April 2010 Prof. Dr.-Ing. habil. Volker Schwieger accepted the chair of a Professor for „Engineering Geodesy and Geodetic Measurements“ he was offered by the University of Stuttgart and became head of the Institute for Applications of Geodesy to Engineering. As the institute copes a wide area in research and teaching it was renamed as Institute of Engineering Geodesy Stuttgart (IIGS) in September 2010. The IIGS is part of the faculty „Aerospace Engineering and Geodesy“. Furthermore, IIGS is still member of FOVUS (Traffic Research Centre of the University of Stuttgart) and thus continues the close collaboration with the faculty of „Civil and Environmental Engineering“. Since December 2010 IIGS has taken over the leadership of FOVUS.

The institute’s main tasks in education focus on surveying, geodetic and industrial measurement techniques, kinematic positioning and multi-sensor systems, statistics and error theory, engineering geodesy and monitoring, GIS-based data acquisition, and transport telematics. Here, the institute is responsible for the above-mentioned fields within the curricula for „Geodesy and Geoinformatics“ (currently Diploma and Bachelor study courses) as well as for „Geomatics Engineering“ (Master in English language). In addition IIGS provides several courses in German for the curricula of „Civil Engineering“ (Bachelor and Master) and „Technique and Economy of Real Estate“ (Bachelor). Furthermore, two lectures are given in English to students within the master course „Infrastructure Planning“. Finally, eLearning modules are applied in different curricula, e.g. for geodetic measurement techniques or for cartographic animations. The main research is therefore closely connected to teaching and focuses on: kinematic and static point positioning, analysis of engineering surveying processes and construction processes, machine guidance, monitoring, transport and aviation telematics, process and quality modelling. The daily work is characterized by intensive co-operation with other engineering disciplines, especially with aerospace engineering, civil engineering, and traffic engineering.

Research and development

Artificial Neural Networks for Propagation of Data Quality within Processes

Management of data quality is one main focus at the Institute of Engineering Geodesy Stuttgart (IIGS). Besides the development of models to describe and quantify data quality, methods for propagation of data quality within processes are part of research activities. The aim is the causal connection of the quality of input and output data. Due to the complexity of many processes within data handling, often no accurate formal description connecting quality parameter of input and output data is available. Therefore black-box qualified methods are necessary, which have the ability to recognize and model the connections without knowing the process flow in detail. Research showed that artificial neural networks (ANN) are capable for solving this task.

ANN are designed as meshed cells/neurons which are able to process information, following the natural prototype of the human brain. These ANN can be designed quite different but all of them have the talent of learning and the capability to abstract. A class of problems, respectively an unknown connection between input data space and output data space, can be learned using examples (supervised learning) or with the information „right/wrong“ (reinforcement learning). Later the ANN is capable to handle any data out of the input data space and predict the corresponding output data. Besides that, ANN are capable for advanced clustering of data, but this is not solve the given problem.

For the propagation of data quality within processes, feed-forward networks are used. Neurons are arranged in layers and the flow direction is fixed within feed-forward networks (compare Fig. 1). Back coupling to previous (relative to the direction of flow) is not allowed. The main advantages of ANN are the complex, parallel data processing, the robustness against noisy and defective input data and the real-time capability of a trained network. Feed-forward networks are trained using training examples. Within the training phase, all network parameters can be determined and the network is capable to handle any input data out of the trained input data space.

An appropriate preparation of data is necessary for using an ANN to propagate data quality. All relevant (quality) parameters of the training data have to be grouped into input and output vectors and normalized. Within the training phase, the best net configuration has to be identified by testing. The more complex the task and number of quality parameters, the more complex has to be the net in general. If the network is trained sufficiently, it is capable to predict from every input vector out of the trained data range the corresponding output vector.

The usability of ANN for propagation of data quality could be shown within a simple geodetic testing example. Regarding polar point determination, standard deviations could be calculated with sufficient accuracy by ANN. It could be also shown, that mapping of availability, consistency and completeness of data is possible by using ANN.

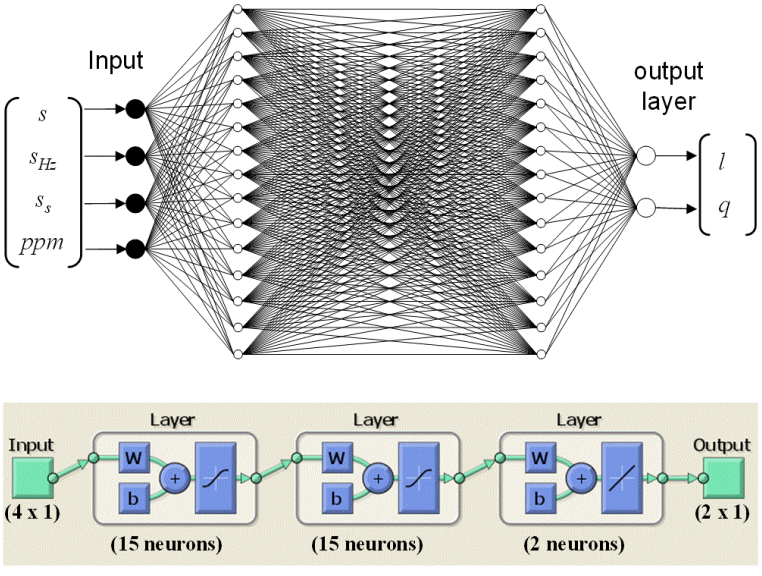

Fig. 1: Example of a feed-forward ANN with 4 input and 2 output variables (first example for research „polar point determination“)

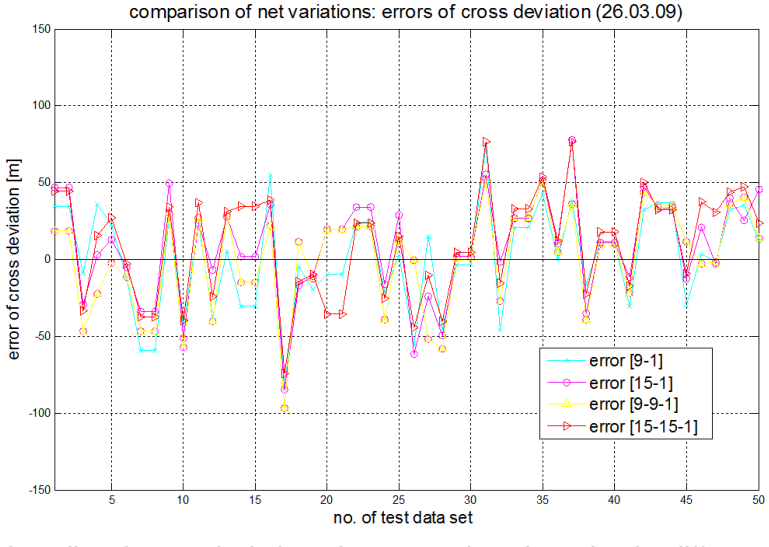

Fig. 2: Errors of predicted cross deviation of 50 example trajectories for different net dimensions (second example of research)

Within another real example, data out of the closed research project Do-iT was used (the aim of Do-iT was the determination of traffic information out of mobile phone data). The highly complex calculation process for determining trajectories of mobile phone users from mobile phone data, leads as well to complex dependencies between quality of input data and output data. The formulation of an accurate analytical relation is not possible. However, as the analysis showed, propagation of data quality works with ANN. The cross deviation of trajectories can be determined with a standard deviation of approx. 35-45 m, using a number of input parameters such as the density of the radio cell network and the density of the digital road network. The cross deviation was defined for evaluation of the calculated trajectories and describes the mean normal deviation of all positions of each user from the estimated trajectory. Fig. 2 shows the errors of 50 randomly chosen examples of trajectories for different net dimensions. The error of the predicted cross deviations ranges mainly between $\pm$ 50 m.

The fields of application for ANN to propagate data quality will be further investigated at the Institute. Particularly the use of so called dynamic networks to describe timeliness of data may be part of the research. Furthermore there are more real examples necessary to deepen the knowledge.

Validation of an Infrastructure for the Exchange of Features between Digital Road Maps

Within the EU research project ROSATTE, the IIGS mainly focused on the project validation and all related topics in 2010. The ROSATTE project, that started in 2008 and lasted until the end of 2010, mainly developed an exchange format description to transfer road sign information in a unified way between different digital road maps. This is especially important to be able to build up an up-to-date data basis for driving assistance systems (ADAS) to come. So far, electronic maps in the cars were hardly up-to-date, because they could only be updated by buying a new DVD with the current map content. In the future, such an update should also be possible via mobile communication. Therefore, also the commercial map providers need to assure, that there databases are always up-to-date.

The exchange format developed in ROSATTE was prototypically implemented in five European test sites. Therefore the data interface at the local road authorities was extended to be able to support the ROSATTE data interface. This interface must be able to support both, full data supply as well as the changes within a certain period of time. These changes are referred to as incremental updates.

In ROSATTE, basically new or changed road sign features in digital road maps are exchanged. In the original road authority database, they are mostly modeled as attributes of one or more road objects. Alternatively, they could also be modeled as self-contained objects that are referenced to one or more road objects. The road sign features (or attributes) therefore do not have an own geo-referencing, they are just referenced to another object that itself has a geo-reference. This is especially important, since the road sign information should be transferred between different digital road maps. For this exchange it is now necessary to create a so-called „location reference

code“. With their help, the location of the road sign features is no longer described by a reference to another proprietary road object and its geo-reference (e.g. an ID), but will be described by the coordinates and other describing attribute information of the road objects themselves. This should give an unambiguous description of the road sign features that is independent from the road maps but still contains enough context information to be able to insert the road sign feature not only at the geometrically but also topologically correct location in the receiving map. The mentioned context information may not only come from the directly involved road objects but also from other surrounding objects that add specific context information. AGORA-C or OpenLR are the two methods that are commonly used to create such location referencing codes.

Within ROSATTE, a process chain starting at the local road authority in the test sites (where the data is generated and provided) up to the commercial map providers, TeleAtlas and Navteq (where the data is received, decoded and integrated into their proprietary road map databases) was implemented.

The IIGS was responsible to support partners during the development as well as for the validation of the final results. For validation purposes, the partners provided images of the data at the local road authorities and the data that was finally received and integrated at the map providers. These images were made available to the IIGS and evaluated. The difficulty at the generation and integration of the updates was especially the fact, that the road sign features are based on different road maps that show also differences in the road geometry. Because of that, a fully automated validation procedure was not feasible. Both datasets from the sending and receiving side were overlaid with the help of a GIS software and then inspected manually. The assessment itself mainly consisted of two parts: The objects were checked with regards to their topological correctness and their geometrical accuracy. The topological correctness could only be answered with either „yes“ or „no“, whereas the geometrical accuracy was determined by the distance measure between the two objects in the map. A detailed definition of the two parameters is given in Table 1. Fig. 3 also describes the geometrical accuracy parameter exemplarily at an intersection.

With the help of this validation methodology it was now possible to evaluate the data provided by the local road authorities and the map providers with a standardized and transparent method. As a result, it could be shown that the road sign information exchange infrastructure developed within ROSATTE is working properly. However, also some weak points turned up. First that was the location referencing problem, already mentioned before. After intensive development efforts good results could be achieved, indeed. However, more development efforts will be necessary up to a real implementation and practical use of these methods.

Parameter	Definition
Topological correctness	Integration result needs to (1) Follow same route as original (2) Has the same direction as original (3) Start- and endpoints need to lie on the topological correct link (does not matter where exactly on that link)
Geometric accuracy	The geometrical accuracy is a distance that is being measured as follows: (1) Identify reference location in the receiving map provider map - At intersections: same distance from intersection point to location point in both maps - Apart from intersections: project the original point on a road element in the sending map orthogonally onto the corresponding road element in the receiving map (2) Measure the distance between reference location and integration result in the receiving map (3) Distance is to be judged according to application requirements

Table 1: Parameter definitions

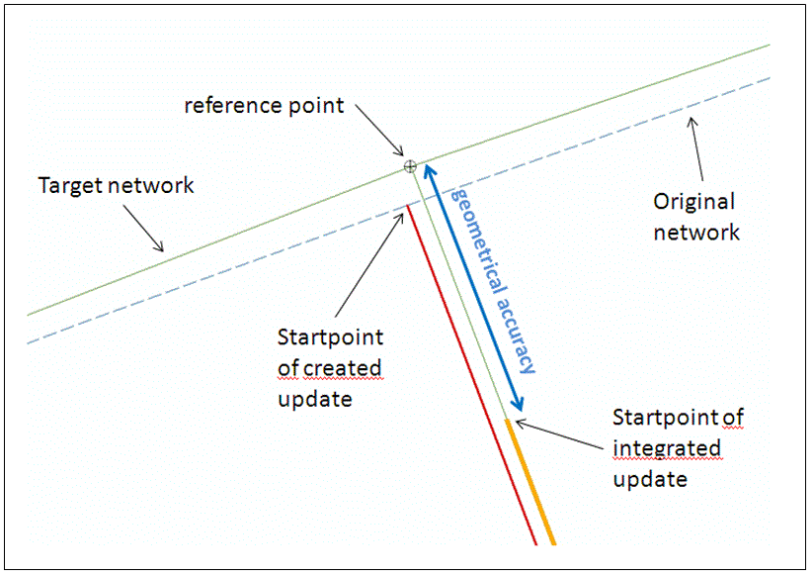

Fig. 3: Geometrical Accuracy

Secondly, the validation results also show that the existing differences in the attribute modelling in the sending and receiving databases theoretically are overcome by the definition of a standardized exchange data format. The practical realization, e.g. the mapping of the attributes from the local road authority database via the standard exchange format up to the receiving map provider database, consistently lead to misinterpretations of the original information. A further harmonization of the data formats would most probably be necessary in the future.

Having in mind the achieved results, the IIGS will continue working in the field of location referencing. The aim is to further increase the level of accuracy and also reliability of these algorithms.

Quality Assurance of Engineering Geodesy Processes

The main content of the project EQuiP (Efficiency optimization and quality control of engineering geodesy processes in civil engineering), which is sponsored by the German research foundation (DFG) is the efficiency orientated integration of engineering geodesy processes in construction processes due to consideration of measures of quality insurance. In this context, the Institute for Engineering Geodesy (IIGS) developed a quality model for engineering geodesy processes.

The quality model, consisting of characteristics and parameters should describe completely the geometric quality of a high rise building. The characteristics form the first hierarchy level of a quality model. The parameters substantiate the characteristics. Characteristics and parameters are derived from the requirements of a product (geometry of a building). There are geometric

parameters like the tolerance or standard deviation and parameters, regarding the processes which determine the geometry of a building. In Table 2 the characteristics and parameters of the quality model are shown on the base of specific requirements.

Requirements	Parameters	Characteristics
Compliance with the tolerance and the absolute position in space	- Standard deviation	**Accuracy**
	- Tolerance correctness	**Correctness**
Adherence to the topological relation between the elements	- Topological correctness	
Completeness of the elements in the house construction	- Number of missing elements - Number of odd elements	**Completeness**
Completeness of the measurement processes	- Adherence to the plan	
Reliability of the measurement processes and measuring equipment	- Condition density - Minimal detectable error - Vulnerability to failures	**Reliability**
Adherence to timescale	- Time Delay	**Timeliness**

Table 2: quality model for engineering geodesy processes

These quality parameters are related to single products or processes. To describe the quality of several processes or finished products, an appropriate computational procedure to propagate the quality parameters through the process has to be described for each parameter. For the standard deviation for example the law of variance propagation or the Monte Carlo Method can be used. But also simple mathematical operation like an addition or averaging can be used for propagating some of the parameters. On the basis of a detailed process model, quality parameters can be propagated to have a complete description of the quality of the engineering geodesy processes and products through the whole construction process.

Project QuCon: Real Time Quality Index for Houses Construction Processes

Within the EU-project QuCon (Development of a Real Time Quality Support System for the Houses Construction Industry), a real time quality assurance tool (software) which is suitable for the houses construction process should be developed.

During the project, a chronological construction process model and an application-oriented quality model with concrete quality characteristics were developed. The focus of IIGS within this project is the development of a real time quality index which describes the quality of the construction process and product in real time.

The quality control during the construction process will be realized by the so-called „Checkpoints“ (see yellow boxes in Fig. 4). One checkpoint consists of many check items which enable the users to compare the real project state and the requirements, so that the quality can be measurable and estimable.

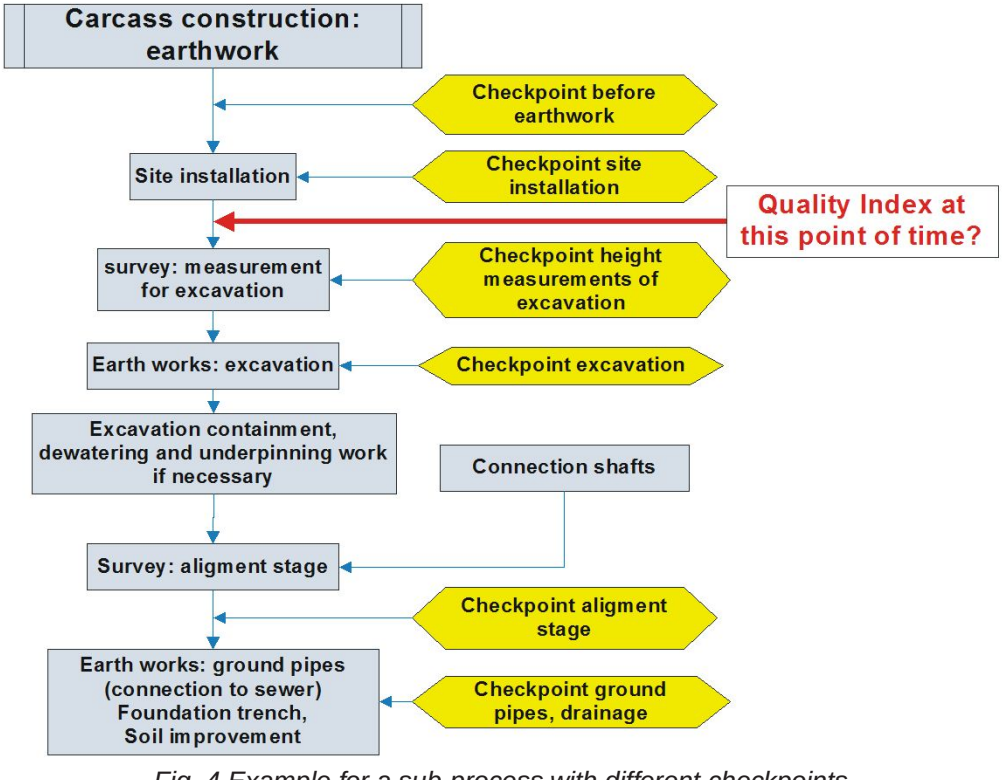

Fig. 4 Example for a sub-process with different checkpoints

A real time quality index can be calculated by the weighed mean of the checkpoint scores. The scores of the checkpoints can be determined as the weighed mean of the check items. The determination bases on the quality model, the scores and the weightings. The process quality can be determined by comparing of the planned and actual cost and time consumption. The determination of product quality bases on the completeness, the correctness and the accuracy of the product (see Fig. 5).

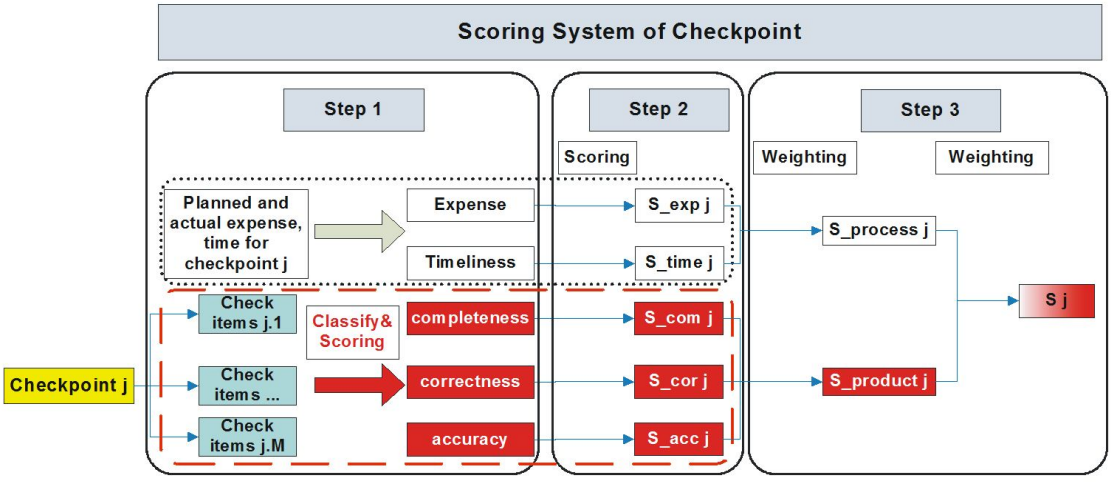

Fig. 5 Determination of the quality score of one checkpoint

Using the software, the process and product quality can be documented, accessed and monitored in real time. The user can have an overview of the current project state through the real time quality index, scores of the checkpoints, the process as well as the product. In this way, the reasonable decision and remediation can be carried out, so that the quality of the construction process can be improved and assured in real time.

Worldwide PPP - Analysis of Kinematic GPS-Measurements for TanDEM-X Evaluation

As part of the DLR TanDEM-X mission, a terrain model of the earth will be created. For the evaluation of the TanDEM-X terrain model, GNSS or rather GPS-measurements are used. For the analysis of the GPS measurements, different methods (e.g. PDGPS, PPP) were investigated and proposed. For reasons of efficiency Precise Point Positioning (PPP) was used as kinematic evaluation method to analyze world-wide kinematically gathered GPS tracks.

The work done in this project was in order of the German Remote Sensing Data Center within the German Aerospace Center (DLR) in Oberpfaffenhofen.

Approach

For data acquisition Dual-frequency-GPS-receivers were used. The GPS-antennas were attached on the roof of measurement vehicles (commonly passenger cars, cf. Fig. 6). The data was acquired on tracks of several thousand kilometers.

Fig. 6: Antenna (LEICA GX 1230) on the roof of a passenger car (Source of the figure: Report „Messung von GPS Tracks in Russland“ from GCI)

Altogether, 15 kinematic GPS-tracks were recorded on all continents of the earth (cf. Fig. 7).

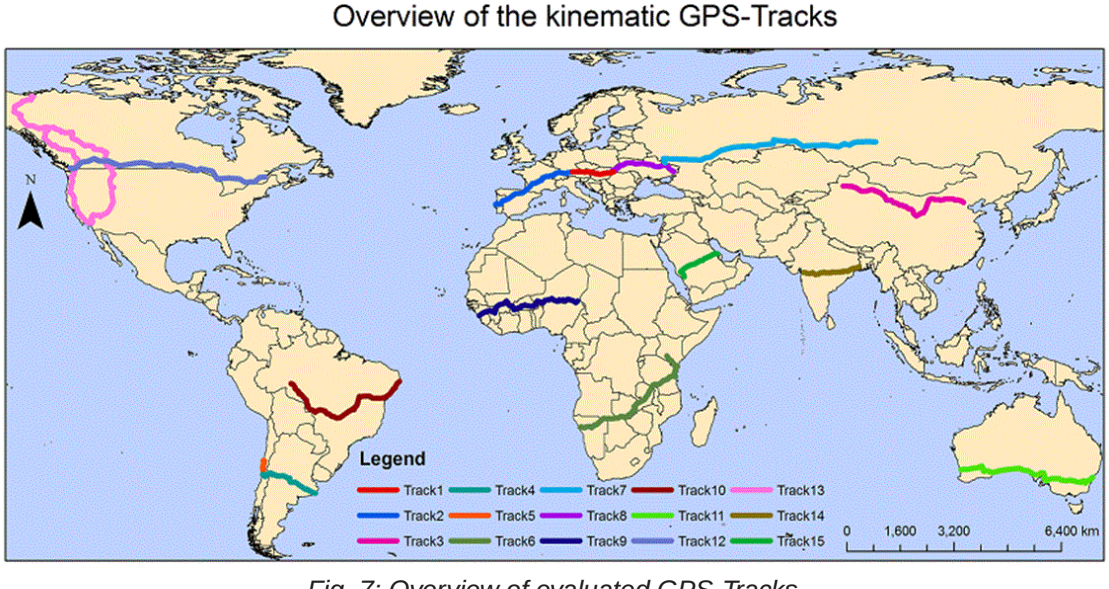

Fig. 7: Overview of evaluated GPS-Tracks

The raw data collected on the vehicles are available in RINEX-format (Receiver Independent Exchange Format). To increase reliability of the analysis results, two strategies are used (cf. Fig. 8). On the one hand, the raw data are processed with two different software packages, which are the „GPS-Inferred Positioning SYstem and Orbit Analysis SImulation Software (GIPSY-OASIS (GOA II))“ of the American „Jet Propulsion Laboratory (JPL)“ and the „Canadian Spatial Reference System (CSRS) PPP Online Service“ (CSRS, 2009) of the „Natural Resources Canada“ (NRCan). The results are then compared with one another and averaged. On the other hand, an evaluation of these final results is realized through PDGPS. In this method different reference stations are selected along the GPS-tracks. Then the trajectory points within a radius of 20km around the respective reference station are evaluated.

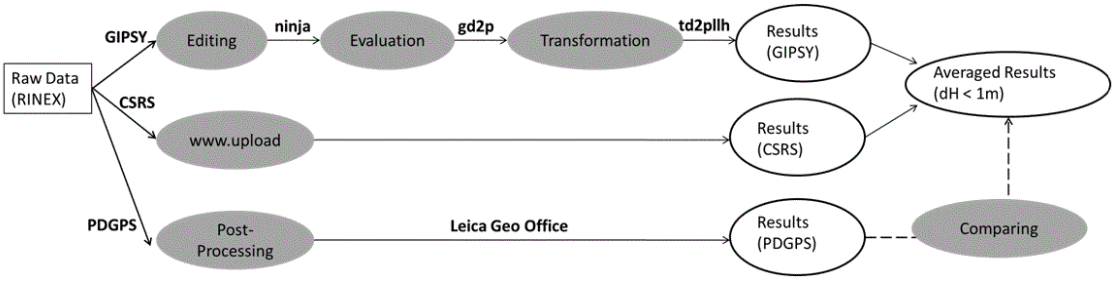

Fig. 8: Evaluation process

Results

Altogether, trajectories with a summed up length of approx. 54,778km were recorded and analyzed. Approx. 65% of all tracks, which were evaluated by both software packages, had a height difference smaller than 1m. The comparison of the results between the two software packages yielded a RMS, which is smaller than 0.7m in the height difference. The correlation between the height differences and the internal accuracies is mostly existent, but nevertheless cannot be used as a reliable indicator. The evaluated tracks were visualized. There are always some gaps in the visualized tracks. These gaps were mostly caused by occultation during data recording (cf. Fig. 9).

Fig. 9: Measurement from under a bridge

Kinematic low-cost GPS

There are already several investigations concerning the use of low-cost GPS receivers for static measurements. In some extent the results of these receivers in monitoring of glacial movements or land slide were very good. So it was not only interesting to investigate the static mode but also tracking and monitoring of fast moving objects like motor vehicles. Up to now, in most cases expensive geodetic GPS- or GNSS-receivers were used for this task. Additionally DGPS-services like SAPOS were also applied. The investigation of the institute should study, if it would be possible to use low-cost GPS receivers for tracking and recording of vehicle trajectories.

The trajectory was measured additionally by the total station Leica TCRP 1201, so the position accuracy of the GPS results could be evaluated. This trajectory, also being recorded in the kinematic mode, was considered as the reference trajectory. The used GPS receivers were geodetic receivers (Leica 1200-series) and receivers from ublox, type AEK-4T.

Fig. 10: Installed ublox receiver and 360° prism

To do GPS- and tachymeter measurements at the same time, the rover was placed (alternately the Low-Cost and the geodetic receiver) centered on a 360° prism (see Fig. 10). The construction was fixed on a car roof by a bracket. Therefore only the height offset between antenna- and prism-center had to be considered for evaluation the data. For the kinematic surveying of the trajectory the local reference station was realized by geodetic receivers but also the use of a low-cost receiver as a reference station was tested.

The first step of the evaluation was to calculate baselines with a Leica receiver as reference station and to compare the accuracies of the kinematic surveying by the geodetic and by a low-cost GPS receiver. In addition the lateral deflections of each GPS-trajectory to the reference trajectory were computed. To assess the position accuracy of the GPS-receivers the mean values of the lateral

deflections were used. Each receiver achieved a mean value of better than 2cm. This means that the accuracy of both receivers is almost equal.

In a second step the baseline evaluation was done with an ublox receiver as reference station. Compared to the results of a geodetic receiver as reference station thereby the accuracies were slightly larger with mean values of 3cm.

Under good environmental conditions the low-cost solution is applicable in the field for the reached accuracy level. This solution has the advantage that the acquisition costs are clearly reduced compared to a geodetic GPS-receiver. Furthermore the current costs for DGPS- services are also reduced or even eliminated.

Activities of Prof. Dr.-Ing.Dr.sc.techn.h.c.Dr.h.c. Klaus W. Linkwitz in 2010: Formfinding of Lightweight Surface Structures

The two-hour-lecture „Analytic Formfinding of Lightweight Surface Structures“ was incorporated into the 4-Semester Master Course “Computational Mechanics of Materials and Structures (COMMAS)“ for foreign students. It was given as a 32-hour compact course in the summer semester 2010. The additional appertaining practical computer exercises were performed on Windows-XP-computers of the CIP-pool of the course „Water Resource Engineering and Management (WAREM) of the department “Civil- and Environment Engineering“ in the University Campus Pfaffenwald. The exercises were intensified, since a final graded project-work was demanded from the students.

Publications

Beetz, A., Schwieger, V.: Enhancement of the Control Quality by an Automatic Calibration Procedure using the Example of a Construction Machine Simulator. 2nd International Conference on Machine Control & Guidance Bonn, 09.-11.03. 2010

Berkhahn, V.; Berner, F.; Hirschner, J.; Kutterer, H.; Rehr, I.; Rinke, N.; Schweitzer, J.; Schwieger, V.: Effizienzoptimierung und Qualitätssicherung-ingenieurgeodätischer Prozesse im Hochbau. In: Der Bauingenieur, Nr. 11,S. 491-501, 2010.

Kosmann, D., Wessel, B., Schwieger, V.: Global Digital Elevation Model from the TanDEM-X and the Calibration/Validation with Worldwide Kinematic GPS-Tracks. XXIV FIG International Congress, Sydney, Australia, 11.-16.04.2010.

Metzner, M.: Deformation Analysis of a Temporary Bridge in Southern Germany, FIG Commission 5 and 6 Workshop, Blue Bay Recreation Centre, Zyryanovsky Region, Kazakhstan, 3-7 September 2010

Scheider, A., Schwieger, V. (compilation): GNSS 2010 Vermessung und Navigation im 21. Jahrhundert. 100. DVW-Seminar, INTERGEO-Akademie. Köln, 04.-05.10.2010.

Schützle, R.: Networks for Mobility, „Quality Management for a Road Safety Feature Exchange Infrastructure“

Schweitzer, J., Zheng, B, Schwieger, V., Kosmann, D.: Evaluation of the TanDEM-X Digital Elevation Model by PPP GPS - Analysis and Intermediate Results. XXIV FIG International Congress, Sydney, Australia, 11.-16.04.2010.

Schwieger, V.: Positionsbestimmung von Fahrzeugen, Themenheft Forschung No 7 „Intelligente Fahrzeuge“, Rektor der Universität Stuttgart, Stuttgart 2010/11

Schwieger, V, Zhang, L., Wengert, M.: A Quality Model for Residential Houses Construction Processes. XXIV FIG International Congress, Sydney, Australia, 11.-16.04.2010.

Schwieger, V., Beetz, A., Wengert, M., Schweitzer, J.: Echtzeit-Integration ingenieurgeodätischer Messsysteme in Bauregelkreise. 16. Internationaler Ingenieurvermessungskurs. München, 23.-27.02.2010.

Schwieger, V., Foppe, K., Neuner, H.: Qualitative Aspekte zu Softwarepaketen der Ausgleichungsrechnung. 93. DVW-Seminar: Qualitätsmanagement geodätischer Mess- und Auswertverfahren. Hannover, 10.-11.06.2010.

Weston, N.D., Schwieger, V.: Cost Effective GNSS Positioning Techniques. FIG Publication No 49, FIG Commission 5 Publication. The International Federation of Surveyors, Copenhagen, Denmark, 2010.

Zheng, B., Schwieger, V., Kosmann, D.: Evaluierung des TanDEM-X Geländemodells mittels kinematischen GPS. In: 100. DVW-Seminar: GNSS 2010 Vermessung und Navigation im 21. Jahrhundert. INTERGEO-Akademie, Köln, 04.-05.10.2010.

Presentations

Schweitzer, J.: Qualitätssicherung ingenieurgeodätischer Prozesse im Bauwesen. Geodätische Woche, Köln, 06.10.2010.

Schwieger, V.: Map Matching Applications. Seminar SE 3.05 „GPS/INS-Integration und Multisensor-Navigation“, Carl-Cranz-Gesellschaft e.V., Oberpfaffenhofen, 10.11.2010.

Schwieger, V.: Cost-Effective GNSS. XXIV FIG International Congress, Sydney, Australia, 13.04.2010.

Schwieger, V.: Quality in Engineering Geodesy Processes.Wuhan University, China, 22.03.2010.

Schwieger, V.: Accurate High-Sensitivity GPS for Short Baselines.Wuhan University, China, 24.03.2010.

Schwieger, V.: Recent Developments in Machine Guidance at University Stuttgart. Wuhan University, China, 24.03.2010.

Schwieger, V.: Qualität in Ingenieurgeodätischen Prozessen. Geodätisches Kolloquium, RWTH Aachen, 21.01.2010.

Schwieger, V.: GNSS, Multi Sensor Systems und Mobile Phone Positioning, Tutorial „Positioning and Map Matching for Traffic Applications“ des 5th International Symposiums „Networks for Mobility“, Stuttgart, 29.09.2010.

Diploma Thesis

Bauer, Bauer: Post-Processing Dokumentation von Baumaschinentrajektorien mittels Low-Cost GPS

Frank, Jacek: Untersuchung zur Anwendbarkeit künstlicher neuronaler Netze bei der Beschreibung von ingenieurtechnischen Prozessen

Scheider, Annette: Nachweis einer vulkanischen Struktur auf der Schwäbischen Alb mittels gravimetrischer Messungen und unterstützender Höhenbestimmungen (gemeinsam mit Geodätischen Institut Stuttgart)

Master Thesis

Hu, Wenjuan: Time series analysis for construction monitoring

Zhang, Xiaoxin: SAPOS HEPS for RTK. Applications in move

Study works

Hasert, Roman: Ausarbeitung eines Qualitätsprüfplanes für Geodaten

Langer, Marko: Analyse und Verbesserung der Qualität von Geodaten

Education

Basic Geodetic Field Work (Beetz, Zhang)	5 days
Geodetic Measurement Techniques II (Metzner, Zhang)	2/1/0/0
Geodetic Measurement Techniques I (Metzner, Zhang)	3/1/0/0
Geodetic Seminar I, II (Fritsch, Keller, Kleusberg, Schwieger, Sneeuw)	0/0/0/4
Integrated Field Work (in German) (Laufer, Zheng,)	10 days
Statistics and Error Theory (Schwieger, Laufer)	2/2/0/0
Surveying Engineering I (Schwieger, Zheng)	2/1/0/0
Surveying Engineering II (Schwieger, Zheng)	2/1/0/0
Surveying Engineering III (Schwieger, Scheider)	2/1/0/0
Surveying Engineering IV (Schwieger, Beetz, Frank)	2/1/0/0
Thematic Cartography (in German) (Metzner, Schützle)	1/1/0/0

Multisensor Systems for Terrestrial Data Acquisition (in German) (Schwieger, Schweitzer)	1/1/0/0
Causes and Impacts of Deformations in Structures (Laufer)	1/1/0/0
Transport Telematics (in German) (Metzner, Schützle, Scheider)	2/1/0/0
Reorganisation of Rural Regions (Meyer)	1/0/0/0
Integrated Field Work (Laufer, Zheng,)	10 days
Terrestrial Multisensor Data Acquisition (Schwieger, Schützle)	2/1/0/0
Thematic Cartography (Metzner, Schützle)	1/1/0/0
Transport Telematics (Metzner, Schützle, Schweitzer)	2/1/0/0
Kinematic Measurements and Positioning (Schwieger, Beetz)	2/1/0/0
Acquisition and Management of Planning Data (Metzner, Frank)	2/1/1/0
GIS-based Data Acquisition (Schwieger, Schweitzer)	1/1/0/0
Data Management and Analysis (Metzner, Frank)	1/1/0/0
GIS-based design of traffic transport structures (Metzner, Frank)	1/1/0/0

Institute of Geodesy

Geschwister-Scholl-Str. 24D, D-70174 Stuttgart,
Tel.: +49 711 685 83390, Fax: +49 711 685 83285
e-mail: gis@gis.uni-stuttgart.de or firstname.secondname@gis.uni-stuttgart.de
url: http://www.uni-stuttgart.de/gi

Head of Institute

SNEEUW NICO, Prof. Dr.-Ing.

Emeritus

GRAFAREND ERIK W, em. Prof. Dr.-Ing. habil. Dr.tech.h.c.mult. Dr.-Ing.E.h.mult.

Academic Staff

BAUR OLIVER, Dr.-Ing. (until 31.10.)
KELLER WOLFGANG, Prof. Dr. sc. techn.
KRUMM FRIEDRICH, Dr.-Ing.
REUBELT TILO, Dr.-Ing.
WEIGELT MATTHIAS, Dr.-Ing.
WOLF DETLEF, Prof. Dr. rer. nat. habil.

Research Associates

ANTONI MARKUS, Dipl.-Ing.
CAI JIANQING, Dr.-Ing.
CHEN QIANG, M.Sc., Wuhan/China (since 29.9.)
DEVARAJU BALAJI, M.Sc.
IRAN POUR SIAVASH, M.Sc.
TOURIAN MOHAMMAD, M.Sc.
WU GELI, M.Sc., Wuhan/China (since 10.12.)

Administrative/Technical Staff

HÖCK MARGARETE, Phys. T.A.
SCHLESINGER RON, Dipl.-Ing. (FH)
VOLLMER ANITA, Secretary

Guests

FÖLDVÁRY L, Dr., Budapest/Hungary (3.5.-31.7.)
ISSAWY E, Prof. Dr., Cairo/Egypt (3.8.-26.10.)
JIANG W, Prof. Dr., Wuhan/China (1.8.-27.9.)
LI H, PhD student, Tongji/China (1.1.-23.1.)
LI J, Prof. Dr., Wuhan/China (1.8.-31.8.)
LIN Y, Dr., Tongji/China (1.1.-23.2.)
SAFARI A, Ass. Prof., Tehran/Iran (4.1.-31.3.)
TSOULIS D, Ass. Prof. Dr., Thessaloniki/Greece (7.6.-15.8.)
VARGA P, Prof. Dr., Budapest/Hungary (22.2.-19.3., 18.5.-18.6., 22.11.-21.12.)
WANG Z, Dr., Wuhan/China (12.7.-27.9.)
XU X, Dr., Wuhan/China (1.1.-20.2.)
YAO Y, Dr., Wuhan/China (1.4.-22.9.)
ZHANG X, Prof. Dr., Wuhan/China (12.7.-27.9.)

Additional Lecturers

ENGELS J, PD Dr.-Ing. habil., Stuttgart
HAUG G, Dr.-Ing., Stadtplanungs- und Stadtmessungsamt, Esslingen/Neckar
SCHÖNHERR H, Präsident Dipl.-Ing., Landesamt für Geoinformation und Landentwicklung Baden-Württemberg, Stuttgart

Research

Derivatives of the range-rate observations for regional gravity field improvement

Modeling of the gravity field

The observations of satellite missions play an important role in the determination of the gravity field of the Earth. In the analysis, the field is usually modeled in terms of spherical harmonics. These harmonic and orthogonal base functions have stable recursions, but they obstruct a regional improvement because of their global support. A regional improvement can be achieved by separating the signal and the model into a global and a residual part. The global part is calculated by spherical harmonics with a known set of coefficients and removed from the signal.

The residual signal is analyzed by a superposition of radial base functions, which are characterized by a centre, a scale factor and a shape. An example of three base functions with different centers and shapes is visualized in the Figure 1, where the height at each center is normalized to one.

In general, the analysis by radial base functions can be formulated as an optimization problem of the base function parameters, minimizing the norm of the differences between the superposition and the residual signal. This leads to a linear problem of the scale factors or to a nonlinear optimization of several parameters per base function.

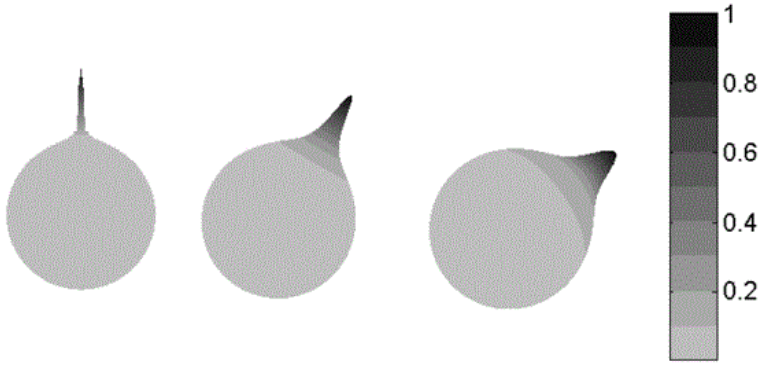

Figure 1: Example of three base functions for the analysis of a residual signal

Derivatives of the range-rate observation

The GRACE mission provides the distance and the changing of the distance between two satellites, the so called range-rate (cf. Figure 2). Removing the non-gravitational effects by corrections, the measurements have to be linked to the parameters of a residual gravity field. This link is the target function in the subsequent optimization problem.

For the numerical determination of the optimum, the partial derivatives with respect to the base function parameters are required. These derivatives are usually generated by variational equations. In regional analysis, a differential equation has to be solved for every arc in the orbit and for each parameter. For numerical reasons the equations should be solved in separate integrations, although the reference field and the orbit are identical.

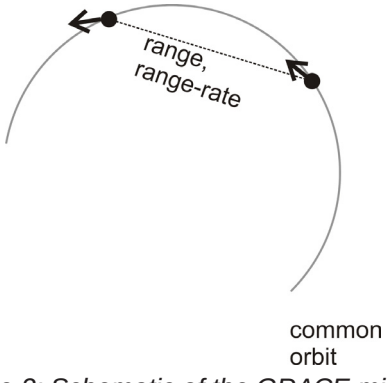

Figure 2: Schematic of the GRACE mission

A closed solution is developed to avoid repeated integrations. The changing of the positions and velocities with respect to a circular reference orbit are described by the Hill differential equations in a rotating coordinate system (cf. Figure 3). For a circular orbit the disturbing force of a radial base function is represented in a Fourier series. Assuming a constant rotation of the Earth, the deviation of the orbit is achieved by a Laplace-transform. The procedure is repeated for the second satellite and the results are transformed into a common coordinate system. The algorithm is summarized in Figure 4 and provides an approximation of the residual range-rate caused by the radial base functions. The formula can be differentiated with to respect to all parameters of the base functions by inserting the known derivatives of the force into the algorithm.

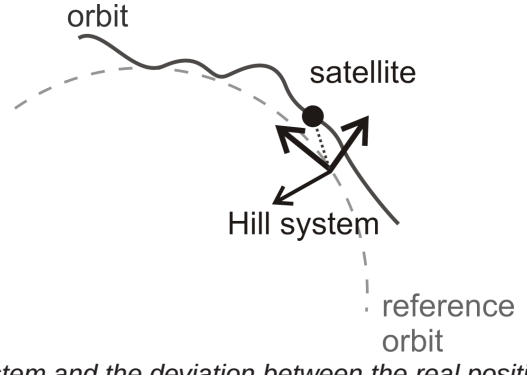

Figure 3: Rotating Hill system and the deviation between the real position and the reference orbit

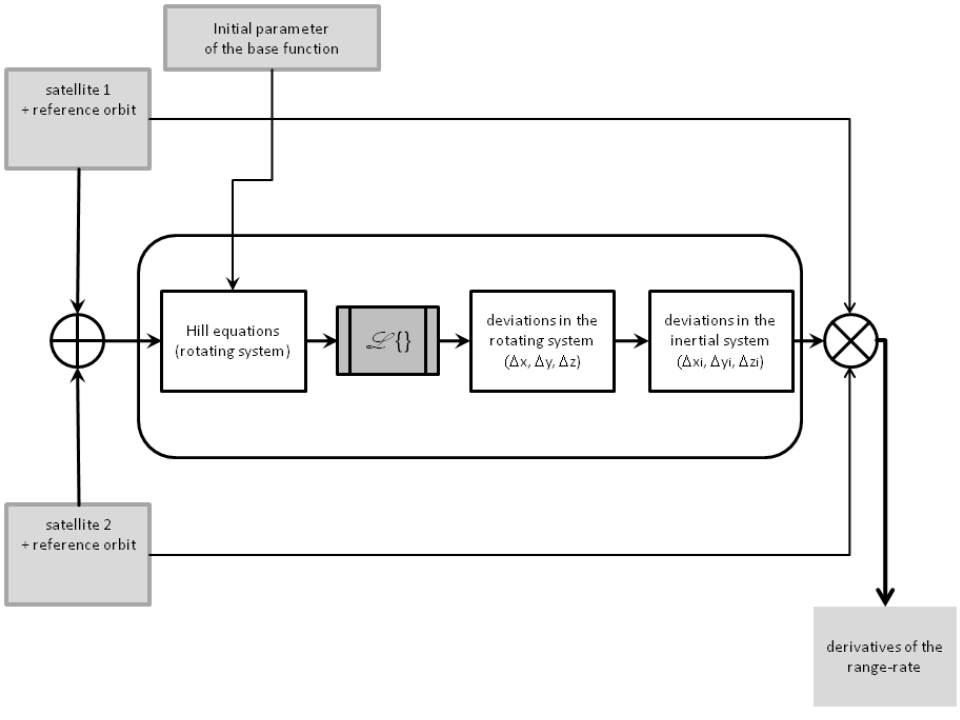

Figure 4: Calculating the closed solution from the orbit data and the initial parameters of the radial base functions

The derivatives of the range-rate with respect to the parameters of a base function are visualized in Figure 5. The base function is located in the middle of the arc, which is correlated with the maximum of the derivative with respect to the co-latitude.

The closed solution and the variational equation fit up to 0.1 - 1 % for an arc of 7.5 min, which can be explained by the different approximations. The limitations of the closed solution are the circular orbit and the implicit restriction of an isotropic reference field. The variational equations require several numerical integrations, but they are more flexible and can be used for an arbitrary orbit.

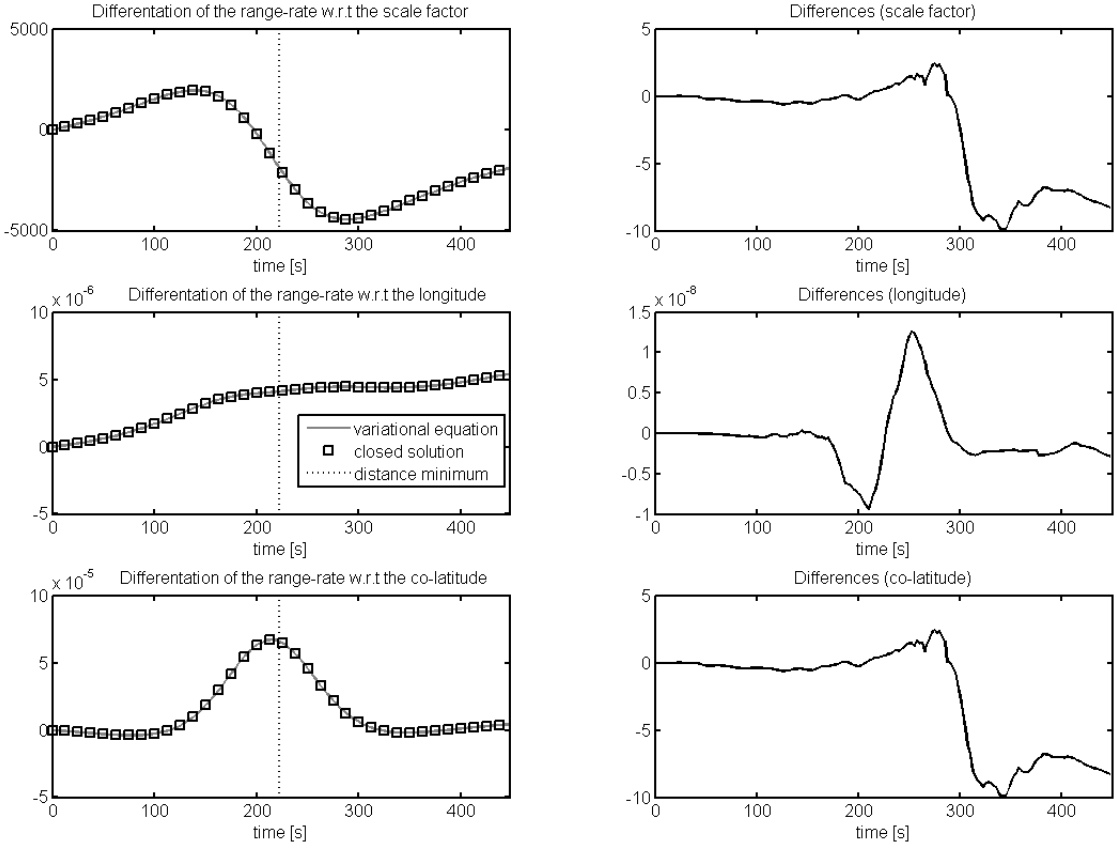

Figure 5: Derivatives of the range-rate with respect to the parameters of a base function in the middle of the arc

Global assessment of mass changes detected by space-borne gravimetry

Mass transport in the Earth's system is one of the main indicators of present-day global climate change, most notably with regard to sea-level variation estimates and forecasts. Since 2002, the Gravity Recovery And Climate Experiment (GRACE) satellite mission allows inference of mass variations on and beneath the Earth's surface from time-variable gravity measurements in space. The assessment of GRACE-derived secular continental mass variations on a global scale provides an improved understanding of mass transport. The delineated areas in Figure 6 cover continental areas exhibiting a dominant GRACE signal. The signal inside these areas is caused mainly by glaciological and hydrological phenomena (rather than GRACE errors).

Eustatic sea-level modeling translates mass gain or loss over land areas to uniform water changes over the world's oceans. Table 1 presents the impact of GRACE-derived secular continental mass variations (cf. Figure 6) in terms of sea-level change equivalent (the signals over the Canadian Shield and Fennoscandia have been corrected for global isostatic adjustment, GIA, effects).

Most notably, present-day continental mass variations as observed by GRACE reveal both secular mass decline and accumulation. Whereas the former contribute to uniform sea-level rise of +(1.33±0.03) mm/yr, the latter result in sea-level drop of -(0.75±0.11) mm/yr. The net effect was +(0.58±0.12) mm/yr. After application of GIA corrections over the whole of Antarctica, this value adjusts to +(0.84±0.14) mm/yr. This estimated non-steric ocean mass trend includes both the land ice and land water contributions. As main result, land-hydrological mass accumulation in a few regions (e.g., central Africa and the Amazon Basin) compensates about half the impact of (melt) water influx to the oceans. As such, consideration of mass accumulation (rather than focusing solely on mass loss) is important for reliable estimates of sea-level change from GRACE.

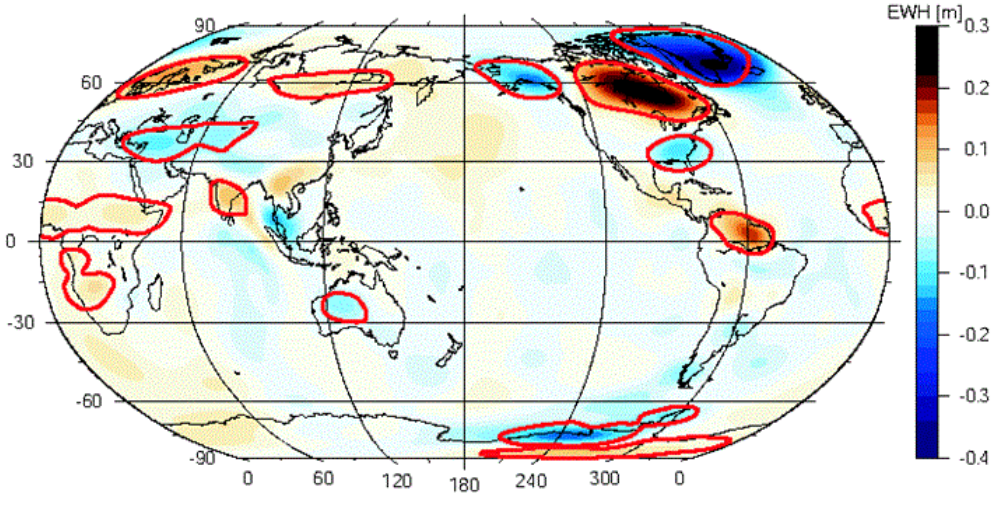

Figure 6: Secular trends from GRACE in terms of equivalent water height (EWH). Pattern extracted from gravity field time-series from March 2003 to February 2009. A regression line was fitted to the time-series of residual EWH values at each point of a global 1° x 1° grid. Delineated areas indicate the regions with dominant signal.

Region	Change
Greenland	3.46±0.06
Antarctica 1	1.49±0.08
Middle East	1.09±0.13
Alaska	0.84±0.06
Mississippi Basin	0.76±0.08
Australia	0.33±0.06
Africa	-1.20±0.18
Amazon Basin	-1.22±0.13
Siberia	-0.74±0.06
Antarctica 2	-0.20±0.08
India	-0.38±0.05
Canadian Shield	-0.15±0.61
Fennoscandia	-0.57±0.11
Sea-level rise	7.98±0.20
Sea-level drop	-4.48±0.67
Total change	3.50±0.70

Table 1: Eustatic sea-level change equivalent (mm) from March 2003 to February 2009, GIA corrections applied

Greenland ice mass loss by means of point-mass modeling

Greenland ice mass loss is one of the most serious phenomena related to global climate change. In this context, both the quantification of overall deglaciation rates and its spatial localization are highly significant. Point-mass modeling is a viable approach to derive high-resolution mass-balance patterns from GRACE (Gravity Recovery And Climate Experiment) gravimetry. The method infers mass variations on the Earth's surface from gravitational signals at satellite altitude. Due to downward continuation the determination of surface mass changes from observations in space is an ill-posed problem, i.e., pertinent regularization deserves particular consideration.

In order to demonstrate the performance of the method, Figure 7 presents the results of a (closed-loop) simulation study. In the synthesis step, 71 point-mass changes were defined along the east coast of Greenland (Figure 7, left panel). The individual magnitudes range from -0.4 km^3 in the north to -27.8 km^3 in the south; the total variation is -1000 km^3. In a second step forward modeling of the point-mass changes yielded 1338 gravitational disturbances at satellite altitude (not shown here). In a final step, the point-mass variations were recovered from the synthesized gravitational signal. To this end, the Greenland area was covered with 234 (equidistant) point-mass variation candidates. Noteworthy, the individual simulated mass-change magnitudes as well as the geometrical mass-change distribution have been recovered correctly (Figure 7, right panel). Comparison with the simulation input quantifies the error to be less than 0.1%.

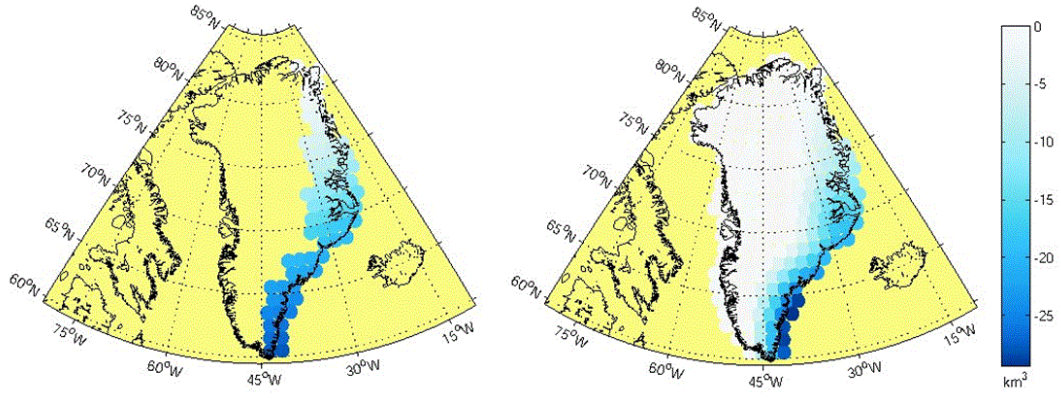

Figure 7: Simulation study. Left panel (synthesis): 71 simulated point-mass variations on the Earth's surface (total variation -1000 km^3). Right panel (analysis): Solution with optimal regularization parameter in terms of the L-curve criterion (total variation -999.5 km^3).

Application of the approach to a series of GRACE monthly gravity field solutions from April 2002 to March 2009 resulted in a volume-change rate of -(299$\pm$6) km^3/yr (the uncertainty is in terms of formal errors). This estimate does not account for global isostatic adjustment corrections; however, these are more than one order of magnitude smaller. Figure 8 depicts the corresponding spatial pattern of recovered point-mass changes. The pattern points to ice-mass decline along the whole Greenland coast line. Most notably, Figure 8 confirms dominating deglaciation in the south-east.

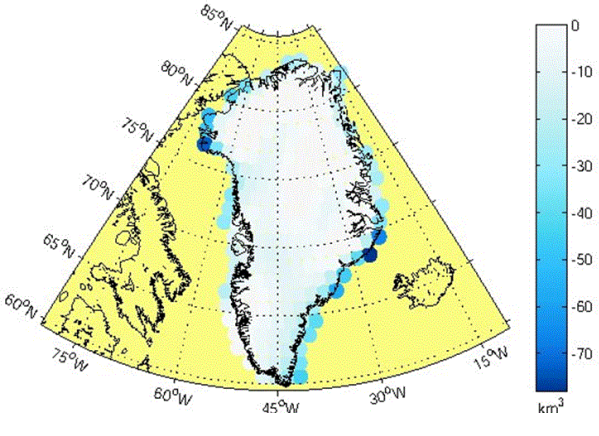

Figure 8: GRACE data analysis from April 2002 to March 2009. Spatial pattern of recovered point-mass changes; the overall change rate is -(299$\pm$6) km^3/yr.

GOCE Gravity Field Recovery - GOCE real data analysis by means of rotational invariants

Launched on 17 March 2009, ESA's Gravity field and steady-state Ocean Circulation Explorer (GOCE) will revolutionize our understanding of one of Earth's most fundamental forces - gravity. Typically, gradiometer data analysis is performed at the level of individual GGs, in particular the main diagonal elements of the gravitational tensor. This approach embraces a variety of methods commonly attributed to the space-wise or time-wise methods. Alternatively to the classical approach, our institute is engaged in GOCE real data analysis by means of rotational invariants.

Due to the colored noise characteristic of successive gradiometer observations, the stochastic model assembly of the rotational invariants constitutes a highly challenging task on its own. Basically, the invariants' variance-covariance information can be deduced from the gravitational gradients by error propagation. But the huge number of gradiometer data and the size of related variance-covariance matrix prohibits this possibility. According to our actual study, the time series of these invariants have similar stochastic characters to these gravitational gradients, see Figures 9-12. Based on successful experiences from IGG, University of Bonn, the GOCE invariants can be also considered as equidistant time series and therefore be decorrelated by means of numerical filters. In this context, autoregressive moving-average (ARMA) filters are tested and applied to approximate the stochastic model of these invariants. The stochastic models of GOCE invariants in the form of various filters will be implemented in real data analysis and their effects on gravity field recovery will be analyzed based on two months of GOCE data.

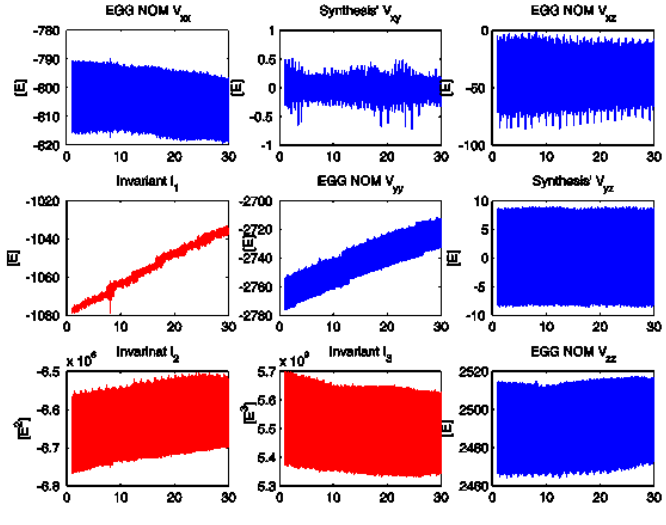

Figure 9: Time series of GOCE gravity gradients EGG NOM and three invariants (in red) in November 2009

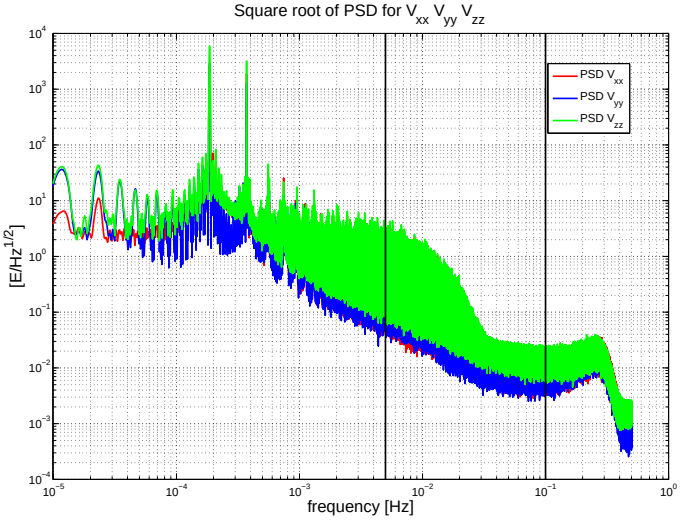

Figure 10: Spectral characteristics of GOCE gravity gradients EGG NOM (main diagonal) in November 2009

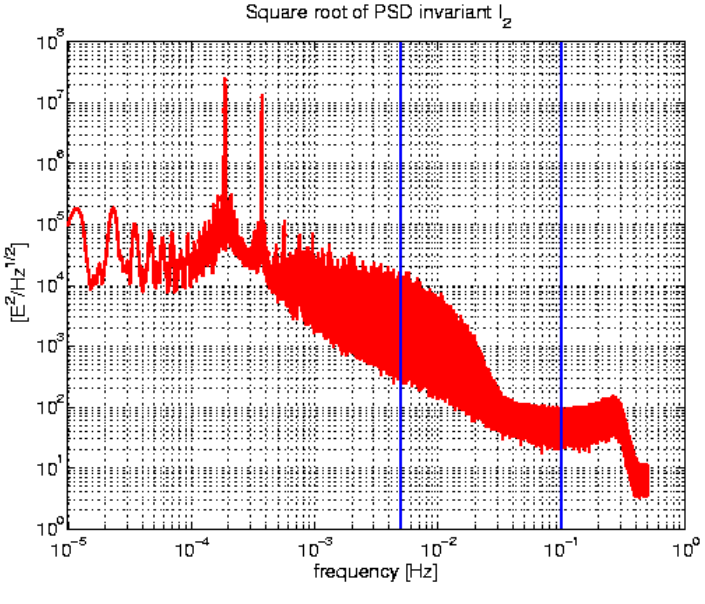

Figure 11: Spectral characteristics of GOCE invariant I_2 in November 2009

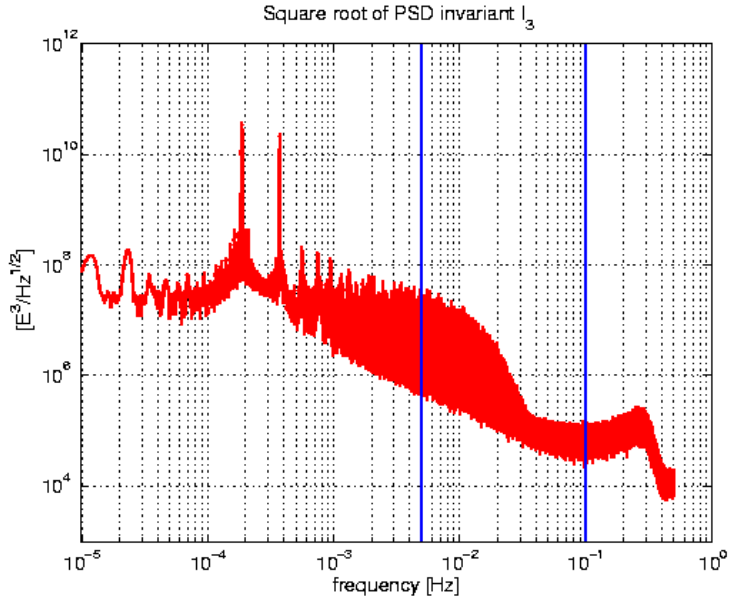

Figure 12: Spectral characteristics of GOCE invariant I_3 in November 2009

Assessment of gravity recovery simulations of future satellite missions by EOF and Canonical Correlation Analysis (CCA)

One of the most fundamental challenges in spaceborne gravimetry is the separation of the time-variable gravitational signals into their individual geophysical sources. Also, the question of which satellite mission scenario is better for retrieving the gravitational signals of the geophysical sources has a crucial importance for formation flight design. That is especially the case when we are challenging the orbital sampling problem and the aliasing effect of high frequency geophysical phenomena.

Empirical Orthogonal Functions (EOF) analysis has been shown to be a valuable tool in support of solving the signal separation problem and signal identification. The Canonical Correlation Analysis (CCA), on the other hand, can be considered as a tool for the correlation search of the satellite mission recovery results and the models of input. The method can be used in a closed-loop gravity field retrieval, i.e. the CCA looks for the correlation between the models used as the input of the flight configuration and the recovered solution which comes out of the mission scenario. The idea, then, is the analysis of correlation levels between input and output may provide a tool for the decision on choosing the better mission scenario.

The Hydrology model PCR-GLOBWB (Utrecht university) was used as the reference for comparing the recovered solutions from the satellite mission scenarios through EOF and CCA (Figure 13).

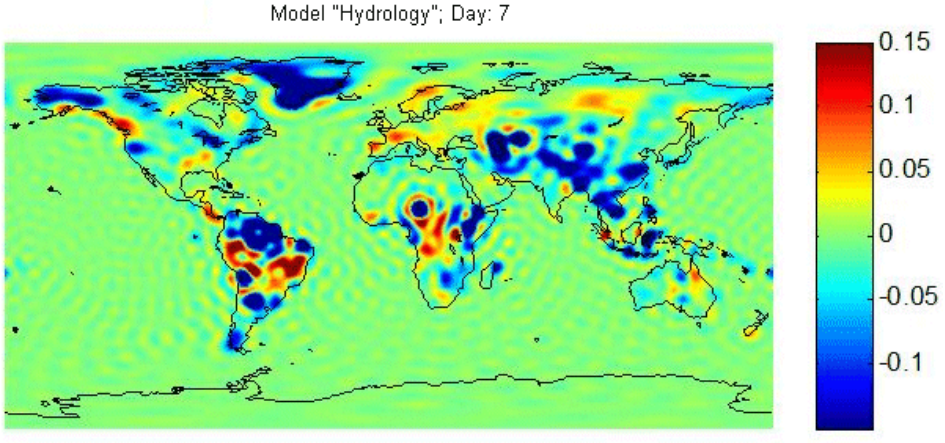

Figure 13: Equivalent Water Height (EWH) anomaly map for 7 January 1996

Three scenarios from the ESA study „Monitoring and Modeling Individual Sources of Mass Distribution and Transport in the Earth System by Means of Satellites" were chosen. The recovery only solved for „hydrology + tides" in all the three scenarios of Table 2 in terms of Stokes coefficients up to degree 50.

Scenario	Pair	Configuration
1	BEN1.5	Bender satellite configuration in polar orbit - 5 days solution
2	SC1234.2	Four tandems in polar orbits, 2 days time-shifted with identical ground tracks - 2 days solution
3	SC1234.8	Four tandems in polar orbits, 2 days time-shifted with identical ground tracks - 8 days solution

Table 2: Satellite mission scenarios

The EOF analysis is used as an approach for signal separation of the recovered solutions of satellite mission scenarios and the data from the hydrology model. The aim is to look for the scenarios which provide the modes (signatures) with higher correlation with the modes resulted from the hydrology model. In the approach, the Stokes coefficients are sorted by order. The EOF analysis, then, is separately done on C_{lm} and S_{lm} coefficients matrices. The difficulty of this correlation search is shown in Figure 14.

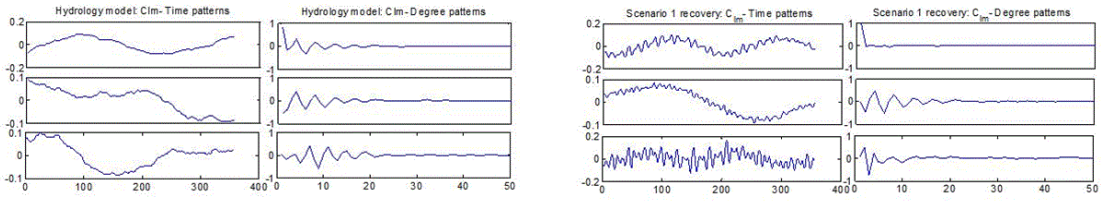

Figure 14: The first three modes of the C_{lm} coefficients of the first order (m=1) of the hydrology model (left) and the scenario 1 (right).

In contrast to EOF analysis, in CCA we directly try to find the correlation between two data sets. The resulting modes of the analysis are indeed the joint modes of the datasets. Here, we look for the correlation between the hydrology model and the recovery solutions of the three suggested scenarios. In all the analysis, and for all the orders, the first modes have very large contribution to the signal power indicated by singular values (Figure 15).

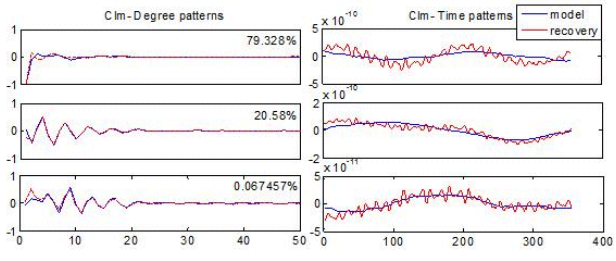

Figure 15: Example of the first three joint modes for the first order (m=1) of C_{lm} coefficients with their contribution to the whole signal power as percentages (right).

Comparing the satellite mission scenarios, the second and third suggested scenarios provide the cleaner Equivalent Water Height (EWH) maps, whereas the third one with longer time solution shows a minor superiority over the second scenario (Figure 16).

The CCA approach was also used to reconstruct the recovery solutions from the first joint modes with the highest singular values, providing cleaner maps, but also smoothing some of the geo-physical signals which might be lain in the other modes. This is certainly a disadvantage for the method if used as a filter.

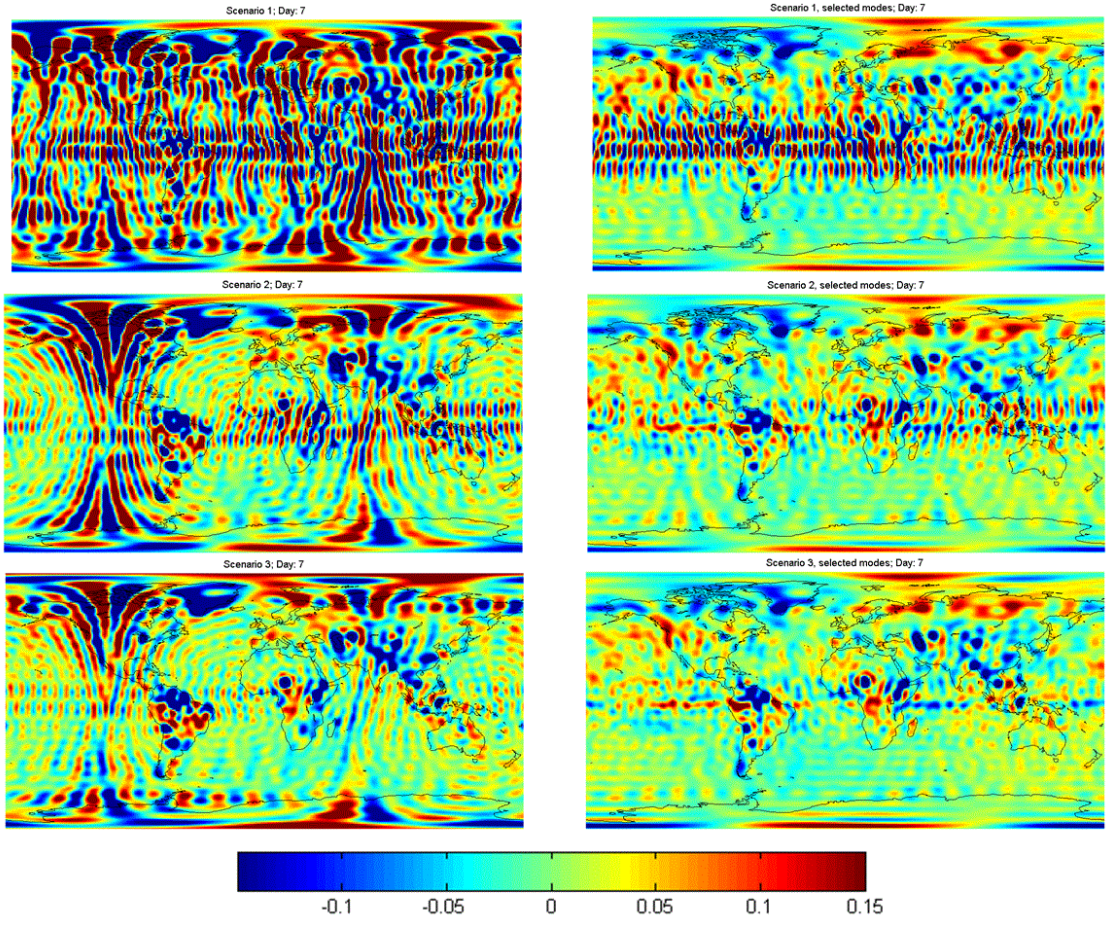

Figure 16: EWH anomaly maps for the three scenarios (left) and the maps resulted from at least 95% of the power of the whole signals analyzed by CCA.

Future satellite formations for the detection of time variable gravity fields

Within the two common projects „Assessment of a Next Generation Gravity Mission for Monitoring the Variations of Earth's Gravity Field" (ESA) and „Zukunftskonzepte für Schwerefeldsatellitenmissionen" (BMBF) with project partners from science and industry concepts for future multi-satellite missions for the detection of time variable gravity fields are investigated.

One of the main problems of the GRACE-mission is the sensitivity of the range-rate measurements, which leads to the typical North-South striping error pattern of GRACE solutions. These striations are due to the anisotropy involved with the leader-follower formation of GRACE, which allows range-rate measurements only in North-South directions and neglects signals in East-West and radial directions. By means of sophisticated formations, the sensitivity and isotropy of the range-rate measurements can be improved. Such formations are (i) the PENDULUM, where the satellites fly approximately parallel at the equator (and behind each other at the poles), (ii) the CARTWHEEL, where the two satellites generate a 2:1 relative elliptic motion once per revolution in the orbit plane and (iii) the LISA formation, a combination of pendulum and cartwheel, where the two satellites perform a circular motion in a plane tilted to the orbit plane. The relative motion of the satellites of these formations is shown in the Hill-frame in Figure 17. In contrast to the North-South directed measurements of GRACE, the PENDULUM generates measurements in East-West direction over the equator (and possibly in North-South direction over the poles), the CARTWHEEL produces measurements alternating twice per revolution in radial and North-South direction and LISA performs measurements alternating in all three directions.

As shown by the triangle plots of formal spectral errors in Figure 17 and the degree-RMS curves in Figure 18, the advanced formations are able to improve the sensitivity by approximately one order of magnitude compared to the GRACE-formation. Additionally, these formations lead to a higher isotropy as shown by the covariance functions in Figure 17. The North-South structures caused by the inline-formation are eliminated and isotropic circular covariance patterns appear. The higher isotropy is also visible in the triangle plots of formal errors, where the accuracy of spherical harmonic coefficients of higher order is improved.

Unfortunately, there is a constraint of the laser instrument on the maximum range-rate which proved to be 10 m/s. With this constraint the advanced formations in the implementation displayed cannot be flown. In order to match this constraint either the satellite-distance has to be reduced significantly, or the line-of sight-angle of the pendulum has to be diminished. Both limitations lead to a loss of sensitivity. For the LISA-formation, the tracking of the satellites and the instability of the formation are significant problems. The technical realisation of the sophisticated formations, which is comparatively difficult, is studied by industrial partners within the mentioned projects.

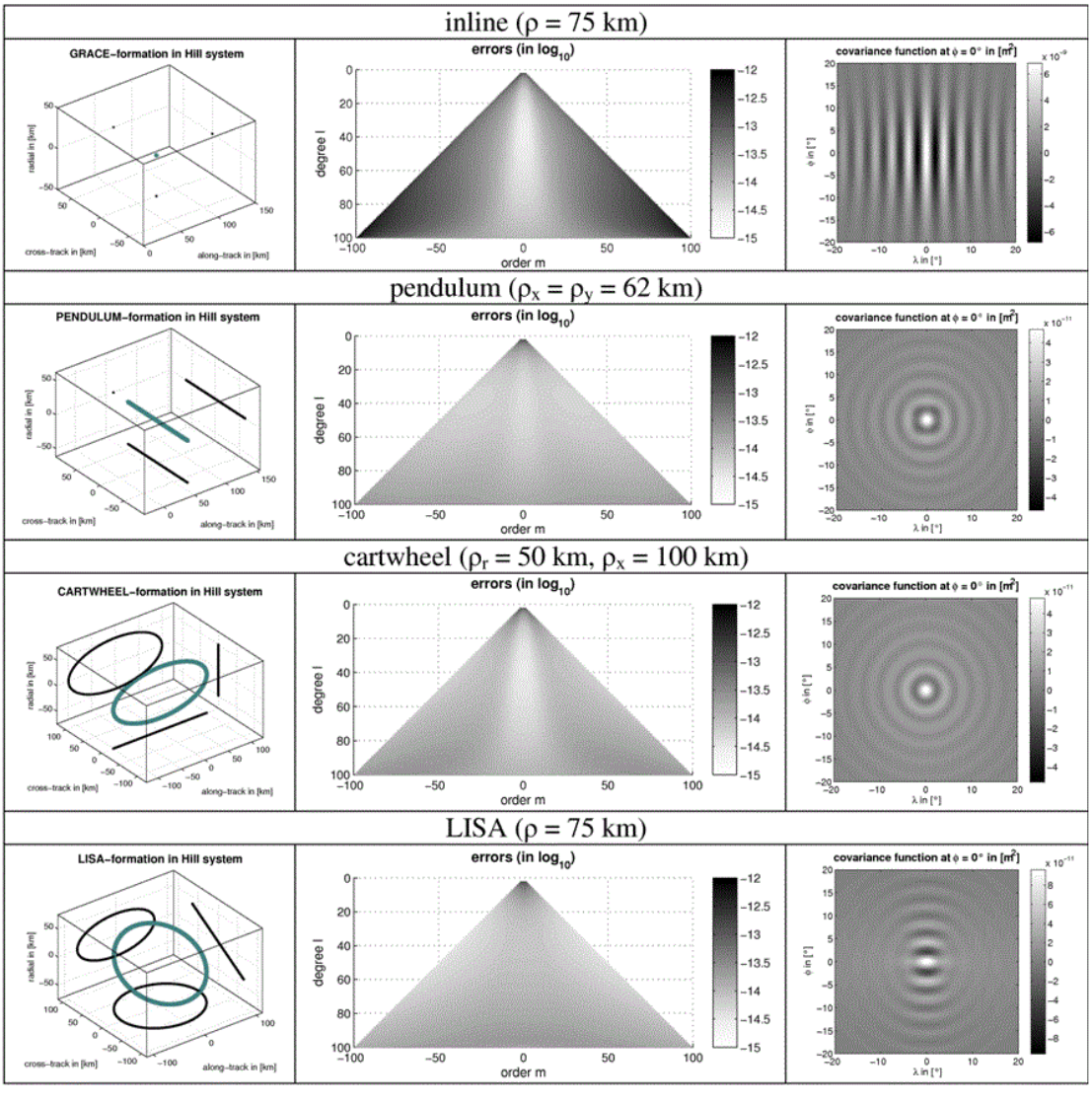

Figure 17: Formal errors, covariance functions and relative motion in the Hill-system of the four natural formations

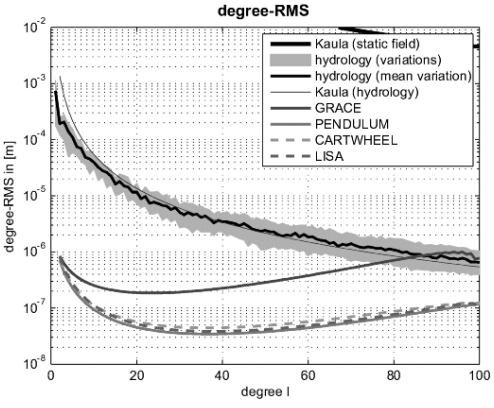

Figure 18: Degree-RMS of the four natural formations

Sensitivity analysis of future satellite formations and configurations of them

By means of „Quick-Look-Tools“ (QLT) error propagation of future satellite missions is studied. With such Quick-Look-Tools the influence of a variety of important parameters as orbit height, inclination, satellite distance, instrumental noise and measurement type can be studied. For this reason the QLT are an important tool for designing future missions, although temporal aliasing - one of the main problems for time variable gravity field detection - cannot be investigated with them.

A sensitivity analysis of the formations is shown in Figure 17 and Figure 18 and described in the previous section. One of the ideas for a future mission design is to combine formations in different inclinations (and repeat patterns), the so-called Bender-design. It was already shown by several studies that such a design has capabilities for temporal de-aliasing and advantages concerning sensitivity, especially for short estimation periods, e.g. 4 or 7 days. By means of Quick-look-tools, the sensitivity of Bender-designs can be studied. Figure 19 and Figure 20 show the results of a sensitivity analysis of Bender-designs using a polar inline formation and inclined inline/pendulum/cartwheel formations. The inclinations used are I = 97° (sun-synchronous, SSO) and I = 63° (low inclination). As visible from Figure 19 and Figure 20, the sensitivity and isotropy can be increased by means of a Bender-formation compared to the single polar inline formation. Adding an inclined inline-formation already leads here to a very promising result concerning the formal errors, although still North-South patterns are visible in the covariance-functions. In case of an inclined pendulum, it has to be taken care which satellite is the leader. Very promising results are obtained for the Bender configurations with an SSO-pendulum with the left satellite as leader or with the (I=63°)-pendulum with the right satellite as leader, where also a high level of isotropy is reached. The Bender-configurations applying the inclined cartwheel also perform quite well. In total, the most promising results are obtained by the Bender-configuration with the SSO-pendulum with the left satellite as the leader.

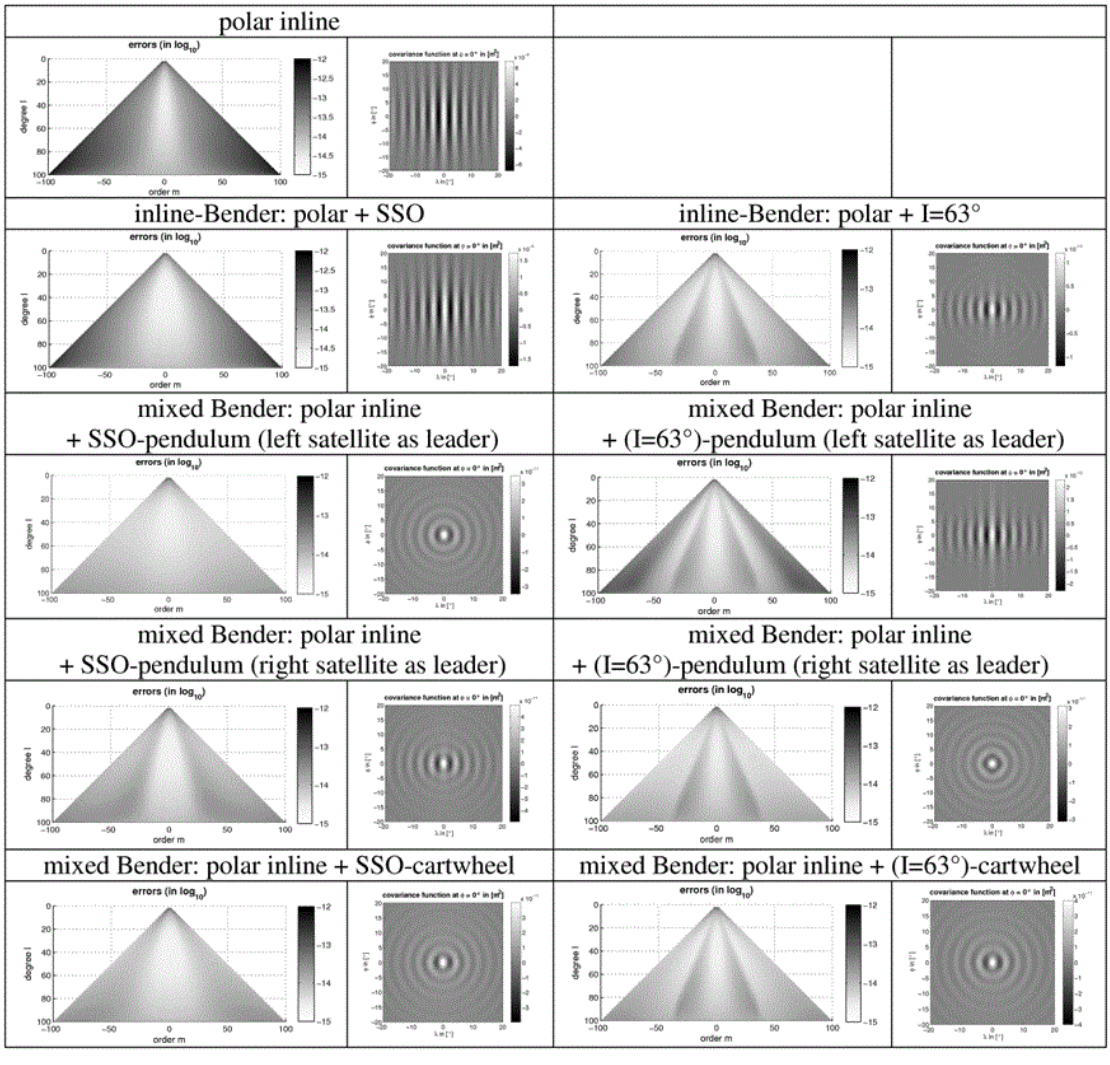

Figure 19: Formal errors and covariance-functions of mixed-Bender configurations (polar inline + SSO/(I=63°) inline/pendulum/cartwheel)

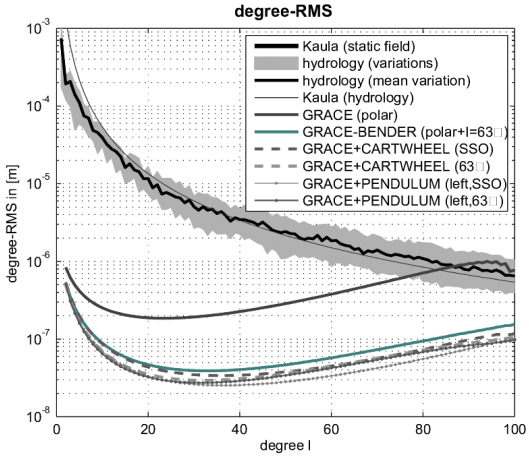

Figure 20: Degree-RMS of mixed Bender-configurations

Filtering on the sphere

The processing of time-variable gravity field data from GRACE satellites has renewed the interest in filtering on the sphere. The unfiltered data from GRACE has a characteristic stripe-like error structure, which completely dominates the signal. Different types of filters have been designed to recover the signal from noisy data, but the central problem has been the choice of the filter. In other words, a typical user has to dig through a basket full of filters to choose appropriate filter. Choosing the filter is further complicated by the fact that there are no standard guidelines to choose the filters and to assess their performance. As a first step towards developing performance measures for assessing filters, it is essential to understand the filtering mechanism of the filters.

Filtering a field on the sphere can be carried out by designing suitable filters either in the spatial or spectral domain. Here, spectral domain refers to the representation of the function on the sphere in terms of spherical harmonics. A general filter kernel on the sphere arises from a normalized weighting function - also known as two-point function, whose weights are determined by the (spherical) distances and directions between the filter kernel location and other points on the sphere. Then the filtered value of the field at the filter kernel location is obtained by averaging the product of the field with the filter kernel. This is the spatial side of filtering, which can also be performed in the spectral domain.

In the brief explanation of filtering provided above, it must be clear that the parameters that control the weights of the filter are the location (latitude and longitude) of the filter kernel and the distances and directions between other points. A variety of filter kernels can be designed by playing around (restricting) with these three parameters: location-independent (homogeneous), direction-independent (isotropic), and distance-independent. Distance-independent kernels are

possible, but they do not serve any purpose in the framework of GRACE data analysis and so it will not be discussed any further. Now that the parameters are well-known the classification can be visualized as a matrix as shown in Table 3.

		Isotropy	Anisotropy
Homogeneity		Distance	Distance and direction
Inhomogeneity	Longitude-independent	Latitude and distance	Latitude, distance and direction
	Location-dependent	Latitude, longitude and distance	Latitude, longitude, distance and direction

Table 3: Classification of filter kernels based on the three parameters location, distance and direction.

In Table 3, the kernels in anisotropic column can further be classified into symmetric and asymmetric kernels. Symmetry is inherent in isotropic kernels and hence, such a classification is not possible in their case. Therefore, there are about eight different classes of filter kernels that can be designed, and all of these different classes of filter kernels exhibit a unique spectral structure. However, only the homogeneous isotropic and longitude-independent inhomogeneous anisotropic filter kernels are widely used in the GRACE community due to their ease of design and use. Two examples are illustrated in Figure 21.

It should be noted that these filter kernels can further be classified in the ways they are designed. When the weighting functions are designed by the use of analytical functions then the filter kernels are called deterministic, and when they are designed by some statistical minimization principles then the kernels are called stochastic. Popular examples of deterministic and stochastic filter kernels are Gaussian homogeneous isotropic filter and Wiener filters, respectively.

The classification brings forth certain implications to the idea of convolution in the classical sense and performance assessment of filters. Convolution in the classical sense is only possible with the homogeneous kernels as they retain their spatial structure throughout the sphere. In fact, in older geodetic literature there is mention of convolution of type I, which uses the homogeneous isotropic kernels, and convolution of type II, which uses the homogeneous anisotropic kernels. In the case of performance assessment of filters, it is evident from the table that inhomogeneous filter kernels must be evaluated at a series of latitude or locations and thus brings a complexity towards comprehending the overall performance of the filter as well as visualization challenges.

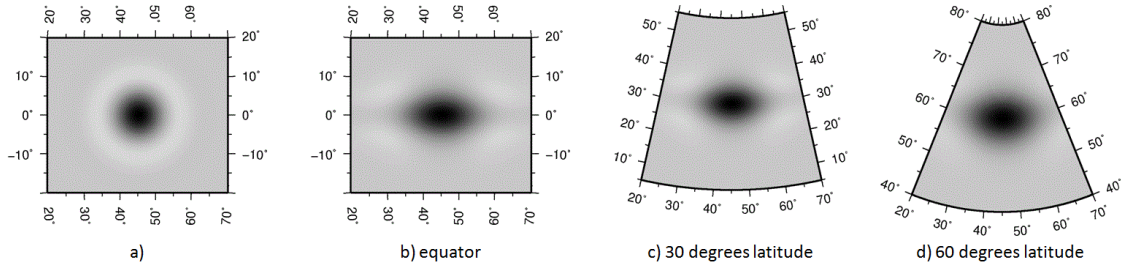

Figure 21: Examples of homogeneous isotropic (a) and longitude-independent inhomogeneous anisotropic filter kernels (b, c and d). Panel (a) is the homogeneous isotropic diffusion filter and panels (b), (c), (d) are Gaussian inhomogeneous anisotropic filters at the respective latitudes.

The global continental water balance using GRACE spaceborne gravimetry and high-resolution consistent geodetic-hydrometeorological data analysis

Over landmasses and for monthly time scales water storage changes from hydrology dS_H/dt correspond to mass change rates from GRACE dM/dt according to:

$$\frac{dS_H}{dt} = \frac{dM}{dt} = P - R - ET_a,$$

where P is the aggregated measured precipitation for the individual catchment, R is the total measured catchment runoff and ET_a is the spatial mean of actual evapotranspiration. On the other hand, water storage changes from the atmospheric water dS_A/dt are also comparable with rate of mass change from GRACE:

$$\frac{dS_A}{dt} = \frac{dM}{dt} = -\nabla\vec{Q} - R,$$

with the divergence of the vertically-integrated average atmospheric moisture flux $\nabla\vec{Q}$ over a catchment.

The error properties of all components of the continental and atmospheric water cycle including the correlations between the different products used for the mass change rates of GRACE, hydrology and hydro-meteorology are investigated and compared (Table 4).

	ERA-INTERIM	MERRA	NNRP1	NNRP2	OpAnl	GPCC v4	GPCP
GFZ	0.49±0.26	0.40±0.32	0.28±0.33	0.30±0.32	0.45±0.26	0.32±0.37	0.32±0.37
JPL	0.46±0.27	0.37±0.32	0.30±0.33	0.32±0.32	0.44±0.27	0.16±0.43	0.21±0.41
CSR	0.49±0.26	0.41±0.30	0.28±0.32	0.31±0.31	0.45±0.26	0.29±0.36	0.30±0.36
ITG	0.48±0.24	0.40±0.29	0.29±0.30	0.31±0.30	0.45±0.25	0.31±0.38	0.31±0.36
GPCC v4	0.63±0.35	0.54±0.39	0.17±0.49	0.19±0.48	0.62±0.37	1±0	0.82±0.13
GPCP	0.56±0.30	0.48±0.44	0.22±0.44	0.26±0.44	0.52±0.34	0.82±0.13	1±0

Table 4: Average ± standard deviation for correlations of $-\nabla\vec{Q} - R$ from different products of moisture flux divergence and P - R in case of ET_a for two products of precipitation versus dM/dt from different products of GRACE over catchments with available runoff data

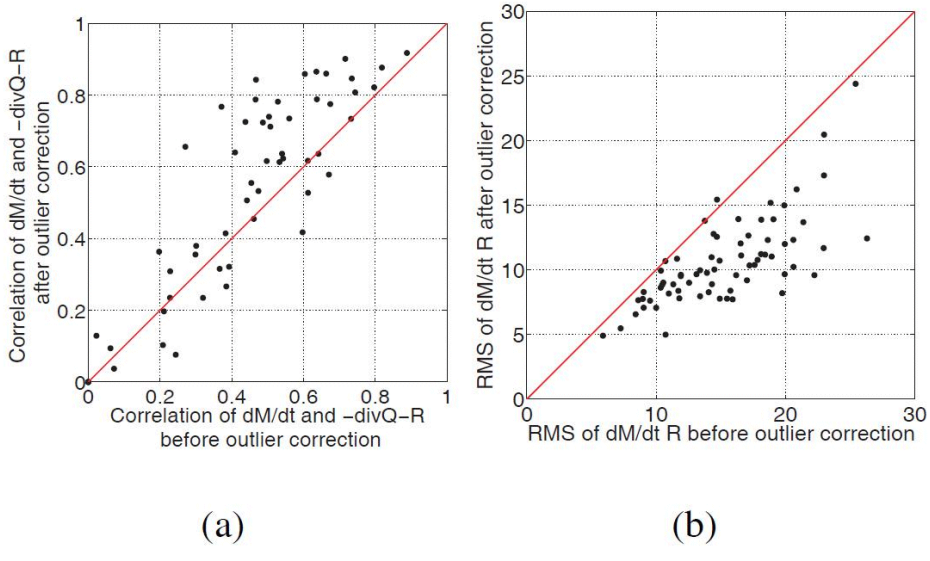

Figure 22: a) Scatter plot of correlation of dM/dt and $-\nabla\vec{Q} - R$ before and after outlier correction, b) Scatter plot of RMS of dM/dt residual before and after outlier correction

Comparisons with hydrologic and hydrometeorologic data reveal different types of GRACE uncertainties: outliers, long-range correlated unknown signals and random errors. The identification and correction of outlier leads to a considerable increase in correlation of GRACE signals and atmospheric data (up to 70%) and a reduction in RMS error (up to 40%).

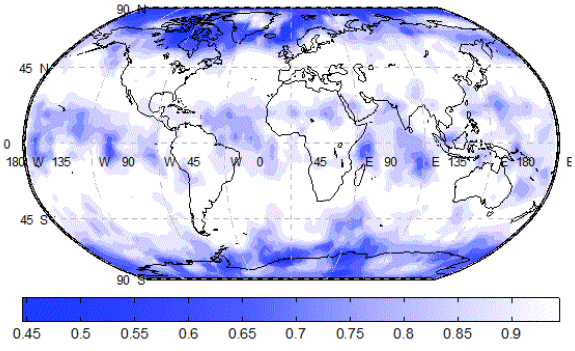

Figure 23: Ratio of RMS of responsible mode for long-range correlation

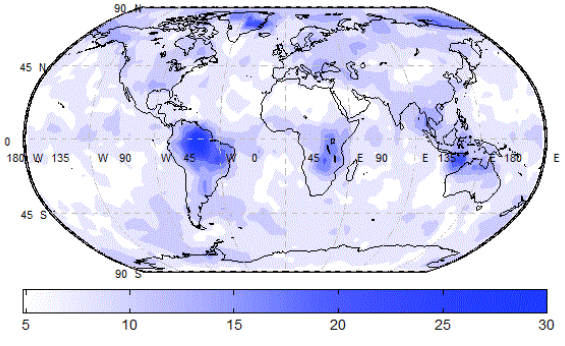

Figure 24: RMS of dM/dt residual after reduction of responsible mode for ICC from the data set

Signal contributions of unknown origin are identified in the mass derivative residuals, which imply a long-range correlation over the globe independent from oceans or land masses. EOF analysis of the mass derivative residuals allow to identify the corresponding signal with a functional form constant over the globe, which is modulated as sine over latitude. The same functional form is found in the zonal averages of the mass derivative residuals. Though the origin of this common signal is unknown so far, it can be eliminated from GRACE signal. As a result the long-range correlation is removed to a large extent.

The elimination of the spatially correlated signal leads to a further increase in correlation of GRACE signals with hydrologic and hydrometeorologic data (up to 30%) and thus is called *correlated error* until its origin is identified. As the mass derivative residual consists of climatic contributions and error, it can serve as an upper limit for the estimation of GRACE errors. The elimination of the correlated error also leads to a tremendous decrease in the RMS of the residual and thus in total noise especially for high latitudes and for equatorial oceans (up to 50%).

The accuracy of GRACE data and the sufficient availability of runoff data are the limiting factors for a statistically based, global scale regionalization of directly determined actual evapotranspiration. For the improvement of GRACE signals, EOF and CCA based filters are used for separation of physical components and errors within the GRACE residuals. For further increase in correlation with hydrology and hydrometeorology, integration of information from measured components of the water cycle into the filter scheme is considered.

As satellite altimetry has the potential to observe runoff, the feasibility of altimetry based discharge measurements for extending the discharge database discharge is studied. The feasibility study confirmed that an increase in number of gauged catchments by a factor of 3 can be expected.

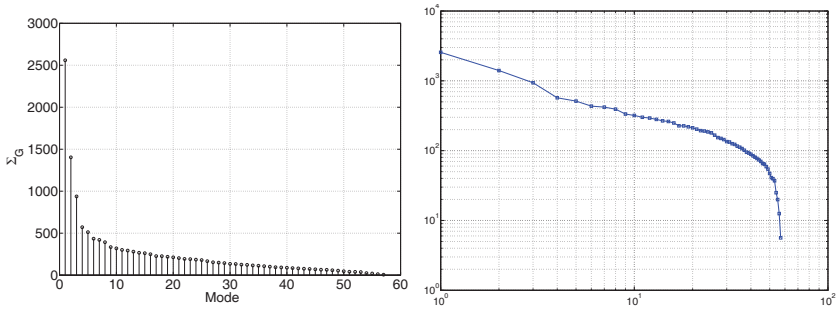

Figure 25: (a) Singular value spectrum of GRACE mass derivative time-series, (b) Log-log scale plot of singular value spectrum of GRACE

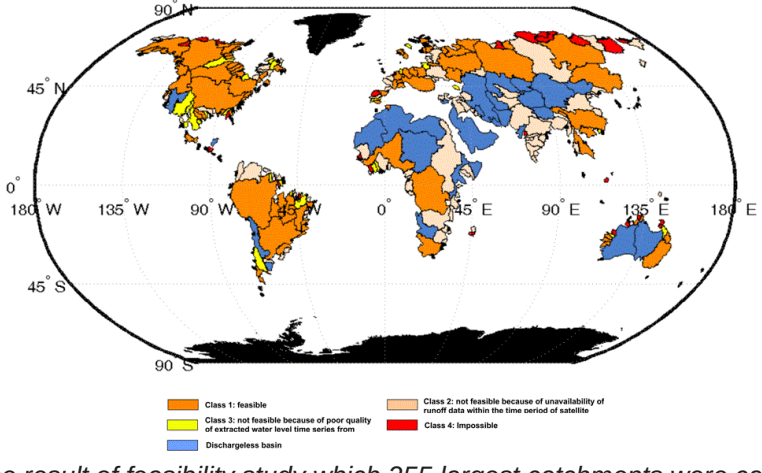

Figure 26: The result of feasibility study which 255 largest catchments were categorized into different classes

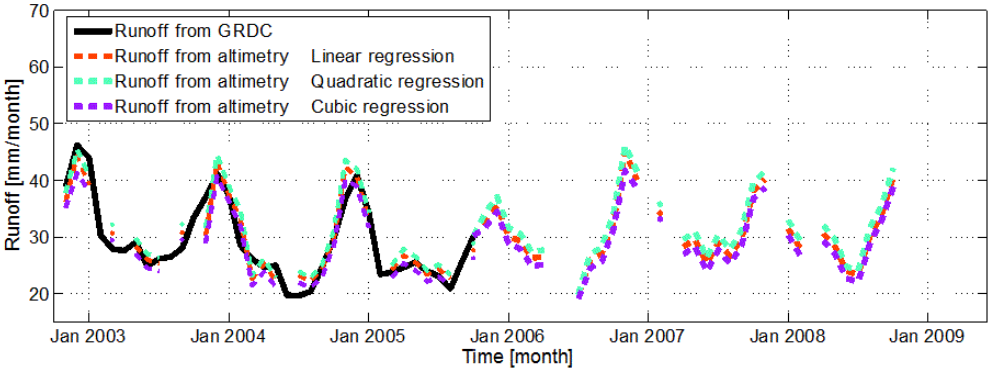

Figure 27: Runoff from insitu measurement (Nov. 2002 - Oct. 2005) and computed runoff from three derived level-discharge relationships for Congo basin

Wavelet decomposition for integral transformations

Galerkin's method

Many problems in regional gravity field modeling lead to an integral transformation

$$S(\vec{x}) = \int \int K(\vec{x}, \vec{y}) s(\vec{y}) d\vec{y}$$

where $S(\vec{x})$ denotes the solution at the evaluation points, $s(\vec{y})$ represents the data at the observation points and $K(\vec{x}, \vec{y})$ is the kernel of the transformation. In two-dimensional planar approximations some of these integrals can be solved by FFT techniques, while in general a numerical quadrature is necessary.

The FFT techniques are generalized by Galerkin's method, representing the signal and the data in a linear combination of orthonormal base functions:

$$S(\vec{x}) = \sum_{k=1}^{n} \beta_k \psi_k(\vec{x}), s(\vec{y}) = \sum_{j=1}^{n} \alpha_j \varphi_j(\vec{y})$$

Inserting the summations into the integral and using the orthogonality of the base functions a linear system

$$\vec{\beta} = A\vec{\alpha}$$

is achieved, where the elements of the matrix are given by

$$(A)_{jk} = \int\int\Big(\int\int K(\vec{x},\vec{y})\varphi_j(\vec{y})d\vec{y}\Big)\psi_k d\vec{x}$$

It should be mentioned, that the elements depend only on the base functions and the kernel, but not on the signal itself. Using the Fourier series for both base functions the matrix becomes diagonal, while in general a full matrix is generated.

Wavelet approach

One-dimensional example

In numerical evaluations the base functions are often constant for a particular area and so the integrals form a wavelet decomposition of the kernel and the data with the rectangular Haar wavelet (cf. Figure 28). In these decompositions the functions are separated into a main part, which is modeled by the scaling function and a difference described by the wavelet. The iterated analysis can be realized by the application of filter coefficients.

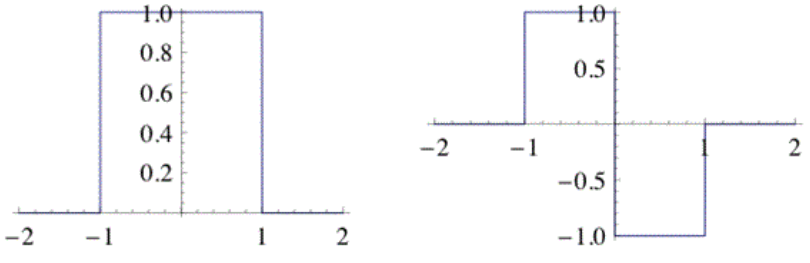

Figure 28: One-dimensional Haar wavelet (right) and scaling function (left)

In a one-dimensional example the normal distribution is chosen as kernel and the Haar wavelet as base function. Figure 29 visualizes the kernel and its approximation by the wavelet decomposition of order 2.

In case of 6 observations the Galerkin matrix contains 36 elements, but almost half of them are negligible for the computation (cf. Figure 30). The matrix can further be compressed by iterating the wavelet decomposition or by using orthogonal wavelets of higher order.

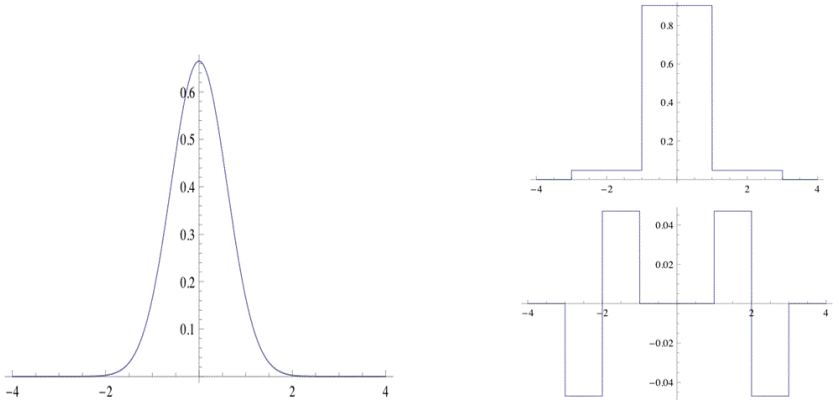

Figure 29: Normal distribution and its wavelets decomposition of order 2

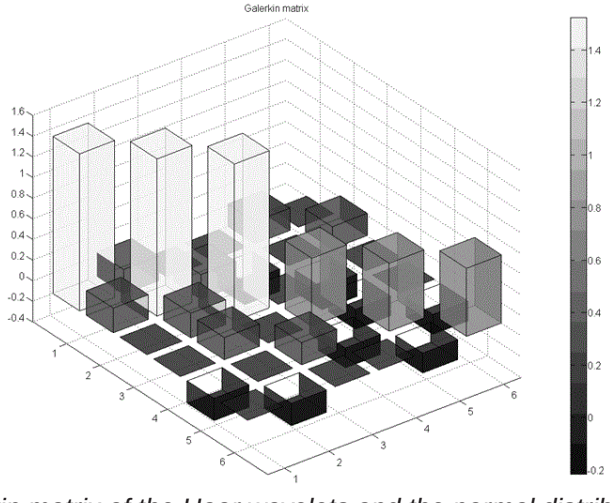

Figure 30: Galerkin matrix of the Haar wavelets and the normal distribution kernel for 6 observations

Two-dimensional application

In the simulation study a two dimensional field of gravity anomalies and the corresponding disturbing potential is created (cf. Figure 31). The potential can be recovered from the anomalies by the planar Stokes integral, either by a numerical quadrature or the wavelet decomposition.

In both methods the Galerkin matrix is computed for a comparison. It turned out that in the numerical quadrature only 88 % of the elements are smaller than the 5% threshold of the maximum. In

the iterative wavelet decomposition this value increases to 97%, 99.6% and 99.95 % in the third iteration. Only the remaining 0.05 % of the entries are necessary to compute a solution, which differs only by a RMS of 4.6 mm compared to the uncompressed values.

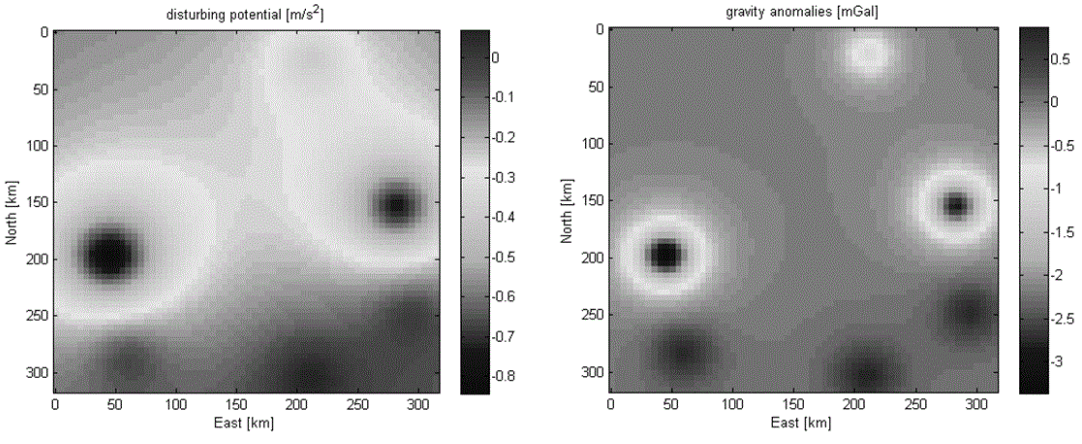

Figure 31: Gravity anomalies and disturbing potential

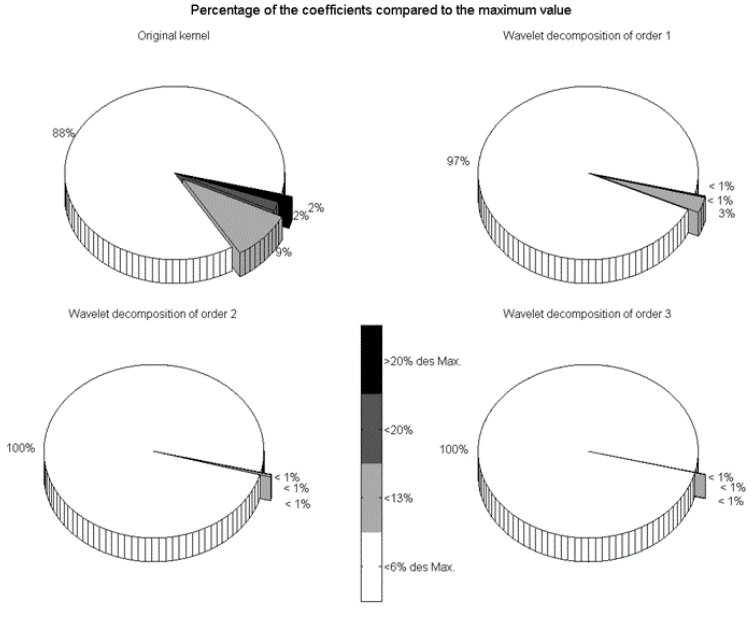

Figure 32: Relative values of the Galerkin matrix for the numerical quadrature (left) and the wavelet decomposition (right) as pie charts.

Development of a windshield for gravimetric observations

Gravimetric observations are affected by wind causing a higher noise level as high-frequency vibrations are introduced. Especially on unstable ground this effect can quickly exceed 10 μGal. The Guide to High Precision Land Gravimeter Surveys by Scintrex Limited (August 1995) suggests to use a simple windshield, e.g. a piece of cardboard or an umbrella, to remove this unnecessary source of noise. Experience shows that these measures are inadequate as on the one side the wind is frequently turning and thus makes the umbrella only a limited protection and on the other hand the cardboard is inconvenient to handle and not very resistant during transportation. Therefore, the aim is to design a windshield which is stable, light-weighted, foldable, height-adjustable giving a 360° protection from wind. The concept and the implementation are shown in Figure 33.

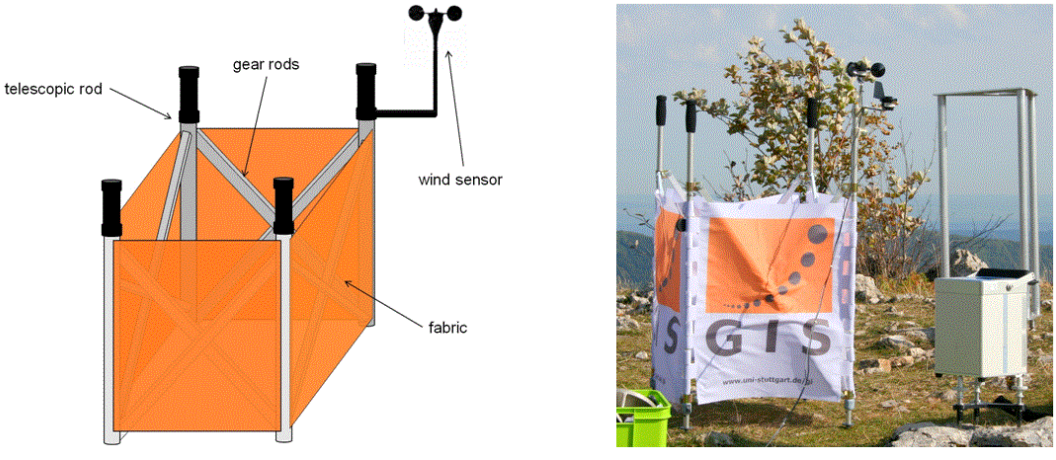

Figure 33: Concept of the windshield (left) and the implementation (right); the Scintrex CG-5 gravimeter and the gradient tripod are also visible on the right.

The windshield consists of a metal frame covered by a wind-resistant fabric. The frame is made of vertical rods, which are height-adjustable and equipped with handles. The stability of the system is ensured by four x-shaped gear rods. The center of the rods is a pivoting point which allows the windshield to be folded horizontally. The dimensions are 60cm x 60cm x 114cm (W x D x H) giving the operator enough space to adjust the settings of the gravimeter inside the windshield. The overall weight is approximately 4 kg which is light enough to be easily transportable but heavy enough to withstand wind gusts up to 35 km/h ($\sim$ 5 Bft.). If desired the windshield can be equipped with a wind sensor. The full setup is shown in the right panel of Figure 33 (including the wind sensor).

In order to test the influence of the wind, test measurements were taken with the Scintrex CG-5 in September 2010 at the Roßberg, Reutlingen, Baden-Württemberg. Two different setups were used. The first one places the gravimeter on its tripod on a solid ground resulting in a stable

setup. The second one is on top of the gradient tripod which is also visible in the background of the right panel of Figure 33. This setup simulates an unstable ground as the gradient tripod is highly sensitive to wind. Measurements are taken as averages of 57 seconds. Corrections for tides are applied and the seismic filter is set to active. This filter is able to handle vibrations, e.g. caused by wind or seismic activities, by rejecting outliers based on a 3σ-criterion. Figure 34 shows the result of the test. On the top, standard deviations given by the instrument are shown. In the middle, the average wind speed is denoted by the black line. The two gray lines are the maximum and minimum wind speed during the 57 seconds of the measurement. The bottom panel shows the number of rejections.

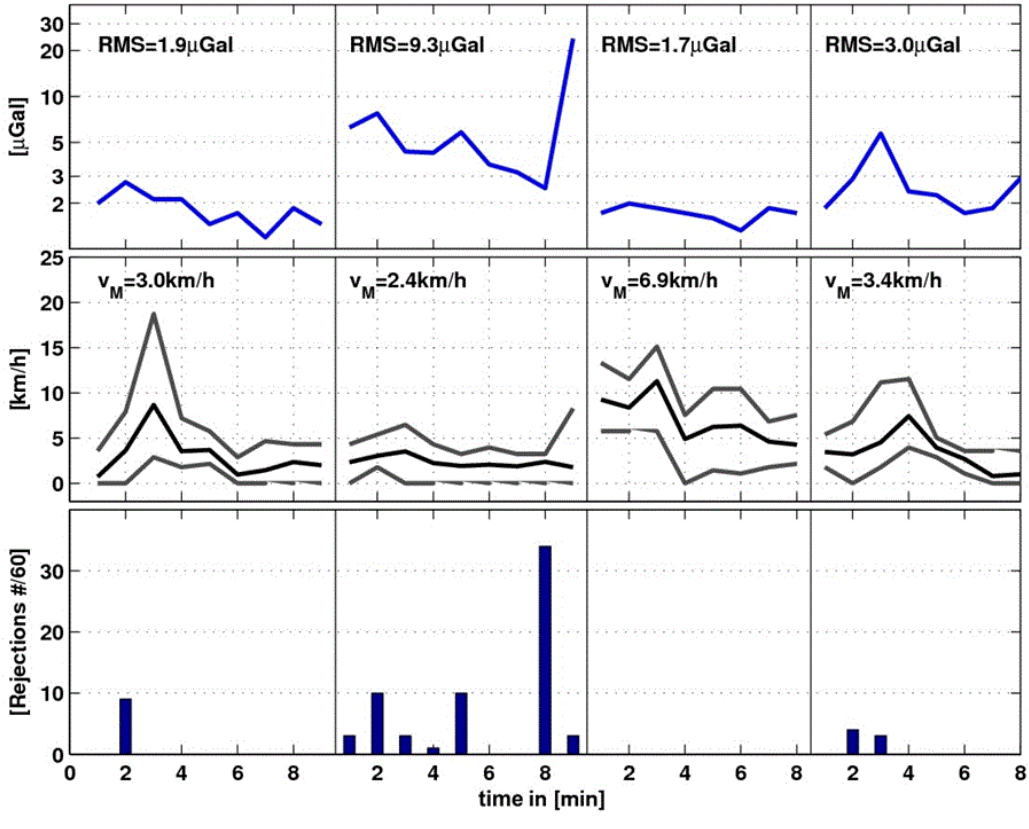

Figure 34: Standard deviation on the top, wind speed in the middle and number of rejections at the bottom; the setup is from left to right: setup without windshield on the ground, setup on the upper level of the gradient tripod without windshield, observation on the ground with windshield and observation with the windshield on the upper level of the gradient tripod

The left most column of the figure shows the results of the measurement on the ground level without windshield. Wind speed was moderate with an average of 3 km/h having a single wind gust of 20 km/h. The RMS of the measurement is 1.9 μGal. The wind gust was intercepted by the seismic filter rejecting the measurements during the event. The second column shows the measurements of the gravimeter on top of the gradient tripod but without the windshield. During this period the wind was calm with no wind gusts. Nevertheless, the gentle breeze still caused a by the factor 5 increased RMS and a high number of rejections due to the instability of the setup. Obviously, the seismic filter is able to handle single wind gusts but not longer periods of wind activity exceeding the filter length. The third column shows the setup on the ground with the windshield installed. Wind speed doubled compared to the left most panel but the RMS is still lower than in the setup without windshield. No measurements were rejected thus already proving the benefit of the windshield. The effect is even more prominent in the fourth panel showing the observations on the top of the gradient tripod and with the windshield. The RMS is cut third although the average wind speed increased by 50% compared to the setup without the windshield. Additionally, there are almost no rejections resulting in a higher reliability of the observations.

In conclusion, the usage of a windshield is beneficial in any setup as it is able to remove high-frequency noise caused by wind. Single wind gusts can be handled by the seismic filter of the instrument but for longer periods of wind activity only a windshield gives proper protection. The concept developed here has proven to fulfill all the requirements and eliminates the influence of the wind with little additional effort enabling gravimetric observations of the highest accuracy.

Theses

Diploma/Master Theses

(http://www.uni-stuttgart.de/gi/education/dipl/diploma_theses.en.html)

KÖRNER M: Untersuchungen zur gravimetrischen Inversion mittels genetischer Algorithmen (Gravimetric Inversion using Genetic Algorithms)

KUSARI A: Comparison of optimal Kalman-filters and the conventional Hatch-filter for carrier smoothed code processing (Vergleich zwischen optimalen Kalman-Filtern und konventionellem Hatch-Filter für die Verarbeitung von trägergeglätteten Code-Beobachtungen)

ROTH M: GOCE data analysis: Optimized brute force solutions of large-scale linear equation systems on parallel computers (GOCE Datenanalyse: Optimierte „brute force“ Lösungen großer linearer Gleichungssysteme auf Parallelrechnern)

SCHEIDER A: Nachweis einer vulkanischen Struktur auf der Schwäbischen Alb mittels gravimetrischer Messungen und unterstützender Höhenbestimmung (Detection of a volcanic structure in the Swabian Alb by gravity measurements with additional determination of heights)

SCHMID S: Assessing hydrological changes in the Murray-Darling Basin (Abschätzung hydrologischer Änderungen im Murray-Darlin Becken)

XIANG C: A Geodetic Approach to Euler Deconvolution

Study Theses

(http://www.uni-stuttgart.de/gi/education/dipl/study_reports.en.html)

FRIEDERICHS T: Analysis of Geodetic Time Series Using Allan Variances (Analyse Geodätischer Zeitreihen mittels Allan-Varianzen)

GERST S: Noise Performance of the Modernized GPS- and GALILEO-Systems (Rauschverhalten der modernisierten GPS- und GALILEO-Systeme)

LORENZ CH: Photography-aided gravity modeling of solid bodies (Fotografisch unterstützte Schweremodellierung ausgedehnter Körper)

Publications

(http://www.uni-stuttgart.de/gi/research/index.en.html)

Refereed Journal Publications

ARDALAN A, R KARIMI AND E GRAFAREND: A new reference equipotential surface and reference ellipsoid for the planet Mars. Earth Moon Planet 106 (2010) 1-13, DOI 10.1007/s11038-009-9342-7

RICHTER B, J ENGELS AND E GRAFAREND: Transformation of amplitudes and frequencies of precession and nutation of the Earth's rotation vector to amplitudes and frequencies of diurnal pole motion. Journal of Geodesy 84 (2010) 1-18, DOI 10.1007/s00190-009-0339-9

VISSER PNAM, N SNEEUW, T REUBELT, M LOSCH AND T VAN DAM: Space-borne gravimetric satellite constellations and ocean tides: aliasing effects. Geophysical Journal International 181 (2010) 789-805, doi: 10.1111/j.1365-246X.2010.04557.x

Other Refereed Contributions

BAUR O, J CAI AND N SNEEUW: Spectral approaches to solving the polar gap problem. In: Flechtner F, T Gruber, A Güntner, M Mandea, M Rothacher, T Schöne, J Wickert (Eds.): System Earth via Geodetic-Geophysical Space Techniques, Springer Berlin Heidelberg 2010, pp. 243-253, doi: 10.1007/978-3-642-10228-8_19

BAUR O, M KUHN AND WE FEATHERSTONE: GRACE-derived linear and non-linear secular mass variations over Greenland. In: Sansò F (Ed.): Proceedings VII. Hotine Marussi Symposium, Springer Berlin Heidelberg New York, in press

GRAFAREND E, Z MARTINEC AND M KLAPP: Spacetime modelling of the Earth's gravity field by ellipsoidal harmonics. In: Freeden W, NM Zuhair and T Sonar (Eds.): Handbook of Geomathematics, 1st ed., part 3, Springer Heidelberg 2010, pp 159-252, DOI 10.1007/978-3-642-01546-5_7

KELLER W: A Geometric Perspective to the Boundary Value Problem of Physical Geodesy. In: Holota P (Ed.): Mission and Passion: Science. A volume dedicated to Milan Bursa on the occasion of his 80th birthday, Prague, Czech Republic, 2009, pp 125-135

REUBELT T, N SNEEUW AND MA SHARIFI: Future Mission Design Options for Spatio-Temporal Geopotential Recovery. In: Mertikas SP (Ed.): Gravity, Geoid and Earth Observation. IAG Commission 2: Gravity Field, Chania, Crete, Greece, 23.-27.6.2008. International Association of Geodesy Symposia, Vol. 135, pp 163-170, Springer, Berlin, Heidelberg, 2010

ROTH M, O BAUR AND W KELLER: Tailored usage of the NEC SX-8 and SX-9 systems in satellite geodesy. In: Nagel WE, DB Kröner, MM Resch (Eds): High Performance Computing in Science and Engineering '10, Springer Berlin Heidelberg, in press

WEIGELT M, N SNEEUW AND W KELLER: Evaluation of EGM2008 by Comparison with Global and Local Gravity Solutions from CHAMP. In: Mertikas SP (Ed.): Gravity, Geoid and Earth Observation. IAG Commission 2: Gravity Field, Chania, Crete, Greece, 23.-27.6.2008. International Association of Geodesy Symposia, Vol. 135, pp 497-504, Springer, Berlin, Heidelberg, 2010

Non-refereed Contributions

BAUR O, N SNEEUW, J CAI AND M ROTH: GOCE data analysis: realization of the invariants approach in a high performance computing environment. Proceedings of the ESA Living Planet Symposium, Bergen, Norway, 28.6.-2.7., ESA SP-686.

CAI J, O BAUR AND N SNEEUW: GOCE gravity field determination by means of rotational invariants: first experiences. GEOTECHNOLOGIEN Science Report Nr. 17 „Observation of the System Earth from Space", 62-69

VARGA P, F KRUMM, F. RIGUZZI, C DOGLIONE, B SÜLE, K WANG AND GF PANZA: Earthquake Energy Distribution along the Earth Surface and Radius. ICTP Publication IC/2010/055. The Abdus Salam International Centre for Theoretical Physics

Poster Presentations

CAI J, O BAUR AND N SNEEUW: GOCE gravity field determination by means of rotational invariants: first experiences. BMBF Geotechnologien Statusseminar: „Erfassung des Systems Erde aus dem Weltraum III", Bonn (4.10.)

IRAN POUR S, N SNEEUW AND T REUBELT: Assessments of gravity recovery simulations of future satellite missions by EOF and Canonical Correlation Analysis (CCA). EGU General Assembly, Vienna, Austria (2.-7.5.)

IRAN POUR S, N SNEEUW AND T REUBELT: Geodetic Error Assessment Tools in the FGM project. BMBF Geotechnologien Statusseminar: „Erfassung des Systems Erde aus dem Weltraum III“, Bonn (4.10.)

KUHN M, S SCHMID, D RIESER, I ANJSMARA, O BAUR AND W KELLER: Monitoring mass transport in the Murray-Darling basin, Australia, using GRACE time-variable gravity, TRMM precipitation and river level/flow observations, Second International Symposium of the International Gravity Field Service, Fairbanks, Alaska, USA (20.-22.9.)

REUBELT T, N SNEEUW, W FICHTER AND J MÜLLER: The German joint research project „concepts for future gravity satellite missions“. EGU General Assembly, Vienna, Austria (2.-7.5.)

SCHLESINGER R, N SNEEUW, R ASAL UND C NWOKE: Vorläufige Analyse zum Schweresignal im Hebungsgebiet Staufen. Geodetic Week, Cologne, Germany (5.-7.10.)

TOURIAN MJ, J RIEGGER, B DEVARAJU AND N SNEEUW: Outlier detection and correction for GRACE data to improve the continental water balance. EGU General Assembly, Vienna, Austria (2.-7.5.)

TOURIAN MJ, N SNEEUW AND J RIEGGER: Feasibility study of extracting runoff data from satellite altimetry over continental surface waters. EGU General Assembly, Vienna, Austria (2.-7.5.)

TOURIAN MJ, N SNEEUW, J RIGGER AND A BARDOSSY: Extracting River Discharge from Satellite Altimetry. Altimetry for oceans and hydrology 2010. Lisbon, Portugal (18.-22.10)

WEIGELT M UND W KELLER: Numerische Aspekte bei der Berechnung von GRACE Schwerefeldern mit Hilfe des Ansatzes der differentiellen Gravimetrie. Geodetic Week, Cologne, Germany (5.-7.10.)

Conference Presentations

BAUR O AND N SNEEUW: Assessing Greenland ice mass loss by means of point-mass modelling: methodology and results, Second International Symposium of the International Gravity Field Service, Fairbanks, Alaska, USA (20.-22.9.)

BAUR O, M KUHN AND WE FEATHERSTONE: Global assessment of GRACE mass-change estimates, Second International Symposium of the International Gravity Field Service, Fairbanks, Alaska, USA (20.-22.9.)

BAUR O, N SNEEUW, J CAI AND M ROTH: GOCE data analysis: realization of the invariants approach in a high performance computing environment. ESA Living Planet Symposium, Bergen, Norway (28.6.-2.7.)

BROCKMANN JM, O BAUR, J CAI, A EICKER, B KARGOLL, I KRASBUTTER, J KUSCHE, T MAYER-GÜRR, J SCHALL, W-D SCHUH, A SHABANLOUI AND N SNEEUW: Real data analysis GOCE Gravity field determination from GOCE. BMBF Geotechnologien Statusseminar: „Erfassung des Systems Erde aus dem Weltraum III“, Bonn (4.10.)

BROCKMANN JM, O BAUR, J CAI, A EICKER, B KARGOLL, I KRASBUTTER, J KUSCHE, T MAYER-GÜRR, J SCHALL, W-D SCHUH, A SHABANLOUI AND N SNEEUW: REAL-GOCE: Gravity field determination from GOCE. BMBF Geotechnologien Statusseminar: „Erfassung des Systems Erde aus dem Weltraum III“, Bonn (4.10.)

CAI J: Bootstrap method and its application to the hypothesis testing in GPS mixed integer linear model. 2010 International Symposium on GPS/GNSS, Taipei, Taiwan (26.-28.10.)

CAI J: Optimal solutions to geodetic inverse problems in statistical and numerical aspects. Geodetic Week, Cologne, Germany (5.-7.10.)

DEVARAJU B, N SNEEUW, MJ TOURIAN, J RIEGGER, B FERSCH AND H KUNSTMANN: Assimilating GRACE, hydrology and hydro-meteorology datasets for estimating monthly water storage changes over continents. EGU General Assembly 2010, Vienna, Austria (2.-7.5.)

KUHN M, O BAUR AND WE FEATHERSTONE: Accounting for leakage effects in GRACE-derived mass estimates, GRACE: Science outcomes and future prospects. Canberra, Australia (26.5.)

ROESE-KOERNER L, B DEVARAJU, W-D SCHUH AND N SNEEUW: Quality description of inequality constrained least-squares estimates. Geodetic Week, Cologne, Germany (5.-7.10.)

ROTH M, O BAUR AND W KELLER: Tailored usage of the NEC SX-8 and SX-9 systems in satellite geodesy. High Performance Computing in Science and Engineering - the 13th Results and Review Workshop of the HLRS, Stuttgart (4.-5.10.)

SNEEUW N: Future Gravity Missions. BMBF Geotechnologien Statusseminar: „Erfassung des Systems Erde aus dem Weltraum III“, Bonn (4.10.)

TOURIAN MJ, B DEVARAJU, N SNEEUW AND J RIEGGER: Canonical Correlation Analysis (CCA) of GRACE, hydrological and hydro-meteorological signals. Geodetic Week, Cologne, Germany (5.-7.10.)

TOURIAN MJ, J RIEGGER, B DEVARAJU AND N SNEEUW: Investigation on Inter Cell Correlations of GRACE monthly solutions over the globe. EGU General Assembly, Vienna, Austria (2.-7.5.)

WEIGELT M UND R SCHLESINGER: Über den Einsatz eines Windschutzes bei gravimetrischen Messungen. Geodetic Week, Cologne, Germany (5.-7.10.)

Books

AWANGE J, E GRAFAREND, B PALÁNCZ AND P ZALETNYIK: Algebraic Geodesy and Geoinformatics. 2nd ed., 377 pages, Springer, Berlin, Heidelberg 2010

Guest Lectures and Lectures on special occasions

AUS DER BEEK T (Center for Environmental Systems Research, Universität Kassel): WaterGAP - a global hydrology and water use model (11.2.)

JIANG W (School of Geodesy and Geomatics, Wuhan University): Research Progress of Gravity Satellite Measurement in China (16.9.)

WANG Z (School of Geodesy and Geomatics, Wuhan University): Parallel Computation for Spherical Harmonic Analysis (16.9.)

ZHANG X (School of Geodesy and Geomatics, Wuhan University): Integer Ambiguity Fixing on Zero-Difference Carrier Phase for Precise Point Positioning (16.9.)

Lectures at other universities

CAI J

Linear Model - classical and modern estimation methods, Wuhan University, Wuhan, China (5.1.)

Geodetic data analysis in statistical and numerical aspects, Wuhan University, Wuhan, China (23.6.)

GRAFAREND EW

Lorant Eötvös and GOCE: satellite gradiometry, Hungarian Academy of Sciences, Budapest, Hungary (21.9.)

KELLER W

Application of SO(3) group representation for satellite-to-satellite tracking, Isfahan University, Iran (17.10.)

SNEEUW N

The Future of Satellite Gravimetry, Kozmikus Geodéziai Obszervatórium, Penc, Hungary (13.9.)

The Future of Satellite Gravimetry, Chinese Academy of Sciences, Beijing, China (21.6.)

Sampling the Earth from Orbit, PPP-Colloquium, Wuhan, China (23.6.)

The Future of Satellite Gravimetry, Shanghai Astronomical Observatory, Shanghai, China (28.6.)

Sampling the Earth from GOCE orbit, GOCE Summerschool 2010, Herrsching, Germany (31.5.-4.6.)

Research Stays

ANTONI M

Faculty of Aerospace Engineering, Delft University of Technology, The Netherlands (4.10.-26.11)

CAI J
School of Geodesy and Geomatics, Wuhan University, China (19.6-10.7.) GRAFAREND EW: Geodetic and Geophysical Research Institute, Seismological Observatory, Budapest, Hungary (20.9.-3.10)

KELLER W
Landwirtschaftliche Universität Wroclaw, Poland (8.3.-21.7.) Universität Teheran, Iran (12.-26.10.)

KRUMM F
Geodetic and Geophysical Research Institute, Seismological Observatory, Budapest, Hungary (22.-26.3.)

SNEEUW N
Geodetic and Geophysical Research Institute, Budapest, Hungary (12.-17.9.)
School of Geodesy and Geomatics, University of Wuhan, Wuhan, China (22.-25.6.)

Lecture Notes

(http://www.uni-stuttgart.de/gi/education/dipl/lecturenotes.en.html,
http://www.uni-stuttgart.de/gi/education/BSC/lecturenotes.en.html,
http://www.uni-stuttgart.de/gi/geoengine/lecturenotes.html)

GRAFAREND E AND F KRUMM
Kartenprojektionen (Map Projections), 238 pages

HAUG G
Grundstücksbewertung I (Real Estate/Property Valuation I), 28 pages
Grundstücksbewertung II (Real Estate/Property Valuation II), 11 pages

KELLER W
Dynamic Satellite Geodesy, 90 pages
Foundations of Satellite Geodesy, 51 pages
Observation Techniques in Satellite Geodesy, 50 pages

KRUMM F AND SNEEUW N
Adjustment Theory, 116 pages

KRUMM F
Map Projections and Geodetic Coordinate Systems, 161 pages
Mathematical Geodesy, 185 pages
Reference Systems, 152 pages

SCHÖNHERR H
Amtliches Vermessungswesen und Liegenschaftskataster (Official Surveying and Real Estate Regulation), 56 pages

SNEEUW N

Analytic Orbit Computation of Artificial Satellites, 90 pages
Geodesy and Geodynamics, 68 pages
Physical Geodesy (Measurement Techniques of Physical Geodesy, Modeling and Data Analysis in the Field of Physical Geodesy), 137 pages

WOLF D

Continuum Mechanics in Geophysics and Geodesy: Fundamental Principles, 100 pages

Participation in Conferences, Meetings and Workshops

CAI J

2010 International Symposium on GPS/GNSS, Taipei, Taiwan (26.-28.10.)
BMBF Geotechnologien Statusseminar „Erfassung des Systems Erde aus dem Weltraum III“, Bonn, Germany (4.10.)
Geodetic Week, Cologne, Germany (5.-7.10.)
GOCE Summer School (Workshop), Herrsching, Germany (30.5.-4.6.)
Joint PPP-Project Colloquium, Wuhan, China (23.6.)
REAL GOCE Project Meeting, München, Germany (15.-16.3.)
REAL GOCE Project Meeting, Stuttgart, Germany (23.9.)

DEVARAJU B

European Geosciences Union (EGU), General Assembly 2010, Vienna, Austria (3.-7.5.)
DFG-SPP1257 Workshop „Mass transport and mass distribution in system Earth“, Dipperz/Fulda, Germany (22.-24.2.)
DFG-SPP1257 Symposium, Review Meeting, Potsdam, Germany (12.-14.10.)
Geodetic Week, Cologne, Germany (5.-7.10.)

IRAN POUR S

BMBF Geotechnologien Statusseminar „Erfassung des Systems Erde aus dem Weltraum III“, Bonn, Germany (4.10.)
Project meeting 2 of „Zukunftskonzepte für Schwerefeld-Satellitenmissionen“ (Geotechnologies - Observation of the System Earth from Space III), GFZ, Oberpfaffenhofen, Germany (4.-5.3.)
Project meeting 3 of „Zukunftskonzepte für Schwerefeld-Satellitenmissionen“ (Geotechnologies - Observation of the System Earth from Space III), Kayser-Threde GmbH, Munich, Germany (7.-8.6.)

REUBELT T

BMBF Geotechnologien Statusseminar „Erfassung des Systems Erde aus dem Weltraum III“, Bonn, Germany (4.10.)
Final Meeting of the project „Assessment of a Next Generation Gravity Mission (NGGM) for monitoring the Variation of the Earth’s Gravity Field“ (ESA Contract 22643/09/NL/AF),

ESA/ESTEC, Noordwijk, Netherlands (25.11.)
Mission Architecture Review of the project „Assessment of a Next Generation Gravity Mission (NGGM) for monitoring the Variation of the Earth's Gravity Field" (ESA Contract 22643/09/NL/AF), ESA/ESTEC, Noordwijk, Netherlands (2.9.)
Progress Meeting 2 of the project „Assessment of a Next Generation Gravity Mission (NGGM) for monitoring the Variation of the Earth's Gravity Field" (ESA Contract 22643/09/NL/AF), TU Delft, Netherlands (24.3.)
Project meeting 2 of „Zukunftskonzepte für Schwerefeld-Satellitenmissionen" (Geotechnologies - Observation of the System Earth from Space III), GFZ, Oberpfaffenhofen, Germany (4.-5.3.)
Project meeting 3 of „Zukunftskonzepte für Schwerefeld-Satellitenmissionen" (Geotechnologies - Observation of the System Earth from Space III), Kayser-Threde GmbH, Munich, Germany (7.-8.6.)
Research period in China (Beijing, Wuhan, Shanghai) within the DAAD-PPP project „Future satellite gravity missions" (20.-29.6.)

SCHLESINGER R
Geodetic Week, Cologne, Germany (5.-7.10.)

SNEEUW N
BMBF Geotechnologien Statusseminar „Erfassung des Systems Erde aus dem Weltraum III", Bonn, Germany (4.10.)
DFG-SPP1257 Symposium, Review Meeting, Potsdam, Germany (12.-14.10.)
DFG-SPP1257 Workshop „Mass transport and mass distribution in system Earth", Dipperz/Fulda, Germany (22.-24.2.)
European Geosciences Union (EGU), General Assembly 2010, Vienna, Austria (3.-7.5.)
Festkolloquium zu Ehren von Prof. H. Drewes, Munich, Germany (26.4.)
Geodetic Week, Cologne, Germany (5.-7.10.)
GOCE Summer School, Herrsching a. A., Germany (31.5.-4.6.)

TOURIAN M
DFG-SPP1257 Symposium, Review Meeting, Potsdam, Germany (12.-14.10.)
DFG-SPP1257 Workshop „Mass transport and mass distribution in system Earth", Dipperz/Fulda, Germany (22.-24.2.)

WEIGELT M
Geodetic Week, Cologne, Germany (5.-7.10.)
GOCE Summer School, Herrsching a. A., Germany (31.5.-4.6.)
IAG Summer School on Reference Frames, Mytilene, Lesvos, Greece (7.-12.6.)

University Service

BAUR O
Chairman of the PR-Commission of the study course Geodesy & Geoinformatics

GRAFAREND E
- Member Faculty of Aerospace Engineering and Geodesy
- Member Faculty of Civil- and Environmental Engineering
- Member Faculty of Mathematics and Physics

SNEEUW N
- Associate Dean (Academic) Geodäsie & Geoinformatik and GEOENGINE, Stuttgart
- Member China Commission, International Affairs (IA)
- Member Examining Board of the Faculty of Aerospace Engineering and Geodesy, Stuttgart
- Member Senate Committee for Structural Development, Stuttgart
- Vice-Chair Examining Board of the Faculty of Aerospace Engineering and Geodesy, Stuttgart

Professional Service (National)

GRAFAREND E
- Emeritus Member German Geodetic Commission (DGK)

SNEEUW N
- Full Member Deutsche Geodätische Kommission (DGK)
- Chair DGK section „Erdmessung“
- Member Scientific Board of DGK
- Member Scientific Advisory Committee of DGFI
- Chair AK7 (Working Group 7), „Experimentelle, Angewandte und Theoretische Geodäsie“, within DVW (Gesellschaft für Geodäsie, GeoInformation und LandManagement)

Professional Service (International)

CAI J
- Luojia Professor at School of Geodesy and Geomatics, Wuhan University, China
- Member of the Institute of Navigation (ION, USA)
- Member of European Geosciences Union (EGU)

GRAFAREND E
- Elected Member of the Finnish Academy of Sciences and Letters, Finland
- Elected Member of the Hungarian Academy of Sciences, Hungary
- Member Royal Astronomical Society, Great Britain
- Corresponding Member Österreichische Geodätische Kommission (ÖGK)
- Member Flat Earth Society
- Elected Member Leibniz-Sozietät, Berlin
- Fellow International Association of Geodesy (IAG)

SNEEUW N
- Präsident IAG InterCommission Committee on Theory (ICCT)

Member Editorial board of Studia Geophysica et Geodaetica
Member Editorial board of Journal of Geodesy
Fellow International Association of Geodesy (IAG)

WEIGELT M
Member Inter-Commission Working Group (IC-WG2): „Evaluation of Global Earth Gravity Models“ (IAG)

Courses - Lecture/Lab/Seminar

Adjustment I, II (Krumm, Baur)	4/2/0
Advanced Mathematics (Keller, Devaraju)	3/2/0
Analytic Orbit Computation of Artificial Satellites (Sneeuw, Baur)	2/1/0
Coordinates and Reference Systems (Krumm, Reubelt)	1/1/0
Dynamic Satellite Geodesy (Keller, Reubelt)	1/1/0
Foundations of Satellite Geodesy (Keller)	1/1/0
Geodesy and Geodynamics (Sneeuw, Reubelt)	2/1/0
Geodesy and Geoinformatics (Sneeuw)	1/1/0
Geodetic Reference Systems (ICRS-ITRS) for Satellite Geodesy and Aerospace (Weigelt)	2/1/0
Geodetic Seminar I, II (Krumm, Sneeuw)	0/0/4
Geometric Data Processing (Keller)	1/1/0
Integrated Field Work Geodesy and Geoinformatics (Keller, Sneeuw)	10 days
Map Projections and Geodetic Coordinate Systems (Krumm, Baur)	2/1/0
Map Projections (Krumm)	1/1/0
Mathematical Geodesy (Krumm)	2/1/0
Measurement Techniques of Physical Geodesy (Sneeuw, Reubelt)	2/1/0
Modeling and Data Analysis in the Field of Physical Geodesy (Baur, Engels, Reubelt)	2/1/0
Observation Techniques and Evaluation Procedures of Satellite Geodesy (Weigelt, Baur)	1/1/0
Official Surveying and Real Estate Regulation (Schönherr)	2/0/0
Orbit Determination and Analysis of Artificial Satellites (Baur, Reubelt)	2/1/0
Physical Geodesy (Sneeuw, Devaraju)	2/1/0
Real-Estate/Property Valuation I, II (Haug)	2/1/0
Reference Systems (Krumm, Reubelt)	2/2/0
Satellite Geodesy Observation Techniques (Weigelt, Devaraju)	2/1/0
Satellite Geodesy (Keller)	2/1/0
Statistical Inference (Krumm, Baur)	2/1/0

Institute of Navigation

Breitscheidstrasse 2, D-70174 Stuttgart,
Tel.: +49 711 685 83400, Fax: +49 711 685 82755
e-mail: ins@nav.uni-stuttgart.de
homepage: http://www.nav.uni-stuttgart.de

Head of Institute

Prof. Dr.-Ing. A. K l e u s b e r g

Deputy: Dr.-Ing. Aloysius W e h r
Secretary: Helga M e h r b r o d t
Emeritus: Prof. em. Dr.-Ing. Ph. H a r t l

Staff

Dipl.-Ing. Doris B e c k e r	Navigation Systems
Dipl.-Ing. Xu F a n g	Navigation Systems
Dipl.-Ing. Michael G ä b	Navigation Systems
Dipl.-Geogr. Thomas G a u g e r	GIS Modelling and Mapping
Dipl.-Ing. René P a s t e r n a k	Remote Sensing
Dipl.-Ing. Bernhardt S c h ä f e r	Navigation Systems
Dipl.-Ing. Wolfgang S c h ö l l e r	Education/Navigation Systems
Dipl.-Ing. Alexandra S e i f e r t	Navigation Systems
M. Sc. Hendy S u h a n d r i	Navigation Systems
Dipl.-Ing. (FH) Martin T h o m a s	Laser Systems
Dr.-Ing. Aloysius W e h r	Laser Systems
Dipl.-Ing. Xue W e i	Inertial Navigation
Dr. Ing. Franziska W i l d - P f e i f f e r	Navigation Systems

EDP and Networking

Regine S c h l o t h a n

Laboratory and Technical Shop (ZLW)

Dr.-Ing. Aloysius W e h r (Head of ZLW)
Technician Peter S e l i g - E d e r
Electrician Sebastian S c h n e i d e r
Mechanician Master Michael P f e i f f e r

External teaching staff

Hon. Prof. Dr.-Ing. Volker L i e b i g - Directorate ESA
Hon. Prof. Dr.-Ing. B r a u n - RST Raumfahrt Systemtechnik AG, St.Gallen

Research Projects

Experiments with different inertial sensors for pedestrian indoor positioning

Pedestrian indoor positioning uses information from the human gait itself to correct inertial measurements for indoor applications. The characteristics of the human gait with its 60% swing time and 40% stance time in one gait cycle can be used to correct the determination of the velocities by applying zero-velocity updates (ZUPT) at detected stance phases. From the inertial raw data we detect the midstance, the relevant part of the stance phase. Among other sensors, we tested a hybrid MEMS sensor from Bosch, with a single gyroscope and dual accelerometer (SG-DA) integrated into one chip. The SG-DA sensor was attached to the ankle or foot of the pedestrian; one accelerometer pointing in the forward direction, the other accelerometer pointing in the upward direction. The measurement axis of the gyroscope was orthogonal with respect to the two accelerometers (see Fig. 1). The raw data is used to detect the stance phases, see in Fig. 2. At the stance phases pseudo measurements are applied to the velocities and the angle which replace and advance to original measurements and eliminate the drift in the resulting positions, see Fig. 3.

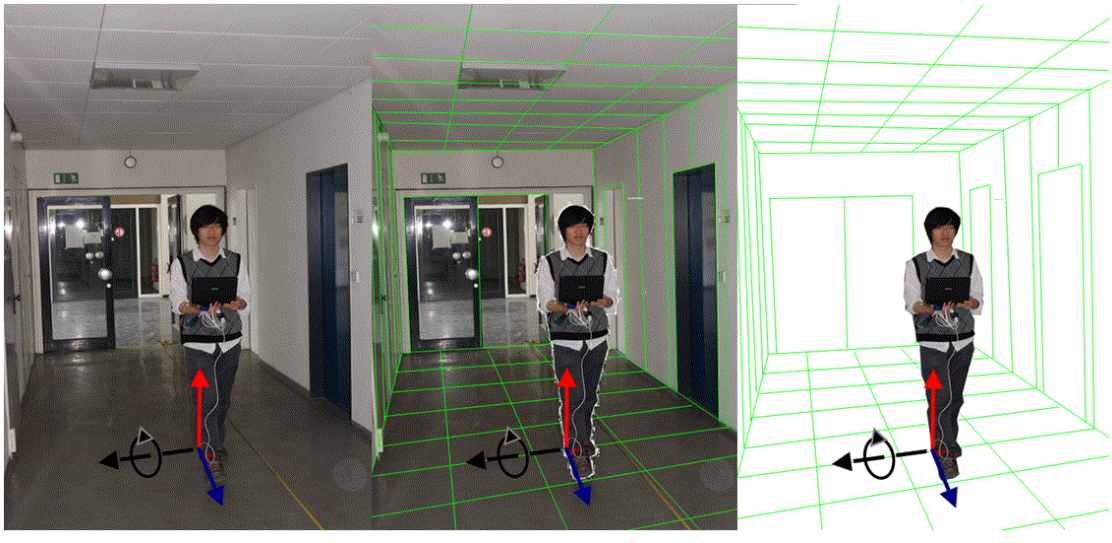

Fig. 1: SG-DA sensor at the right foot. Accelerations measured in front (blue) und upward (red) direction. Turn rates measures around the orthogonal axis with respect to the two accelerometers.

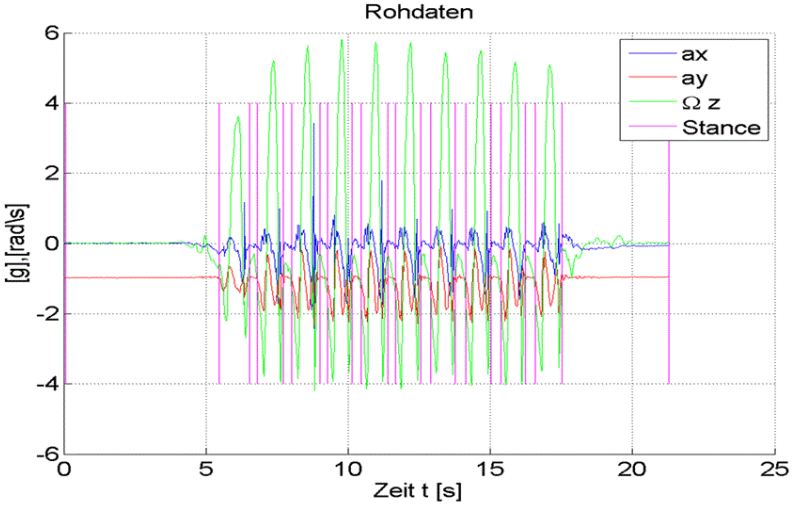

Fig. 2: SG-DA sensor raw data with automatically detected stance phases. Accelerations measured in front (blue) und downwards (red) direction are plotted in the unit g. Turn rate are plotted green in the unit rad/s.

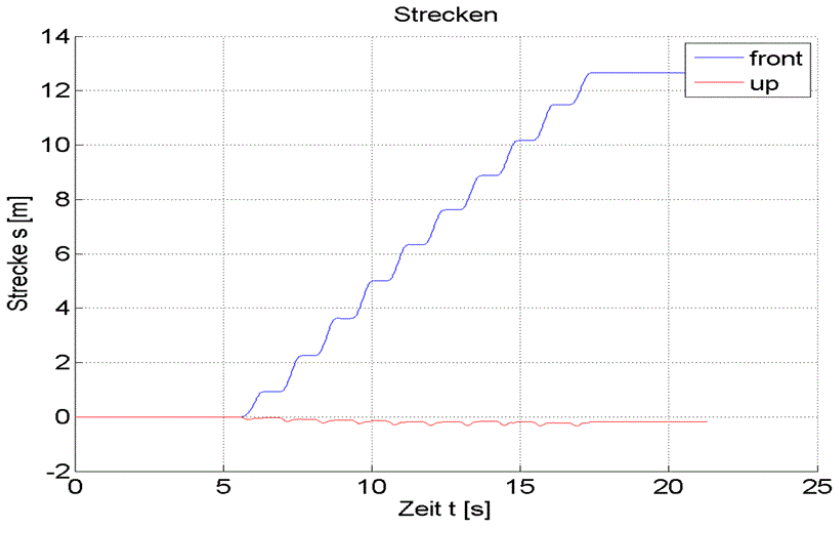

Fig. 3: Resulting positions in front (blue) and upward (red) directions.

μblox *4* Rennteam

In 2010 the Institute of Navigation was supporting the student racing team of the University of Stuttgart (Rennteam). A low-cost and light-weight positioning solution was developed which meets the requirements of horizontal coordinate accuracy better than one meter and high data rate of 10 Hz in a highly dynamic environment. Two customized receivers with μblox LEA-4T were implemented on a standard circuit board with additional controller area network (CAN) modules. Both receivers can be used as rover or base station. The rover will be connected with the CAN-bus of the car and the GPS observations will be logged to the CAN data logger. The base station can be operated with standard software on a laptop. The proof of concept was given by a Study Thesis and showed, that the requirements could be meet with freely available open source GPS analysis software. This also emphasizes the characteristics of the support, which should be mainly be done by students, as the Rennteam is a students' project. The cooperation will continue in 2011.

An Improvement of the Stochastic Model for Double-Difference GPS Observational Variance-Covariance Matrix (VCM)

Three levels of observation vc-matrix can be defined: the double-difference (DD) observations are assumed totally uncorrelated, hence the vc-matrix is considered to be an identity matrix. The second level is that the observations are only mathematically correlated. It means the DD observations are only uncorrelated within one epoch, and the correlation relations of the observations

remains the same for every epoch. The third level, which is closest to the reality is that the DD observations are correlated physically. The physical correlation is derived from stochastic properties of the observation. It is expected to represent unmodelled random behaviour during the observation (Fig. 4).

Teunissen (2004) suggested the use of elevation dependency to represent the physical correlation. However this method is not efficient for practical purposes, since it is a very time consuming process. Based on the work of Rabbany (1994), an algorithm using the observation vc-matrix model the physical correlation is presented. The algorithm takes temporal correlation into account. The correlation coefficient g(i) is defined by an exponential function.

Recovering the Surface Displacements Using Combined 1-Hz GPS and Strong-Motion Accelerometer

Traditionally strong-motion (SM) accelerometers are utilized to record the rapid movements of the Earth, which typically keeps for tens of seconds. Large drifts, however, often exist in the displacements derived from the accelerations due to offsets. In comparison to SM accelerometer 1-Hz GPS position estimates are directly sensitive to displacement, but many orders of magnitude less precise at high frequencies. With the availability of 1-Hz GPS position estimates and collocated seismic data from the 2003 Mw 8 Tokachi-Oki (Hokkaido) earthquake, it is possible to constrain the long-period instability of seismic displacement during integration of accelerations. A Least-Square Adjustment is constructed to integrate the accelerations into ground displacement and simultaneously to correct unpredictable offsets existing in the acceleration records. In this study the offsets are approximated as step function occurred at possible time in the acceleration records. The seismic data are weighted more heavily than the GPS data, since its digitization precision is 0.015 cm/sec^2 while the accuracies of GPS estimates used for this study are 4mm, 7mm and 15mm for east, north and vertical component. An example showing the result of the constrained integration is shown in Figure 5. The time shifts in the strong-motion time series due to the different distance to the epicenter still need to be explored in the future.

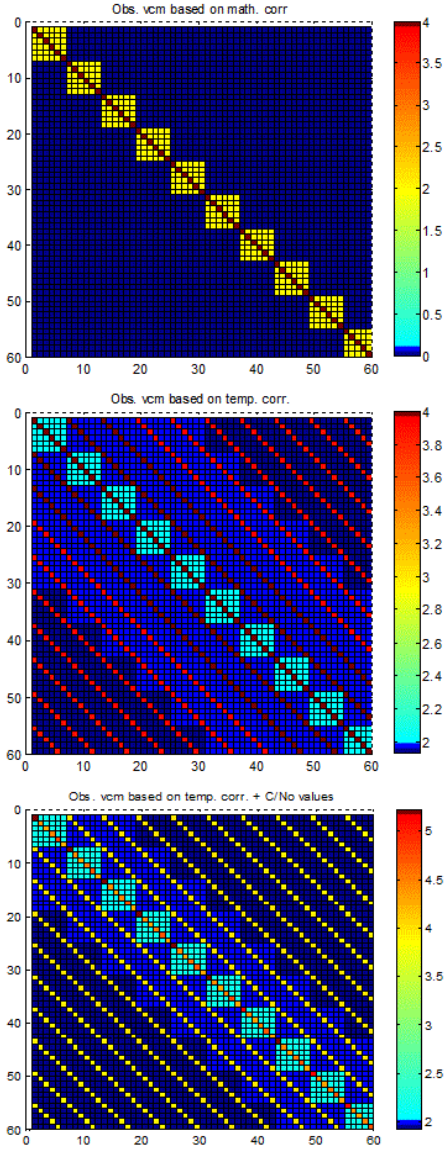

Figure 4: The variance-covariance matrices of observation with: mathematical correlation, mathematical+temporal correlation, mathematical+temporal correlation + C/N0 values of 6 DD in 10 epochs

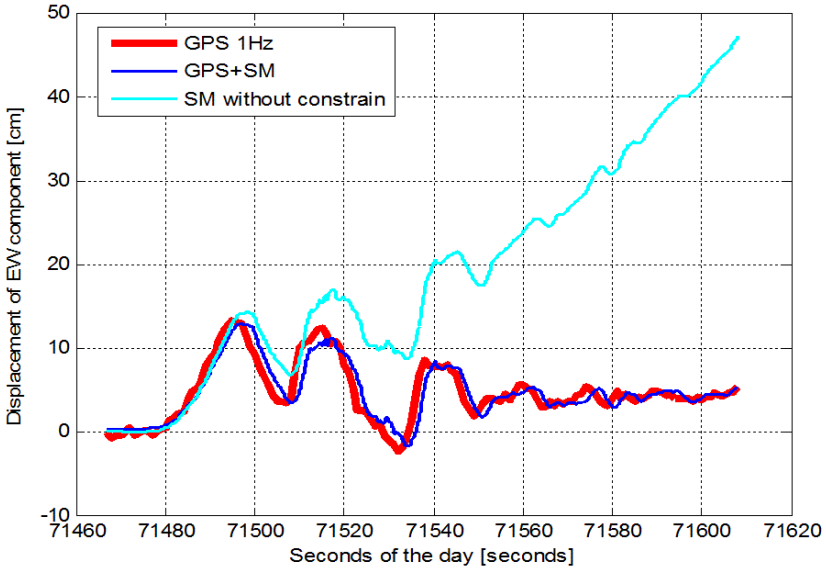

Figure 5: Displacement constrained by a combination of GPS and strong-motion data

Phenologocal Impact on a transferable classification concept for multitemporal TerraSAR-X-data (PI-X)

In early spring 2010 a project proposal within the framework of the TerraSAR-X Science Service System was submitted to the German Aerospace Center (DLR). A couple of weeks later the project proposal was accepted. In this context a package of TerraSAR-X data is guaranteed for free.

PI-X is designed to investigate the impact of the regional and interannual variations of the vegetation development on an automated land use classification, termed for three years. The main focus is in the vegetation covered land surface, with particular emphasis on the agricultural landscape. The variability of the vegetation development depends on different conditions of growth, caused by weather and relief. Due to the coexistence of different natural units, the state of Baden-Württemberg provides a possibility to investigate the above mentioned problem. 3 test sites were chosen in total, to guarantee an observable time shift within the vegetation development. As a start large amounts of data are necessary within in the scope of the project covering the whole vegetation period including the regional and interannual time shift between the test sites. During the project, one question to be answered is, how to schedule data acquisition of TerraSAR-X with the help of meteorological data. Further, another objective in this context is to seek timeframes during which

crops can be distinguished best. This will help to minimize the needed data. All works should result in automated and transferable classification method of the land use. Results can be used for the update of land use information systems at federal or federal state authorities and as an addition to the core or additional services in the framework of DeCover.

Diffuse Air Emissions in E-PRTR

The joint research project „Diffuse Air Emissions in E-PRTR (European Pollutant Release and Transfer Register)“ (EU ENV.C.4/SER/2009/0067), is carried out on behalf and on the account of European Commission - DG Environment and is elaborated in close co-operation between the Institute of Energy Economics and the Rational Use of Energy (IER), Universität Stuttgart and the Institute of Navigation, Universität Stuttgart (INS).

Within the project emission data from EMEP CEIP (European Monitoring and Evaluation Programme, Centre on Emission Inventories and Projections) in a 50x50km^2 grid resolution were re-projected and delivered for viewing on the E-PRTR web site (*http://prtr.ec.europa.eu/DiffuseSourcesAir.aspx*). The main project task, however, is the modelling of geographical information system (GIS) layers of spatially disaggregated emission of key pollutants (NO_x, SO_2, PM10, CO, CO_2) from key diffuse emission sources (transport activities, stationary commercial and residential combustion, diffuse industrial releases) and agricultural NH_3 and PM10 releases for the year 2008 using officially reported emission data from the countries to UNFCCC (United Nations Framework Convention on Climate Change and to the EU Greenhouse Gas Monitoring Mechanism) and UNECE (Convention on Long-Range Transboundary Air Pollution). The spatial scale of the modelled emission maps is a 5x5km^2 grid, covering the EU27 countries and the 4 EFTA countries Iceland, Norway, Liechtenstein, and Switzerland, i.e. close to about 30% of the surface of the globe (Figure 6). The delivered GIS layers are integrated into the E-PRTR register as a new feature and will be made available for viewing on the E-PRTR web site. It is also planned to make the final data sets available for data retrieval.

Further information:
on E-PRTR: *http://prtr.ec.europa.eu/Home.aspx*
on the project results (maps): *http://prtr.ec.europa.eu/DiffuseSourcesAir.aspx*
on methods: *http://147.67.243.36/Public/irc/env/e_prtr/library?l=/prtr_expert_meeting_2/*

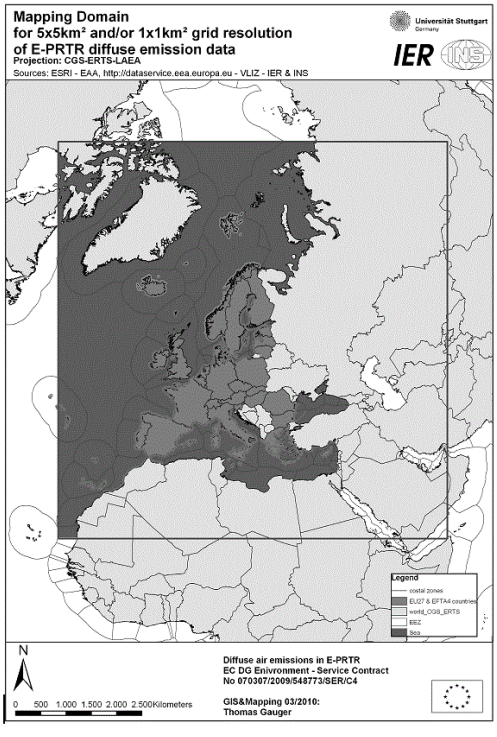

Fig. 6: Map extent of E-PRTR diffuse emission data

Assessment, Prognosis, and Review of Deposition Loads and Effects in Germany

The joint research project „Assessment, Prognosis, and Review of Deposition Loads and Effects in Germany“ (BMU/UBA FE-No 3707 64 200), is carried out on behalf of the German Federal Environment Agency (UBA) and on the account of Bundesministerium für Umwelt, Naturschutz und Reaktorsicherheit (BMU). Within the project national maps of air concentration levels and deposition loads (see Figure 7) are generated using measurement network data, additional model estimates and high resolution land use maps.

From modelled data sets high resolution maps of deposition loads and air concentration levels are calculated using GIS technique. The dose, in terms of deposition loads of air pollutants causing acidification and eutrophication in different forest and non-forest ecosystems in Germany, are compared to ecosystem sensitivity given as critical levels and modelled critical loads in order to provide an impact assessment in the form of exceedance maps for ecosystems. The trend of air pollutant input over time into the respective receptors on the national, regional, and local scale can be identified.

The joint project is elaborated in close co-operation between the Netherlands Organization for Applied Scientific Research (TNO, Dept. Air Quality and Climate), Utrecht, The Netherlands, the working group on Tropospheric Research of the Institute for Meteoroliogy of Freie Universität Berlin (FU Berlin, IfM, AG TrUmF), the Corporation for Ecosystem Analysis and Environmental Data Analysis (ÖKO-DATA, Strausberg), and the Institute of Navigation, Universität Stuttgart (INS). The results of the project are support for the German Federal Environment Agency (UBA, Dessau) in calculation and verification of national data which are implemented in European scale Critical Loads and Levels maps. The project results are national contribution for the protocols within the framework of UN/ECE Convention on Long-range Transboundary air pollution (UN/ECE LRTAP). Moreover the data are supporting EU and national regulations on air pollution control and emission abatement (EU NEC directive, BImSchG, TA-Luft).

Further information:
on the project: MAPESI (Modelling of Air Pollutants and EcoSystem Impact) *www.mapesi.de*
on the methods applied: *http://www.icpmapping.org/htm/manual/manual.htm*
on previous projects: *http://www.nav.uni-stuttgart.de/navigation/forschung/critical_loads*

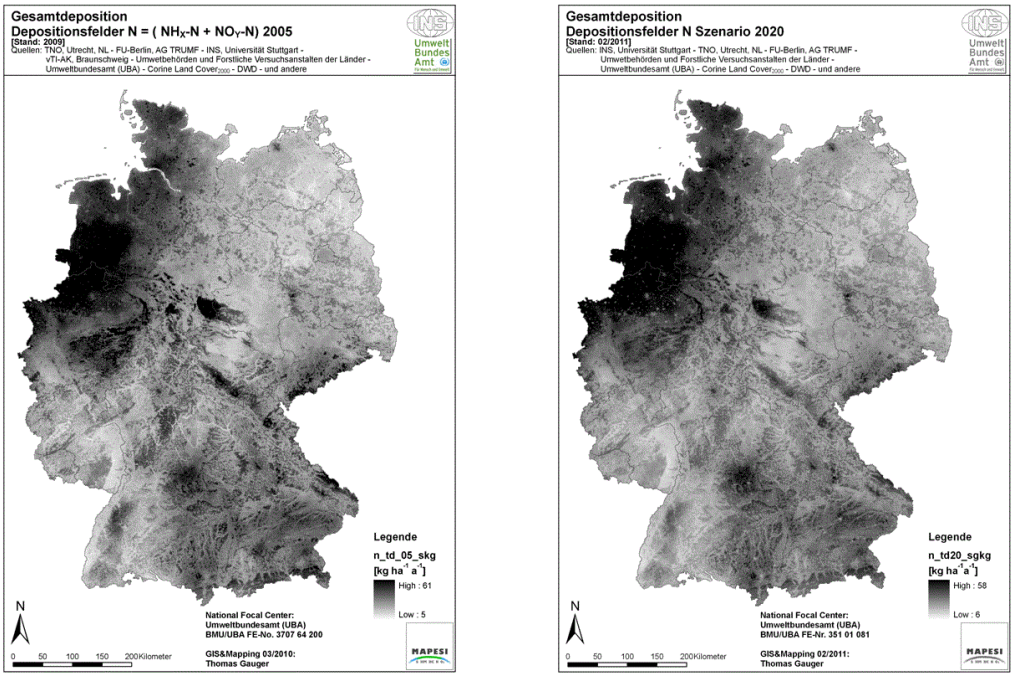

Fig. 7: Total deposition fields of nitrogen in Germany 2005 and prognosis 2020

Publications and Presentations

Schäfer, B.; Wild-Pfeiffer, F.; Xue W.: Erfassung von Bewegungszuständen mittels MEMS-Sensoren. Geodätische Woche 2010, 5.-7. October 2010, Köln

Janák, J., Wild-Pfeiffer, F.: „Comparison of various topographic-isostatic effects in terms of smoothing gradiometric observations“, In: Mertikas, S. (Ed.): Gravity, Geoid and Earth Observation, GGEO 2008, IAG Int. Symposium, Chania, Crete, 23 - 27 June, 2008, Vol. 135 (2010), Springer-Verlag, S. 377-382.

Janák, J., Wild-Pfeiffer, F., Faskova, Z., Mikula, K.: „Refinement of a regional gravity field model using a combination of GOCE data and terrestrial gravity data“, In: Proc. ESA Living Planet Symposium, Bergen, June 28 - July 2, 2010 (ESA SP - 686, Dezember 2010), CD-ROM.

Janák, J.,Wild-Pfeiffer, F., Faskova, Z., Mikula, K.: „Refinement of a regional gravity field model using a combination of GOCE data and terrestrial gravity data“, ESA Living Planet Symposium, Bergen, 30.06.2010.

Janák, J., Faskova, Z., Wild-Pfeiffer, F., Xu, P.: „Challenges of GOCE Satellite Mission in Terms of User Applications“, The Meeting of the Americans, Foz do Iguaçu, 10.08.2010.

Gäb, M., Kleusberg, A.: „Improved tracking of the GNSS signals by coupling with MEMS for land vehicle navigation“. Vortrag und Veröffentlichung im Rahmen der Europäischen Navigationskonferenz (ENC 2010), Braunschweig, 19. - 21.10.2010.

Diploma Thesis

Wang, Kan: „Untersuchung zur Positionierung auf Basis von Galileo Pseudoliten für automatische Allwetter-Andockverfahren in Häfen“; Institute of Navigation, University of Stuttgart, April 2010 (Wehr)

Master Thesis

Cahyadi, Mokhamad Nur: „Evaluation of Loosely and Tightly Coupled Kalman Filtered Post Processing-Solution from an Integrated Navigation System“; Master Thesis; Institute of Navigation, University of Stuttgart, May 2010; (Schäfer).

Zhao, Liang: „Accuracy Assessment of GPS Data Loggers“; Master Thesis; Institute of Navigation, University of Stuttgart, July 2010 (Becker)

Study Thesis

Gao, Yang: „Measurement of physical activity with low-cost sensors“; Study Thesis, Institute of Navigation, University of Stuttgart; June 2010; (Schäfer).

Ellmer, Matthias: „Untersuchung eines Low-Cost GPS-Empfängers zur kinematischen Positionierung eines Rennwagens“; Studienarbeit, Institut für Navigation; Universität Stuttgart; Dezember 2010; (Schäfer).

Baleanu, Camelia: „Evaluierung eines älteren GPS/GLONASS Empfängers für den kinematischen Einsatz“, Institute of Navigation, University of Stuttgart, September 2010 (Becker)

Kruck, G, Gesine: „Untersuchung der C/A-Code Singlepositionierung aus kombinierten GPS und GLONASS Messungen“, Institute of Navigation, University of Stuttgart, June 2010 (Gäb)

Zhong, Jinghao: „Analyse der derzeit empfangbaren SBAS-Ranging Signale“, Institute of Navigation, University of Stuttgart, October 2010 (Becker)

Participation in Conferences, Meetings and Workshops

Wild-Pfeiffer, F.
ESA Living Planet Symposium, Bergen, 28.06. - 02.07.2010
Geodetic Week, Köln, 05.-07.10.2010

Schäfer B.
International Conference on Indoor Positioning and Indoor Navigation (IPIN) 2010, 15.-17.09.2010, Zürich, Switzerland
Geodetic Week, Köln, 05.-07.10.2010

Gäb M.
European Navigation Conference (ENC - GNSS 2010), Braunschweig 19.-21.10.2010
ION (Institute of Navigation) - GNSS 2010, Portland, Oregon, September 21.-24. 2010

Activities in National and International Organizations

Alfred Kleusberg
Fellow of the International Association of the Geodesy
Member of the Institute of Navigation (U.S.)
Member of the Royal Institute of Navigation
Member of the German Institute of Navigation

Wild-Pfeiffer, F.
Meeting „Frauen im DVW“, Intergeo Köln, 06.10.2010

Education (Lecture / Practice / Training / Seminar)

Navigation and Remote Sensing (Wild-Pfeiffer, Schäfer)	2/1/0/0
Introduction of Geodesy and Geoinformatic (BSc)	2/2/0/0
Electronics and Electrical Engineering (Wehr, Fang)	2/1/0/0

Satellite Measurement Engineering (Wehr, Fang)	2/1/0/0
Aircraft Navigation (Schöller, Wehr)	2/0/0/0
Parameter Estimation in Dynamic Systems (Kleusberg)	2/1/0/0
Navigation I (Kleusberg, Xue)	2/2/0/0
Inertial Navigation (Kleusberg, Xue)	2/2/0/0
Remote Sensing I (Wild-Pfeiffer, Pasternak)	2/2/0/0
Remote Sensing II (Wild-Pfeiffer, Pasternak)	1/1/0/0
Satellite Programs in Remote Sensing, Communication and Navigation I (Liebig)	2/0/0/0
Satellite Programs in Remote Sensing, Communication and Navigation II (Liebig)	2/0/0/0
Radar Measurement Methods I (Braun)	2/0/0/0
Radar Measurement Methods II (Braun)	2/1/0/0
Navigation II (Becker)	2/2/0/0
Integrated Positioning and Navigation (Kleusberg)	2/1/0/0
Interplanetary Trajectories (Becker)	1/1/0/0
Practical Course in Navigation (Schöller)	0/0/2/0
Geodetic Seminar I, II (Fritsch, Sneeuw, Keller, Kleusberg, Möhlenbrink)	0/0/0/4
Integrated Fieldwork (Schäfer, Fang)	(SS 2010)

Institute for Photogrammetry

Geschwister-Scholl-Str. 24D, D-70174 Stuttgart
Tel.: +49 711 685 83386, Fax: +49 711 685 83297
e-mail: firstname.secondname@ifp.uni-stuttgart.de
url: http://www.ifp.uni-stuttgart.de

Head of Institute

Director: Prof. Dr.-Ing. Dieter Fritsch
Deputy: apl. Prof. Dr.-Ing. Norbert Haala
Personal Assistant: Martina Kroma
Emeritus: Prof. i.R. Dr. mult. Fritz Ackermann

Research Groups at the ifp:

Geoinformatics

Head: Dr.-Ing. Volker Walter	GIS and Remote Sensing
Dipl.-Ing. Hainan Chen	Data Integration
Dipl.-Ing. Yevgeniya Filippovska	Data Quality
Dr.-Ing. Martin Kada	3D-Visualisation
Dipl.-Ing. Michael Peter	Generalisation

Photogrammetry and Remote Sensing

Head: Dr.-Ing. Michael Cramer	Digital Airborne Sensors
Dr.-Ing. Susanne Becker	Point Cloud Interpretation
Dipl.-Ing.(FH) Markus Englich	Sensor Laboratory
Dipl.-Ing. Mathias Rothermel	Semi-Global Matching
Dipl.-Ing.(FH) Werner Schneider	Digital Photogrammetry Laboratory
M.Sc. Eng. Rongfu Tang	Bundle Block Adjustment Extension

Terrestrial Positioning Systems and Computer Vision

Head: Prof. Dr.-Ing. Dieter Fritsch, Dr.-Ing. Jan Böhm (until Aug. 2010)

M.Sc. Eng. Angela Budroni	Indoor Model Reconstruction
Dipl.-Ing. Alessandro Cefalu	Photogrammetric Calibration and Object Recognition
Dipl.-Ing. Alexander Fietz	Indoor Mapping
M.Sc. Eng. Ali Mohammed Khosravani	Indoor Modeling and Positioning
M.Sc. Eng. Wassim Moussa	Sensor Fusion
M.Sc. Eng. Mohammed Othman	Image Orientation
Dipl.-Ing. Carina Raizner	Objective Stray Light Measurement

External Teaching Staff

Dipl.-Ing. Stefan Dvorak, Amt für Stadtentwicklung und Vermessung, Reutlingen
Dipl.-Ing. Sabine Urbanke, Landesvermessungsamt Baden-Württemberg

Research Projects

Geoinformatics

Indoor Navigation and Modeling

The success of Volunteered Geographic Information (VGI) in projects like OpenStreetMap is closely related to GPS as prevalent and inexpensive sensor system. In such scenarios, the volunteers use their GPS tracks to georeference objects of interest. While VGI has become very popular in outdoor areas, the lack of a suitable positioning sensor prevents corresponding developments in indoor environments. In order to enable indoor data collection, the path of a volunteer must be collected with suitable accuracy while he moves through a building. For this purpose a wide range of experimental and commercial positioning systems are available. However, they either require infrastructure like WLAN networks or RFID beacons, or are based on high quality indoor models. Therefore, they do not allow for an inexpensive and generally available indoor navigation. This can be realized by low-cost inertial measurement systems based on MEMS IMUs. However, position determination by naive integration of such inertial measurements suffers from unfavorable error characteristic with large drifts after short time periods. In order to improve the positional accuracy from MEMS IMU measurements during pedestrian navigation, so-called ZUPTs (zero velocity updates) can be used. A foot-mounted MEMS is used as a pedometer, which considerably improves the quality of the measured trajectory. The accuracy of MEMS IMU indoor navigation is further improved by stair detection and an alignment of the trajectories. The alignment presumes that most parts of indoor routes will be parallel or perpendicular to the main direction of the building.

Since inertial navigation only provides relative coordinates, additional measurements to relate the trajectory to a reference coordinate system are required. For outdoor applications, this reference is usually provided by integration of GNSS positions. Since this is usually not available in indoor environments at suitable accuracies, we use an initial position of the user which can be derived from images of evacuation plans. Such plans are compulsory for public buildings in a number of countries. They consist of an approximate floor plan and escape routes. Furthermore, they provide the current position of the user with respect to the plan, which can be used as starting point for inertial navigation. For scenarios, which imply an active participation of a potential user, we assume that he is willing to collect an image of such a floor plan by a mobile device like a cellular phone. Ground plan information can be made explicit from such images by a raster-to-vector-conversion. This information is then used to support and improve pedestrian navigation similar to map matching in outdoor environments. Furthermore, a floor plan can provide semantic information like stairs, elevators or level number. An approximate indoor model of the respective building can be generated during further processing.

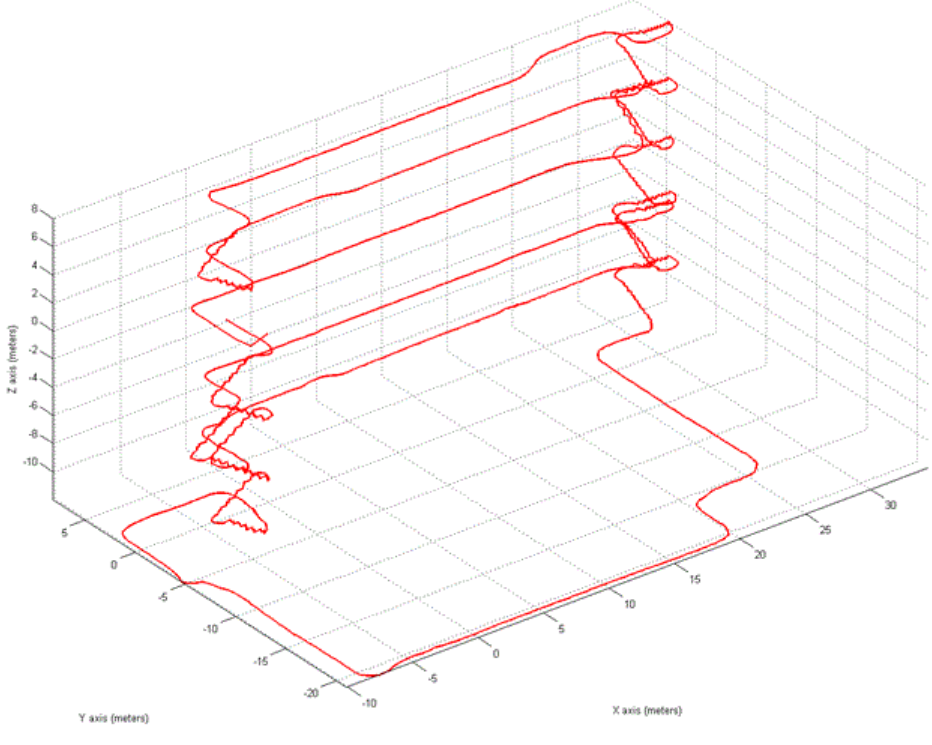

Figure 1: Indoor track using ZUPTs, alignment and height correction.

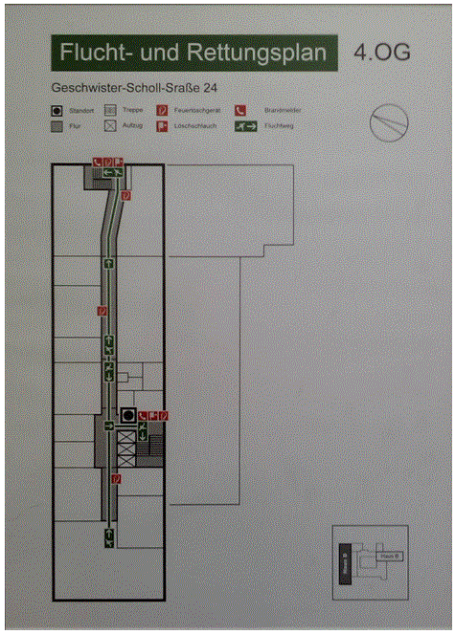

Figure 2: Evacuation plan of the Institute for Photogrammetry, containing information like floor number, address and current position of user

Context information from detailed façade models

In order to provide a geometric basis for spatial world models for context aware applications, methods for the automatic derivation of 3D building structures from sensor data with heterogeneous quality have been developed. Resulting 3D building models can be used for various scenarios. Strategies have been worked out to make the 3D building structures applicable in navigation systems for blind people. Based on façade models in which detailed façade structures are represented by explicit 3D geometry and semantic information, 2D maps can be derived for each floor where windows and doors are described by annotated polygons. Especially the position of doors may be helpful for blind people when searching for the entrance of a building. Figure 3 (left) shows the Central Administrative Building of the University of Stuttgart as 3D model before and after façade reconstruction. The corresponding 2D map of the ground floor is given in Figure 3 (right) where façade elements are marked as filled polygons.

Beside pedestrian navigation, a number of other applications can take advantage of semantically interpreted 3D building models. For example, detailed façade models allow for energetic estimates of a building's heat loss by calculating the ratio of wall to window areas. Furthermore, they are appropriate to complement Building Information Models which are used for facility design, construction and asset management. Façade structures can also be used to simulate high-resolution

SAR images in order to support Persistent Scatterer Interferometry (PSI) focused on single urban objects. However, most applications require not only geometric and semantic knowledge but also quality information about the building structures. Therefore, application dependent quality criteria for façades have been developed which are appropriate to be used in various scenarios. Such evaluation criteria consider the ratio of void to solid of a façade, the form and size of windows as well as their arrangement.

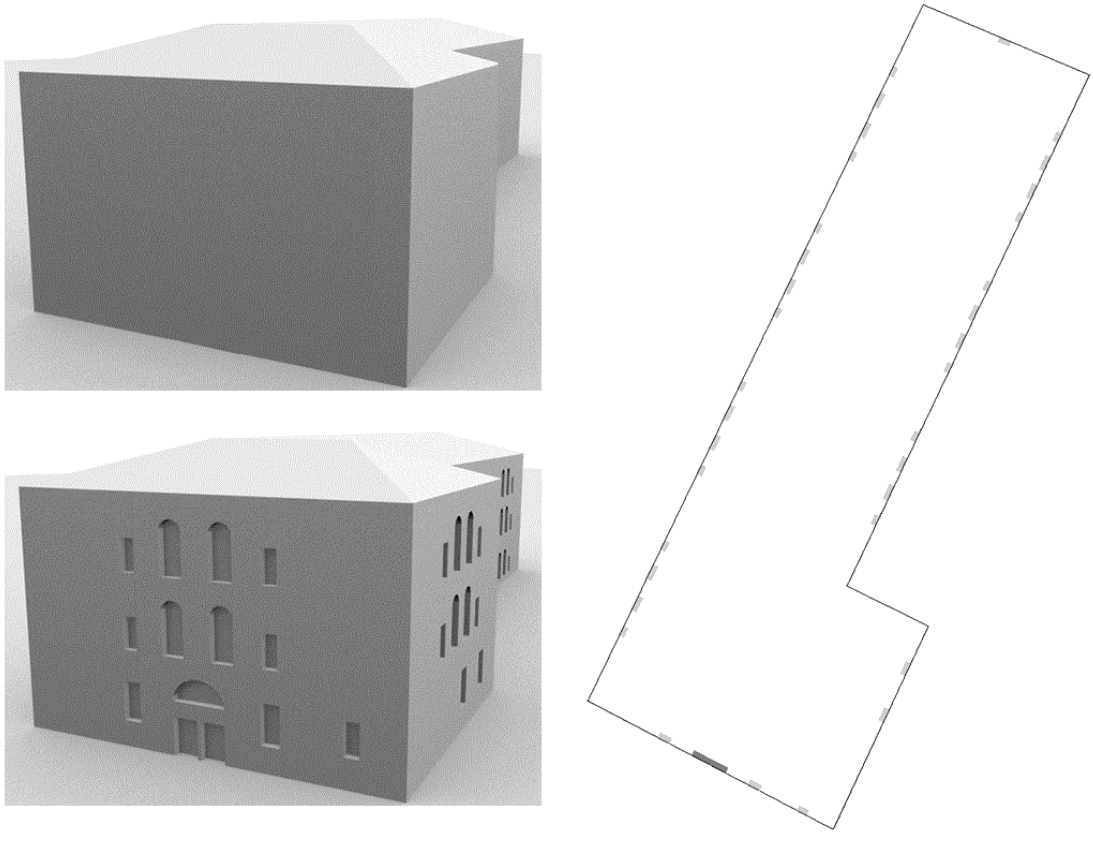

Figure 3: The Central Administrative Building of the University of Stuttgart: 3D model before and after façade reconstruction (left); 2D map of the ground floor (right).

Classification of Maps with Kohonen Feature Maps

Artificial Neural Networks are an approach to simulate biological neural networks. Different types of Artificial Neural Networks have been developed, like single-layer feedforward networks, multilayer-networks, recurrent networks or Self-Organizing Maps. The Kohonen Feature Map has been developed by Tuevo Kohonen and is a type of a Self-Organizing Map which uses unsupervised learning in order to organize the connections between the neurons. That means that the neural network does not know what the correct classification for a specific input is. The function of the network is therefore to categorize different inputs into clusters which have similar characteristics. A Kohonen Feature Map consists of an input layer and an output layer. The layers are represented with neurons which are connected to each other. Objects, that should be classified, are represented with a feature vector which describes the object characteristics. This feature vector is the input for the Kohonen Feature Map. The output is a classification of the objects into different object classes.

In the following, the practical use of Kohonen Feature Maps for the classification of maps in the scale of 1:10,000 is shown as an example. The objects that should be classified are: buildings, stadiums, roundabouts, highways, major roads, side roads and rail track. First, the object characteristics of the different object classes have to be defined with a vector consisting of 0 and 1 values. Altogether ten object characteristics are used which results in an input vector with the dimension 10. In the next step, the numbers of neurons of the Kohonen Feature Map have to be defined. The number of neurons of the input layer corresponds to the number of different object characteristics. The optimum number of neurons of the output layer was estimated by testing. Based on an evaluation of different configurations, we use 30*30 neurons in the output layer. An example of a classification result is shown in Figure 4. The incorrect classified objects are marked with red circles. It can be seen that in some cases small streets were classified as buildings or large buildings were classified as streets. Also two rail tracks were classified wrongly as side roads.

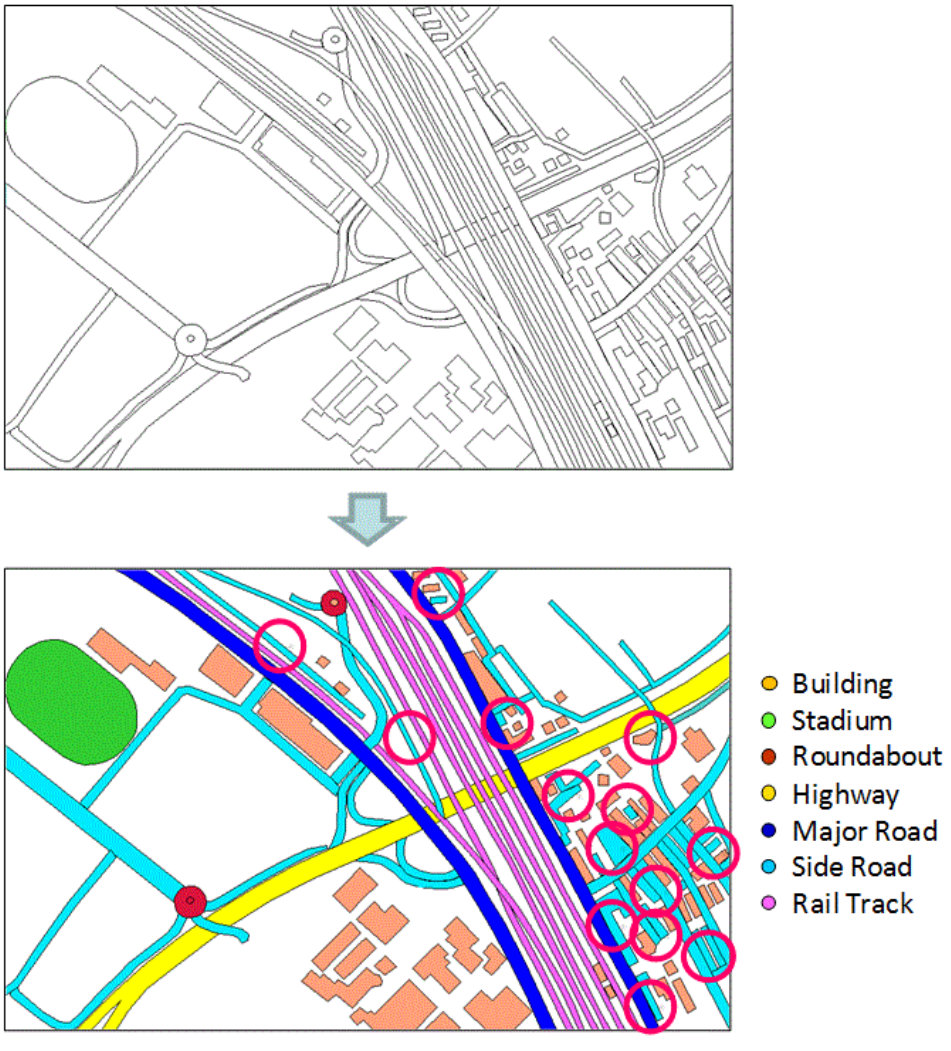

Figure 4: Classification example of a 1:10,000 map. Incorrect classified objects are marked with red circles.

Shape assessment of generalized building ground plans

Along with constantly improving acquisition, processing and visualization techniques, the amount of spatial data that is available today has dramatically increased. As a consequence, various data sets for one and the same area are often available. Thus, there is a rising need to compare such data sets in order to assess their quality and select the best one for a specific application. This work is particularly dedicated to the shape assessment of building ground plans. For different reasons, multiple versions of one and the same building ground plan are available that differ both in geometry and shape. The reasons are for example: data collections at different times, transformations by means of analyses (e.g. 3D building reconstruction), or visualization purposes (e.g. generalization). In this work we want to identify and measure automatically differences between the location, extent and shape of different building ground plans.

A commonly used characteristic for measuring the deviation between the outlines of polygonal objects is the Hausdorff distance. However, on generalized building ground plans the metric performs in some cases less intuitive from a human point of understanding. Examples resulting from a generalization where the Hausdorff distance fails are shown in Figure 5.

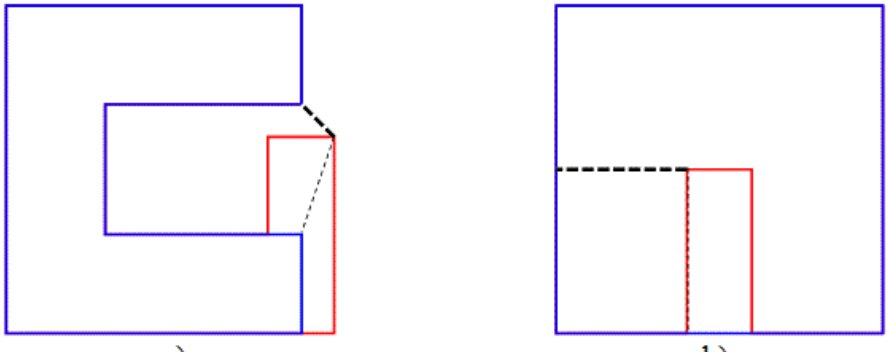

Figure 5: Computed Hausdorff distance (fine dashed line) between two building ground plans compared to what a human might perceive (bold dashed line).

In order to avoid a false identification of the correspondences between the elements of the original and generalized polygon, the computation of a modified Hausdorff distance is not calculated on the entire set of the vertices of the building ground plan but only on the vertices within the eliminated object parts. The difference between the normal Hausdorff distance and the modified Hausdorff distance can be interpreted as difference of shape complexity. Another possibility is to calculate the maximum shortest path within the eliminated object parts. Whereas the original and the modified Hausdorff distance characterize the maximum deviation between the outlines of

two building ground plans, the shortest path rather defines the shape complexity of the eliminated object part. This characteristic can also be considered for the quality evaluation of generalization algorithms. The results are shown in Figure 6.

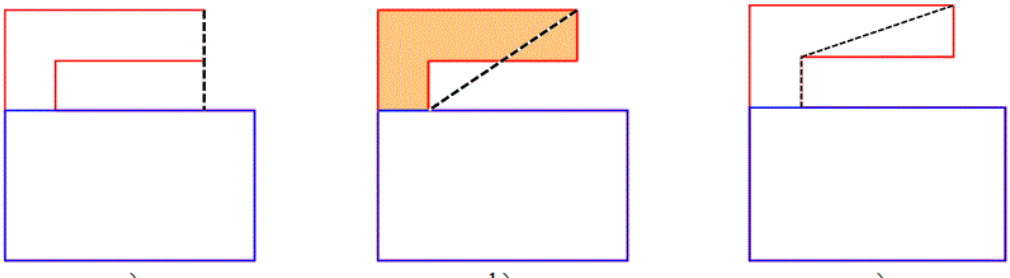

Figure 6: Hausdorff distance a), modified Hausdorff distance b), shortest path within the eliminated object parts c).

Photogrammetry and Remote Sensing

The refinement of digital airborne camera systems is still one of the major research topics. Especially because now the systems are introduced in practice and continuously have to provide consistent and reliable results in operational conditions. This does not only cover the sensor hardware itself, it also includes improvements of process chains, considering both geometry and radiometry aspects.

Today it is obviously that not only people from photogrammetry and the traditional mapping business are using mapping technologies. It is a much more broader spatial community that moves towards automation, asking for more reliable and more robust processes, finally merging of worlds and bridging the gap to computer vision. New applications request for image data, which are more important than former vector maps. Future focus will be more on up-to-dateness, completeness and automation. The need for a complete image mosaic seems to be higher than the final accuracy, at least as long there is „some sort“ of georeferencing available. Robust unconventional mapping also will be one topic of importance especially for unmanned, low-cost and flexible UAV systems and applications. This definitely also will impact the currently still rigorous UAS/UAV flight restrictions.

UAV used in airborne mapping

First investigations on the potential of UAV for airborne mapping with special focus on remote sensing applications have been conducted together with the Institute of Space Systems (IRS) and their „Stuttgarter Adler“ UAV (Figure 7). This fixed wing, remotely controlled airborne vehicle

can be used as flexible platform for remote sensing applications. It has about 4,30m wing span and maximum takeoff weight of 25kg. In April 2010 test flights were done, using a small format 1280 x 1024 pixel CCD industrial camera system. Images were taken from 300m flying height above ground, which corresponds to about 8cm ground sampling distance. Additional control points were provided to investigate the geometrical performance of the system. Figure 8 shows the block configuration with signalized ground control points overlaid. The area covered is about 200m x 400m in size.

Figure 7: The „Stuttgarter Adler“ UAV platform for remote sensing applications (© Institute for Space Systems (IRS)).

It is clearly visible that the block configuration of a UAV image block is much different compared to classical airborne platforms. The irregular distribution of the images, which is due to the aircraft dynamics since no stabilized camera mounting is used and deviations from the flight planning due to navigation errors are clearly visible. This requests for powerful tools for image matching, especially because in our case almost no or only very poor pre-knowledge on the exterior orientation of each image is available. The image matching is based on the SIFT algorithm which is also used for the image orientation and adjustment. This adjustment is based on the „Bundler“ bundle adjustment software, which allows for image orientation without any starting values for camera parameters and exterior orientations. Figure 9 shows the adjusted point cloud in object space and the estimated camera perspective coordinates. The results of this first adjustment were used as starting values for a more sophisticated bundle adjustment to refine the camera geometry through self calibration. From this, object point accuracies in the range of half a pixel (about 5cm) in horizontal and about two pixel (about 20cm) in vertical direction have been obtained, which is quite promising.

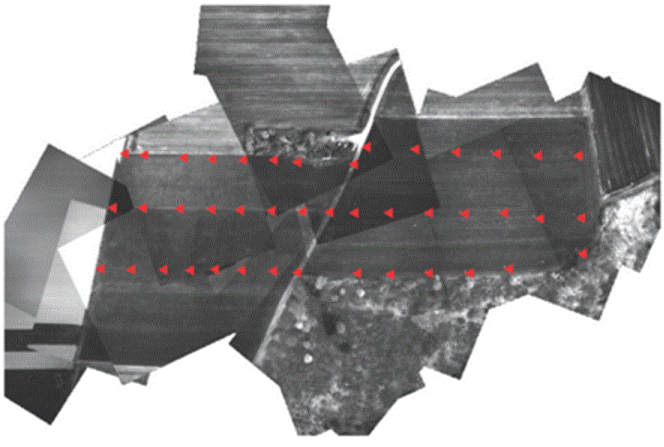

Figure 8: Exemplarily block configuration from „Stuttgarter Adler“ test flight with overlaid control points (triangle symbols).

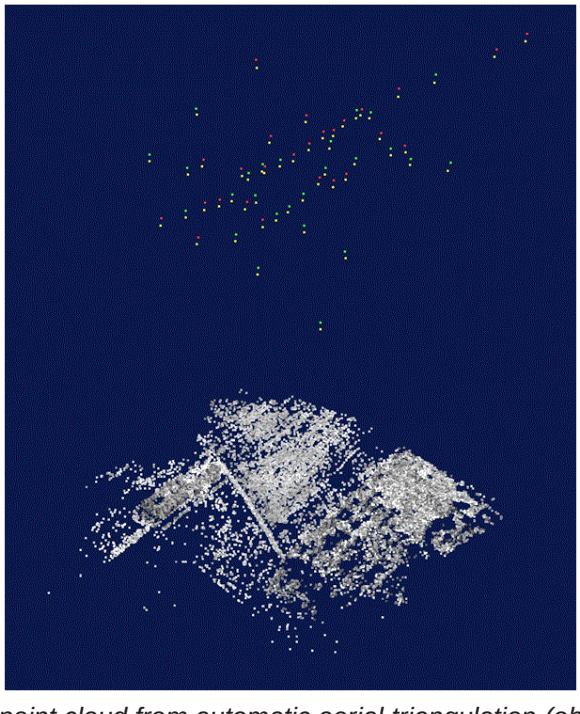

Figure 9: Adjusted 3D point cloud from automatic aerial triangulation (object points and camera station coordinates).

High-end digital airborne imaging

The UAV mapping is the one side of photogrammetric mapping. On the other side there is large format digital imaging, which now has replaced the former analogue mapping cameras completely. In 2010 the first single frame, thus monolithic, very large format digital airborne camera, the now called DMC II product, was introduced by Intergraph/ZI. This product is available as series with 140, 230 or 250 Mpix resolution. In terms of number of pixel per image the DMC II now by far exceeds the number of pixel of the former DMC I product, which was less than 110 MPix. But this was obtained for the virtual image only, which was stitched from 4 individual about 28 MPix camera heads arranged in a tilted configuration to derive a „butterfly“ pattern on the ground. A 230 MPix image now - in terms of number of pixel - is equivalent to an image from traditional airborne mapping cameras scanned with a pixel size of 0.014 mm. It will be interesting to follow, if this monolithic imaging now is superior to the so far realized large format imaging using multi-head layouts, or if both technologies will be used in parallel.

The continuous evolution of sensors and change in concepts always requests for new empirical accuracy testing, not only focusing on the geometry but also on the radiometric sensor performance. A quite extensive test of digital airborne camera systems and the quality of derived products like digital surface models from manual stereo-plotting has been finished in summer 2010 under the leadership of the Institute for Photogrammetry. It was one of the most comprehensive tests in digital airborne systems done so far. This test on Digital Airborne Photogrammetric Cameras was initiated from the German Society of Photogrammetry, Remote Sensing and Geoinformation (DGPF). The results were published in the 02/2010 special issue of the PFG journal.

All new types of sensors, data and products request for commonly accepted certification processes. This is why the Institute for Photogrammetry is also involved in the definition of certification strategies, which are based on defined standards and definitions. The activities in the frame of the European Digital Airborne Camera Certification project and the support of the development of the new ISO/TS 19159 „Calibration and validation of remote sensing imagery sensors and data“ should be mentioned in this context.

Student’s excursions to digital photogrammetric system suppliers

In order to demonstrate our students the most recent developments in airborne imaging we have organized two one day student trips. The two digital photogrammetric camera providers Leica Geosystems in Heerbrugg/Switzerland and Intergraph/ZI in Aalen have been visited in 2010 - both with special focus on airborne sensor development including some insight views into digital sensor assembly and calibration. Figure 10 shows the group in front of the Intergraph/ZI Aalen facilities. It was close to 30 students, about half from the international GEOENGINE M.Sc. program (2nd semester), and the other half from the German Geodesy and Geoinformatics Diploma program (6th semester) who enjoyed this more practical approach in digital photogrammetric image data acquisition.

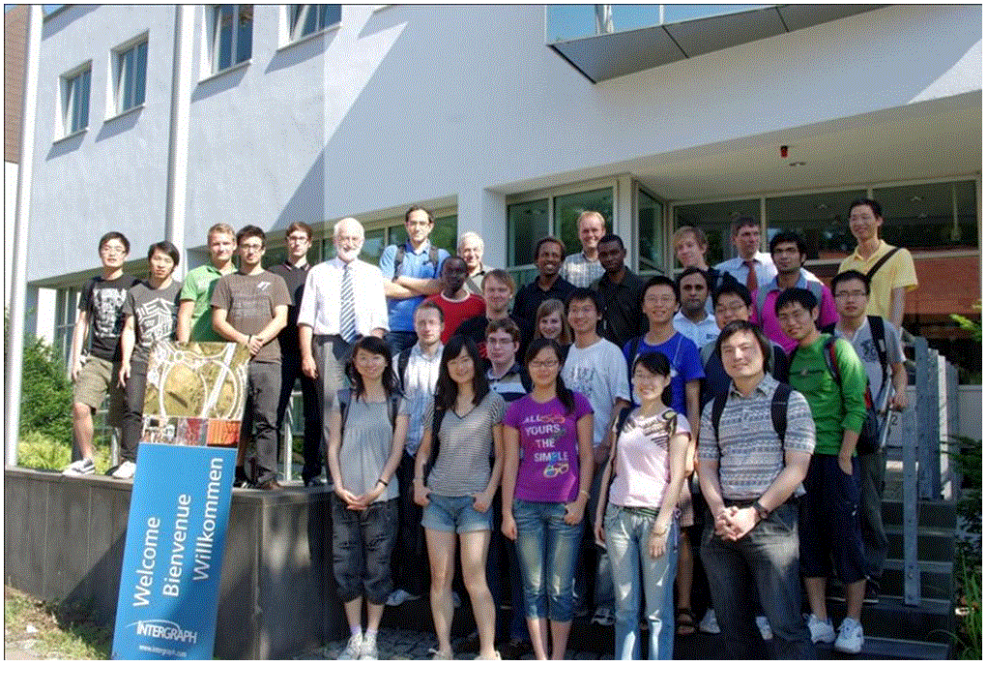

Figure 10: One day student's excursion to the airborne image sensor development at Intergraph/ZI, Aalen.

Dense Image Matching using Semi-Global Matching

Current digital airborne cameras offer excellent signal-to-noise ratio and high image overlap which considerably improve the usability of the collected data for image matching. Comprehensive tests, as for example organized by the German Society of Photogrammetry, Remote Sensing and Geoinformation (DGPF) have shown that meanwhile digital image matching is a valid alternative to airborne LiDAR data collection in the context of dense and accurate Digital Surface Model (DSM) generation.

The increasing applicability of image based DSM generation triggered the further development of matching algorithms. In contrast to automatic stereo tools based on feature extraction and matching, recent algorithms like Semi-Global Matching aim at a very dense multi-matching by a per-pixel stereo measurement. Relating pairs of correspondent pixels across two images is done by minimizing a global matching cost function. For optimal image alignment the cost is expected to be minimal. Since this optimization problem is known to be NP hard for 2 dimensional images, Semi-Global Matching aims for minimizing an approximation of the global cost.

The matching quality of a pair of corresponding pixels can be estimated by the Mutual Information (MI) which is robust against radiometric distortions and based on entropies and joint entropies of images. Using MI, the costs induced by matching a base image pixel p onto a set of i match image pixels q_i can be compared. The tuple of pixels (p, q_i) which constitutes the minimal cost is then considered to be the best match. Since the cost function will not yield correct results for every intensity combination, analyzing costs for each pixel separately will cause a large number of mismatches. Therefore Semi-Global Matching incorporates costs of proximate image regions by aggregation of costs along paths in 16 directions. This strategy approximates global minimization of costs and models the assumption that neighbouring disparities, and therefore depth values in object space, are smooth.

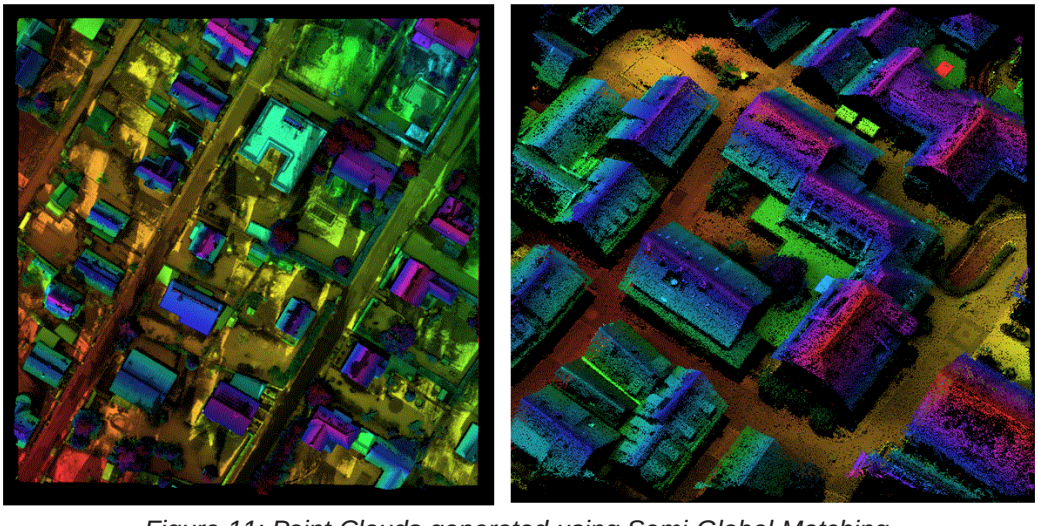

Figure 11: Point Clouds generated using Semi-Global Matching.

Bayesian estimation in aerial photogrammetry

The two most significant developments in aerial photogrammetry in the recent years are the introduction of integrated navigation systems and the advent of digital camera systems. They both greatly change numerous aspects of photogrammetry as well as they also cause many new challenges. Two of these challenges are of our current interest, namely the

- ▷ (1) Variance estimation during aerial triangulation
- ▷ (2) Digital camera calibration from test field data

The first work is motivated by the fact that the proper weighting of heterogeneous observations (like GPS/IMU observations, ground control points (GCPs) and photogrammetric image measurements) has a great impact on the results from aerial triangulation. Typically the variance of

individual observations is manually appointed by photogrammetrists according to their empirical expertise. Nevertheless, additional information involved in the observations directly, can be utilized to refine the empirical knowledge on the observation precision. Within the first phase of this work, Bayesian statistics has been applied to the photogrammetric bundle adjustment, to take advantage of the Bayesian rule, which derives the posterior variance by integrating the prior knowledge and data information.

The mathematical rigorous Bayesian method has been developed and implemented in the bundle adjustment. Its main difference from the traditional adjustment is that the traditional method focuses statically on the initial values of unknowns while the Bayesian method centers dynamically in the approximation of unknowns. Some first results from aerial triangulation using the Bayesian method in comparison to the standard AT are shown in Figure 12. The results are from an airborne image block, flown with the digital airborne camera DMC in the ifp test site Vaihingen/Enz. The ground sampling distance was about 20cm, with each 60% forward and side-lap overlaps. The external accuracy obtained from about 140 independent check point differences is given. A dense control point distribution (47 points) was used in the adjustment.

This and other results show that Bayesian adjustment could achieve similar accuracies as the traditional method in most cases whith some advantages: the covariance information could be available for the adjustment and the Bayesian method may handle the additional self-calibration parameters in a more proper way.

The large computational demand of the Bayesian method needs to be solved in further research. Other statistical methods, such as variance component estimation, could be adopted in future, as well-known alternative to estimate the variance of heterogeneous observations.

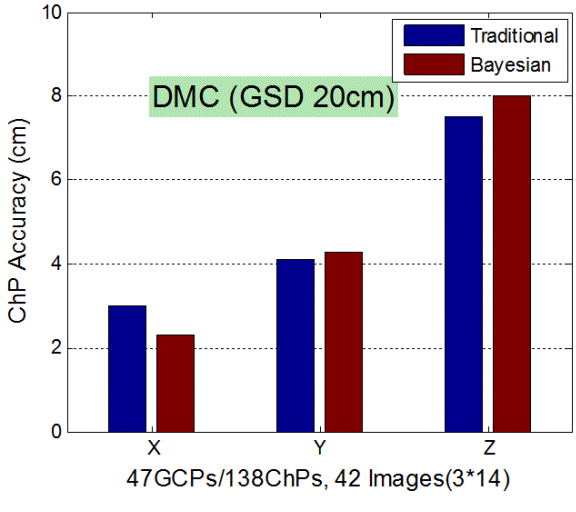

Figure 12: An example of comparison between traditional and Bayesian adjustment.

Terrestrial Positioning Systems and Computer Vision

Optimized Methodology for 3D Scene Reconstruction

Images are everywhere - with the availability of digital cameras, images are taken almost at all times and everywhere and furthermore are also made available to the public. This imaging information now might be used to extract useful information. In this project the focus is on the recovery of 3D information to serve the increasing demand for 3D models. The main objective is to provide an optimized and fully automated methodology for scene reconstruction, which takes a set of unordered images and produces a 3D scene. In particular, our methodology involves mainly two tasks:

- (1) Automatic orientation of a set of unordered targetless close-range images
- (2) Creation of 3D models with a multi-image matching algorithm

Nowadays, automation in image orientation can be considered as solved in aerial photogrammetry, but a general and commercial solution is still pending in case of close-range image blocks. The reconstruction of 3D information from multiple images of a scene has long been an active issue still open in computer vision, graphics and photogrammetry, and it has inspired a wide variety of different approaches and algorithms. The reconstructed 3D objects and their features are highly dependent on the use of the model and the results may differ in terms of accuracy and time needed for their generation. The key issue is to develop a fully automatic data processing pipeline for accurate, efficient and fast dense reconstruction from a set of multiple images of a complex scene taken by a typically hand-held, small format digital camera. For that the following workflow (see Figure 13) has been developed:

- (1) Initial Network Geometry Analysis
- (2) Tie Points Extraction
- (3) Structure and Motion Recovery and
- (4) Dense Reconstruction

We have tested our methodology with different aerial (from UAV) and terrestrial datasets. The comparison with the open source software package „Bundler“ shows that our optimized methodologies (before (BR) and after reduction (AR)) are more accurate and faster. Figure 14 shows the results for the terrestrial data set of a historic castle (Castle-P30 dataset, 30 images with a resolution of 6.3 Mpix each). The Bundler is extremely slow in the matching phase as well as in the structure and motion phase, as it matches every view to each other. Our target is to establish geometrically consistent feature matches only between each connected pair of images. This is demonstrated from the connectivity matrix which is obtained during the initial network geometry analysis stage. To assess the precision of the camera orientations, we rely on the reprojection error in the image space. As it can be seen from Figure 14 left, our methodology gives errors less than the Bundler at all views.

For the dense reconstruction stage, which is the last step in our process chain, we use a Patch-based Multi-View reconstruction method (PMV), which is defined by Furukawa as a match, expand, and filter procedure, starting from a sparse set of matched keypoints and repeatedly expanding these to nearby pixel correspondence before using visibility constraints to filter away false matches. The final results are detailed colored point clouds which are very near to active sensors. As shown in Figure 15, colored point clouds for two datasets are presented. The left part shows results for the aerial UAV based data set (UAVs-P118, 118 images with resolution 1.3 Mpix) and the right part shows results from the Castle-P30 dataset.

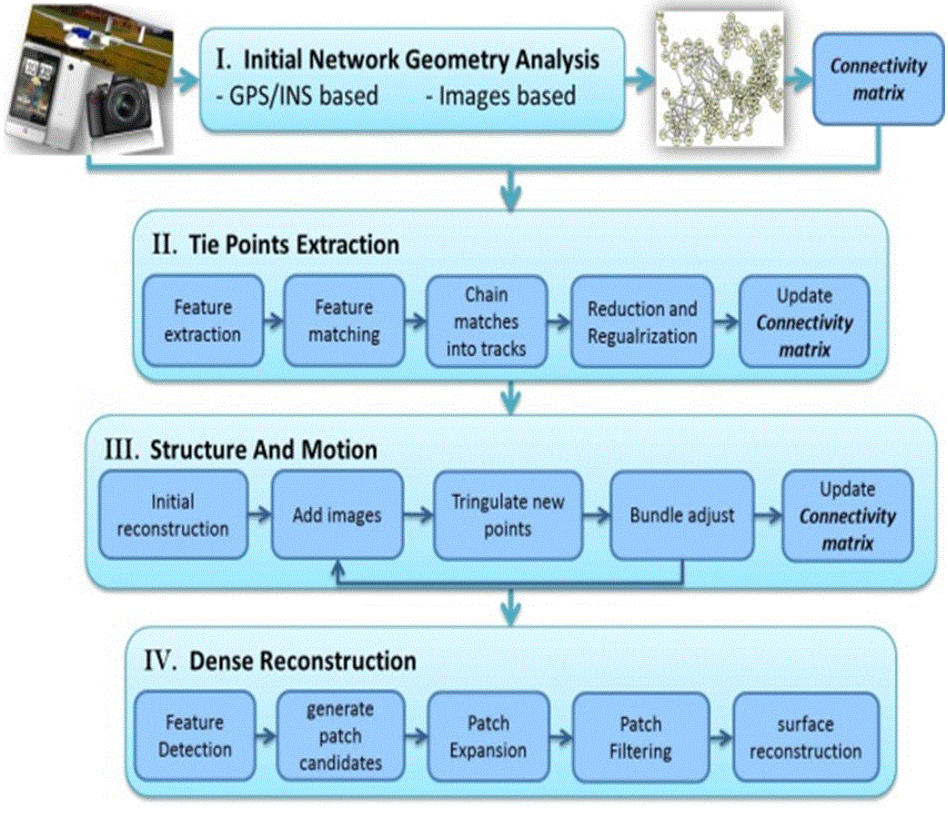

Figure 13: Block diagram of the optimized methodology for 3D scene reconstruction.

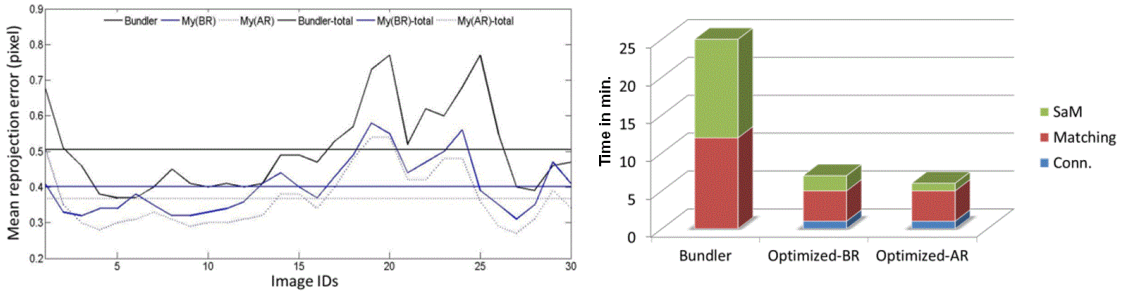

Figure 14: Results and comparison with bundler software.

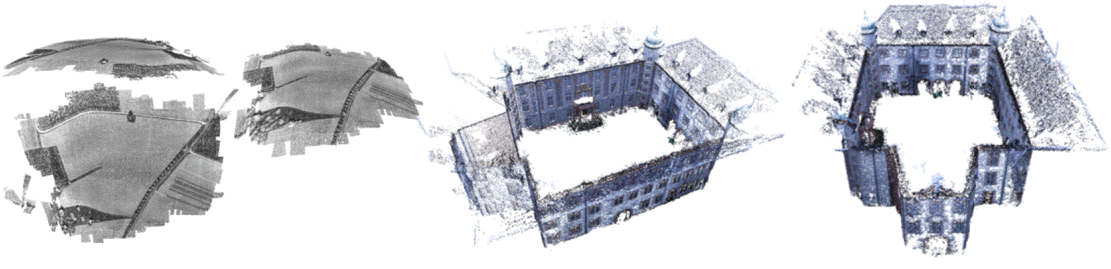

Figure 15: Final results (colored point cloud).

Linking 3D Virtual Reality Models with Content of Bibliographic Repositories - The „Hirsau Abbey“ Project

3D digital preservation and documentation of all cultural heritage sites in the whole world is a very hot topic today. As an example the initiatives of the CyArk Foundation (http://archive.cyark.org/) can be mentioned here.

These „digital“ heritage sites should be easily accessible for the public. For this purpose, a combination of 3D photorealistic models with content of bibliographic resources, which describe the history of the site, is highly needed. The „Hirsau Abbey“ which is an old monastery in the northern part of the Black Forest, Baden-Wuerttemberg, Germany was reconstructed in the last year (Figure 16). Both static LiDAR and close range photogrammetry have been employed successfully for the precise documentation of this cultural heritage study.

This site was also selected as an example for linking contents of bibliographic resources to a 3D model. In particular, this will serve for the special needs of the Verein „Freunde Kloster Hirsau e.V.“ which is a registered association for taking care of the Hirsau site.

Figure 16: The Hunting Lodge, the Cloister and the Lady Chapel in Google Earth.

To do so, we combined successfully the community-based Wikimapia, an online map combined with a wiki system, and the Google 3D Warehouse, which is a free online repository, where you can share and store 3D models. Sites can be found using Google Maps and explored in three dimensions with Google Earth with links to bibliographic resources and related texts. Another option could be to find a model in Google Earth, then move to Google 3D Warehouse, where the model is stored, and then proceed to Wikimapia, where links to bibliographic repositories can be found.

In a first pilot project we have implemented a 3D photorealistic model of one of the ruins of the Hirsau Abbey, which is called the „Hunting Lodge“, with content of bibliographic repositories (Figure 17), and then we extended the implementation to the 3D photorealistic models of the „Cloister“ and „Lady Chapel“.

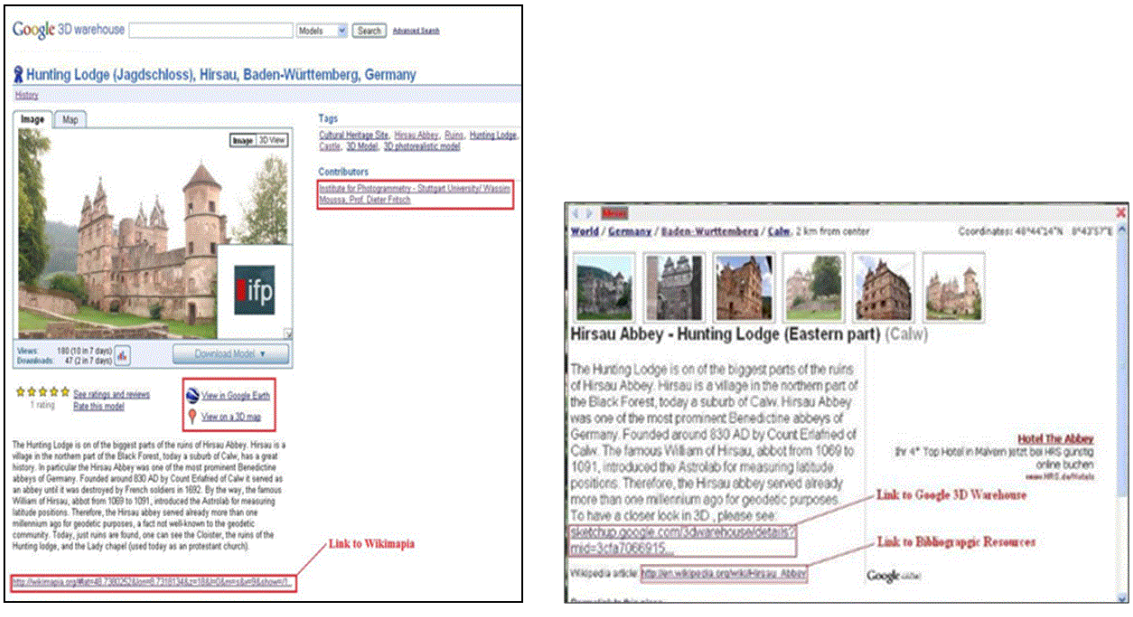

Figure 17: The Hunting Lodge in Google 3D Warehouse (left) and in Wikimapia (right).

You can access the models at: *http://tinyurl.com/63evygd* and *http://tinyurl.com/6kbl5sp*

Automatic 3D Modelling of Indoor Manhattan-World Scenes from Laser Data

A growing attention concentrates upon the development of new automatic techniques for interactive building representations. A higher degree of automation in the reconstruction process may contribute to a fast and dynamic architectural documentation and facilitate the spread of oncoming CAD representations. A progression from 3D to 4D and the use of BIM (Building Information Modelling) is expected. Modern BIM tools enable the automatic updating of objects according to changing contexts. An automatic method to digitize existing architectures can be integrated into a BIM software.

The automatic reconstruction of building models has been mostly restricted to the determination of the outer shapes of buildings. We developed an approach for indoor reconstruction from point clouds. The complexity of our 3D model is compatible with the highest level of details - LoD4 - required by the multi-scale representation CityGML). In particular we reconstruct a 3D model, which incorporates interior architectural details like rooms and interior doors. Also the accuracy of the final CAD model conforms to the CityGML requirements for the LoD4.

Since the subject of indoor reconstruction may cover a wide range of different situations (from cultural heritage to industrial environments), we restrict our domain of application in order to develop a robust method that delivers optimal results in response to one specific issue. The reason lies in the automation of our reconstruction algorithm. An automatic tool in fact is supposed to work independently of external control, thus it requires to be specified into an operational domain, which defines its particular tasks. The domain of our field of application is defined by the Manhattan-world assumption. Many indoor and outdoor city scenes are based on a Cartesian coordinate system, which can be referred to a Manhattan grid.

Our solution to the problem of Manhattan-world interior reconstruction consists of two main subsequent steps (Figure 18). Minor issues are treated in parallel to give a contribution to the final model in terms of output verification (histogram visualization) and detail enhancement (door extraction). A third additional step may be added at the end of the pipeline to allow the application to handle different portions of the data by properly connecting them in a sequential fashion.

The steps we refer to are the sweep reconstruction of the indoor volume and the ground plan cell decomposition. The first is accomplished by a translational (linear) sweep to compute a volume enclosed by orthogonal faces. As a result, each face in the volume is segmented. In the second step, the hypothetical ground plan, represented by one of the previously segmented faces, is divided into rectangular cells whose effective correspondence with the real ground-plan depends on the number of points counted in the cell. The algorithm we propose processes a point cloud (input) in binary format and returns its 3D model as a CAD file.

The data sets under test consist of point clouds of variable point density. The processing time grows with the number of points to be matched with the sweeping plane during the sweep reconstruction. The method was tested on a data set with over 2 million points with a resulting performance comparable to those in response to smaller data samples. It yields that the algorithm robustness is not affected by huge dimension of the input data. Anyway, a further issue may be the connection of adjacent volumes after the single models are separately computed.

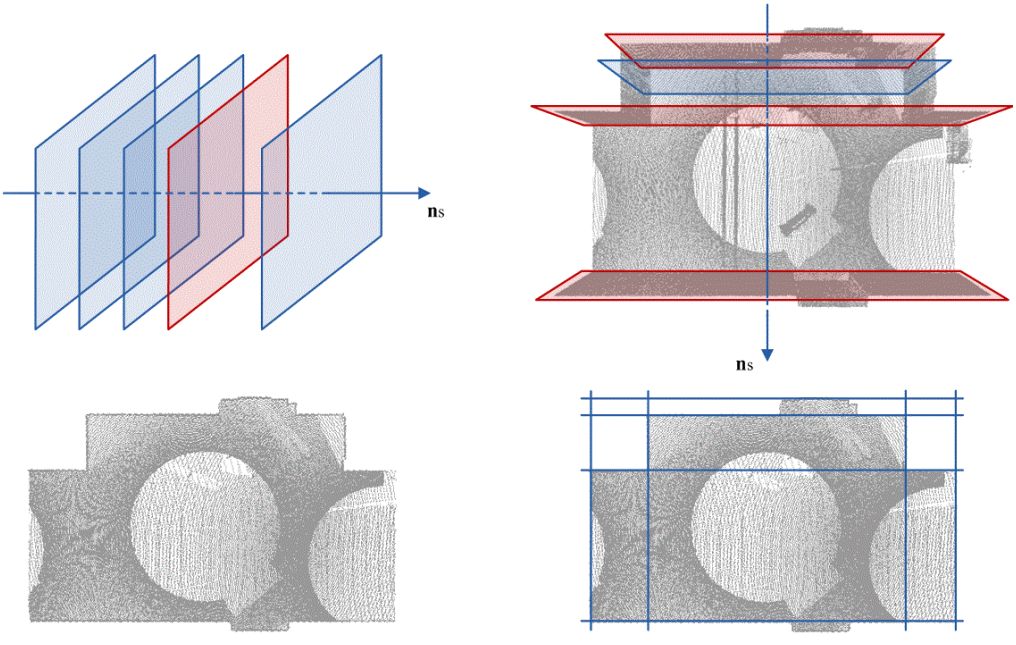

Figure 18: Two main steps for the solution to the problem of Manhattan-world interior reconstruction: Sweep reconstruction of the indoor volume (top) and ground-plan cell decomposition (bottom).

RoboMAP

The project RoboMAP is a cooperation of different partners from science and industry, including the Institute for Photogrammetry. It aims at the development of an inspection system for quality assurance in the automotive industry. The objects to inspect are cylinder heads. In particular the valve seats and the valve stem guides are of special interest. The latter lie in the inner part of the cylinder head and are therefore difficult to access. The different kinds of geometry in combination with other goals, such as inline capability and flexibility regarding measurable object variants, impose the need for a new generation of optical measurement techniques. Tactile methods are not applicable, particularly because of their slow operating speed. A boost of flexibility is achieved by integrating a robot into the system in order to position the multi-sensor in an optimum configuration to the object for inspection. This additional capability is further exploited by integrating a single camera into the system which is used for detecting the cylinder head's pose. Thus there is no need for a predefined object position. Next to a general description of the project, we focus on the calibration of the system. Due to the various kinds of involved sub-systems, the overall calibration will be performed in separate steps in a network of coordinate systems.

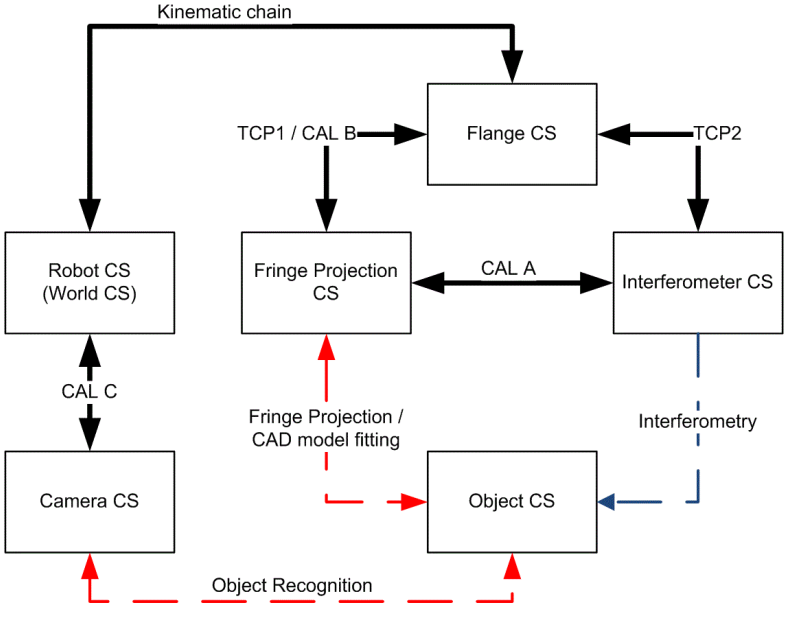

Figure 19: Diagram of the network of coordinate systems; double arrows depict transformations, dashed lines depict sensor measurements.

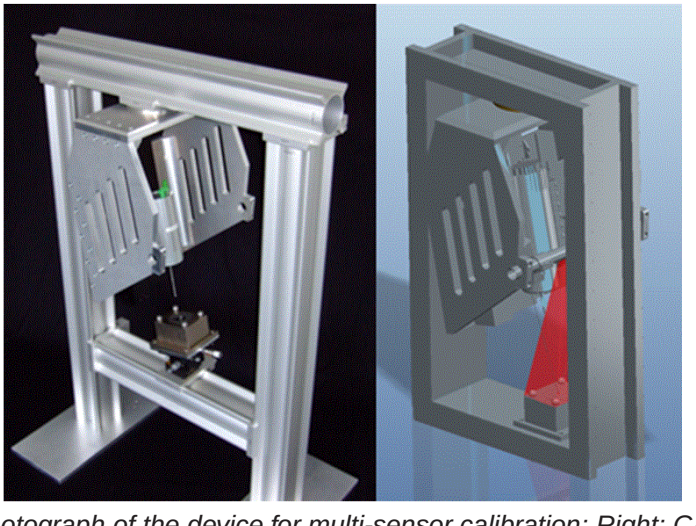

Figure 20: Left: Photograph of the device for multi-sensor calibration; Right: CAD drawing of the device for calibration of the Sensors to the robot hand.

Each component produces or processes geometrical data in its own coordinate system. If the data to process is obtained through another system it has to be transformed accordingly. Figure 19 depicts the linkage of all important coordinate systems. The calibration of the overall system can be understood as the determination of a network of transformation parameters which, if concatenated, enable us to transform any geometrical data into the coordinate system of one of the components.

The sensor coordinate systems needs to be determined with respect to the flange coordinate system (or robot hand coordinate system). These two sets of parameters are referred to as Tool Center Points (TCP) and are directly used by the robot control unit for sensor positioning. Furthermore, the object recognition yields the cylinder head's pose in the camera coordinate system. In order to derive the correct measuring position of the fringe projection system in the robot coordinate system from this result, it has to be transformed accordingly. The necessary calibrations can be classified into the multi-sensor calibration, which includes both TCPs and the transformation between the two sensors and the calibration determining the transformation from the coordinate system of the object recognition camera to the robot coordinate system. The obtained results show that the concept works well. It is recently being integrated to the RoboMAP system for first performance tests.

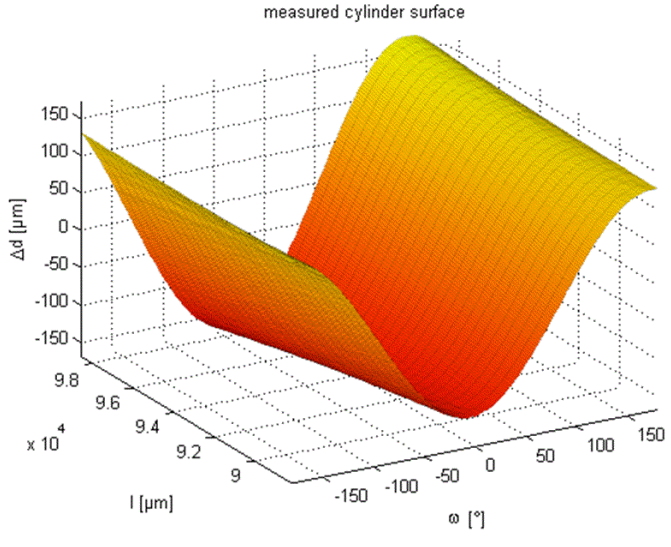

Figure 21: Plot of the cylindrical coordinates of a helix shaped measurement at a cylinder of a calibration object.

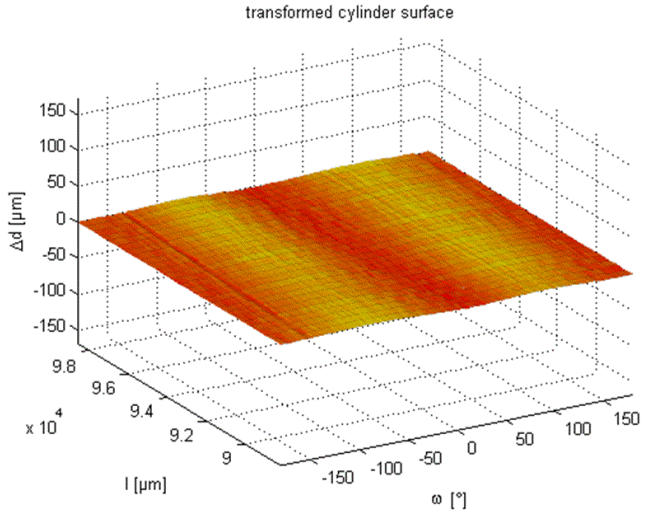

Figure 22: Plot of the cylindrical coordinates of a helix shaped measurement after transformation according to the calibration.

Automated measurement of interiors using a mobile platform

Architects, craftsmen and other groups are engaged in constructional modifications of interiors. The basis of their work is often a detailed and accurate floor plan. The acquisition of the necessary geometrical information plus the following modeling is a time-consuming procedure. Therefore, an automated floor plan measurement with a mobile robotic platform is the topic of this research. This issue implicates a number of fundamental tasks that have to be solved. The existence of a hardware framework to allow processing like the activation of sensors or the wheels is just a basic requirement. For an autonomous operation the system has to be able to locate itself in an unknown environment based on the available sensor data. Simultaneously one or even several maps have to be built up out of the collected data. The system has to know which parts of the environment still have to be surveyed and how it manages to do that. Therefore exploration strategies have to be applied that propose new measurement positions and determine paths to ensure a collision-free navigation.

We developed an approach for a fully automated measuring of a self-contained indoor scene in 2D using a mobile platform (Figure 23). A novel sensor is used, designed for the acquisition of precise floor plan scans, mounted on a mobile robot. The software framework is configured to optimize the accuracy and the completeness of the acquired data. Therefore an exploration strategy was implemented that finds gaps in the data and determines the next best view in an explorative way.

The scene is presented to the system as continuous line segments. Data management builds up the collected point cloud in a homogeneous density, using the relevant and most accurate available information. Existing scan matching techniques are modified in a way to work robust and precise.

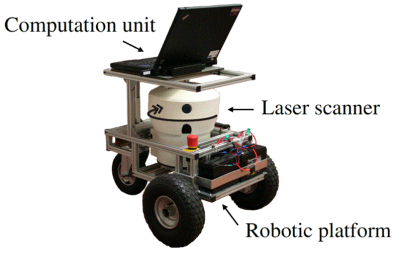

Figure 23: Hardware set-up.

The system setup was tested in an interior scene of ca. 150m^2, consisting of several rooms (Figure 24). To be able to conclude about the systems accuracy, ground truth data was recorded by generating a model of the same scene with a tachymeter. 42 points, spread all over the scene, were measured. Both models were overlaid to calculate the difference vectors. Coordinate differences possess a standard deviation of s_o = 5.2mm with a maximal deviation of 1.2cm. The experiments showed that the system can collect floor plan data with high accuracy.

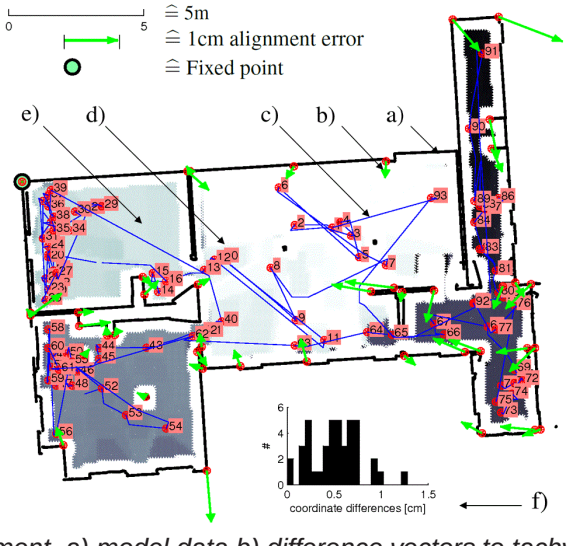

Figure 24: Test environment. a) model data b) difference vectors to tachymeter model c) path d) succession of measuring positions e) background, shaded dependent on the point of time, the area was declared as passable f) histogram of differences to tachymeter model.

Objective Stray Light Inspection of High-Dynamic-Range Cameras

Video based driver assistance systems are gaining increased importance in the domain of night vision improvement or object and lane measurements. Active infrared night vision systems (Figure 25 left) provide an extended visibility at night compared to conventional low-beam headlights, without blinding oncoming traffic. The road scene illuminated by infrared light is recorded by a high-dynamic-range CMOS (HDR) camera and presented as a black and-white image on a display. The HDR camera is able to acquire the outperforming wide luminance range of night sceneries using a nonlinear conversion.

The performance of HDR cameras is especially critical if being exposed to glaring situations in typical street sceneries with uncontrollable illumination. Due to mechanical defects or contamination of the imager or lens, different stray light artefacts might be amplified by the HDR CMOS sensor and occur as beams and fans of varying lengths or different halo sizes as well as sidelight structures in the images, among others. Currently, cameras are tested by visual inspection according to a failure catalogue. In order to ensure the reproducibility and repeatability of test results, to enhance the test coverage and at the same time to reduce test duration, an objective and automated procedure for stray light inspection is developed. While moving the camera by means of a motor unit in dark surroundings, images are acquired which show an external light source mapped as bright spot on dark background at different positions (Figure 25 right).

Figure 25: Night vision system (left) and stray light artefact in form of radial beams (right).

The aim of the newly developed machine learning algorithm is the classification of the cameras into a defect or non-defect class by evaluating a complex feature vector extracted from each image after applying specific digital image pre-processing steps. As stray light artefacts are characterized by blurred intensity differences and show a large range in appearance, an approach based on supervised statistical learning in combination with image processing is applied as opposed to a simple analysis of intensity measures. Supervised statistical learning is subdivided into two steps: (a) training of the classifier model and (b) actual prediction of the class in each image by

application of the classifier model. The performance of the model is evaluated by a k-fold cross-validation (CV). Apart from the predicted artefact probability in each image, the results of the CV are presented by a receiver operating characteristic (ROC) analysis and by the area under the ROC curve (AUC) in percent. The results of the objective stray light inspection conceal an average AUC value of more than 95% for different artefact types (Figure 26). An additional sensitivity analysis evaluates the importance of the individual features with respect to their influence on the classification performance.

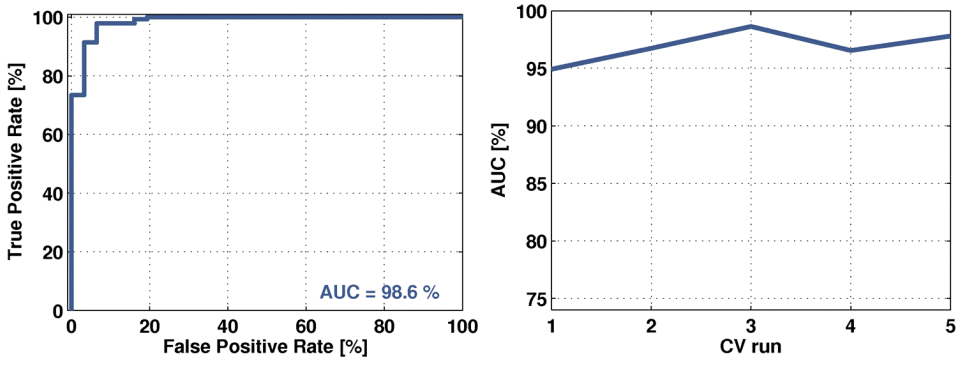

Figure 26: Results of objective stray light inspection on the example of beam artefacts: ROC curve for one CV run (left) and AUC results from 5-fold cross-validation (right).

References 2010

Alshawabkeh, Y., Haala, N., Fritsch, D.: A New True Ortho-photo Methodology for complex archeological alication. Archaeometry, Vol. 52, Issue 3, 517-530.

Auer, S., Balz, T., Becker, S., Bamler, R.: 3D SAR Simulation of Urban Areas Based on Detailed Building Models. Photogrammetric Engineering & Remote Sensing, Vol. 76, No. 12, 1373-1384.

Böhm, J., Pattinson, T.: Accuracy of Exterior Orientation for a Range Camera. International Archives of Photogrammetry, Remote Sensing and Spatial Information Sciences, Vol. XXXVIII, Part 5, 103-108.

Budroni, A., Böhm, J.: Automatic 3D Modeling of Indoor Manhattan-world Scenes from Laser Data. International Archives of Photogrammetry, Remote Sensing and Spatial Information Sciences, Vol. XXXVIII, Part 5, 115-120.

Cefalu, A., Böhm, J.: Development of a Robot Guided Optical Multisensory Inspection System for Inline Inspection of Cylinder Heads. International Archives of Photogrammetry, Remote Sensing and Spatial Information Sciences, Vol. XXXVIII, Part 5, 137-142.

Chen, H., Walter, V.: Hierarchical Quality Inspection of Spatial Data by Data Integration. ASPRS 2010 Annual Conference, San Diego, California, USA, April 26-30, 6 pages (on CD-ROM).

Cramer, M.: The DGPF-Test on Digital Airborne Camera Evaluation - Overview and Test Design, Photogrammetrie - Fernerkundung - Geoinformation (PFG), Heft 2(2010), 75-84.

Cramer, M.: Der DGPF-Test zur Evaluation digitaler Luftbildkameras - Überblick und Testdesign, Tagungsband 19/2010 - Dreiländertagung OVG, DGPF und SGPF, 1-9.

Cramer, M., Grenzdörffer, G., Honkavaara, E.: In situ digital airborne camera validation and certification - the future standard? International Archives of Photogrammetry, Remote Sensing and Spatial Information Vol. XXXVIII, Part 1, 6 pages (on CD-ROM).

Cramer, M., Haala, N.: DGPF Project: Evaluation of digital Photogrammetric Aerial-based Imaging Systems - Overview and Results from the Pilot Center. Photogrammetric Engineering & Remote Sensing Vol. 76, No. 9, 1019-1029.

Fietz, A., Jakisch, S.M., Visel, B.A., Fritsch, D.: Automated 2D Measuring of Interiors Using a Mobile Platform. Proceeding of the 7th International Conference on Informatics in Control, Automation and Robotics (ICINCO 2010), Funchal, Madeira, Portugal, 115-120.

Filipovska, Y., Kada, M.: Shape Assessment of Generalized Building Footprints. International Archives of Photogrammetry, Remote Sensing and Spatial Information Sciences, Vol. XXXVIII, Part 4, 6 pages (on CD-ROM).

Fritsch, D.: E-Government und 3D-Geodaten- Bürgerentscheidungen leicht gemacht. In: Gemeinsam für die digitale Gesellschaft, Initiative D21, Jahresband 2010, S. 65.

Fritsch, D.: Professor Dr.-Ing. Dr. E.h. mult. Fritz Ackermann 80 Jahre - Hochschullehrer, Innovator und Entwickler der modernen Photogrammetrie. Photogrammetrie, Fernerkundung, Geoinformation (PFG) 4/2010, 305-314.

Haala, N., Cramer, M., Jacobsen, K.: The German Camera Evaluation Project - Results from the Geometry Group. International Archives of Photogrammetry, Remote Sensing and Spatial Information Sciences, Vol. XXXVIII, Part 1, 6 pages (on CD-ROM).

Haala, N., Hastedt, H., Wolff, K., Ressl, C., Baltrusch, S.: Digital Photogrammetric Camera Evaluation - Generation of Digital Elevation Models Photogrammetrie - Fernerkundung - Geoinformation (PFG), Heft 2(2010), 99-115.

Haala, N., Hastedt, H., Wolff, K., Ressl, C., Baltrusch, S.: DGPF Projekt: Evaluierung digitaler photogrammetrischer Luftbildkamerasysteme - Themenschwerpunkt Höhenmodelle. DGPF Tagungsband 19/2010 - Dreiländertagung OVG, DGPF und SGPF, 22-31.

Haala, N., Kada, M.: An update on automatic 3D building reconstruction. ISPRS Journal of Photogrammetry and Remote Sensing, Vol. 65, No. 6, 570-580.

Hügel, H., Fritsch, D., Wagner, J.: Orientierung im Raum - 200 Jahre Maschine von Bohnenberger. Austellungskatalog, www.uni-stuttgart.de/Bohnenberger, Stuttgart 2010.

Jacobsen, K., Cramer, M., Ladstädter, R., Ressl, C., Spreckels, V.: DGPF-Project: Evaluation of Digital photogrammetric Camera Systems - Geometric Performance. Photogrammetrie - Fernerkundung - Geoinformation (PFG), Heft 2(2010), 85-98.

Jacobsen, K., Cramer, M., Ladstädter, R., Ressl, C., Spreckels, V.: DGPF Projekt: Evaluierung digitaler photogrammetrischer Kamerasysteme - Themenschwerpunkt Geometrie, Tagungsband 19/2010 - Dreiländertagung OVG, DGPF und SGPF, 11-21.

Kirchgässner, U., Putze, U., von Schönermark, M., Haala, N.: Anforderungen an die Auswertung UAV-gestützter Fernerkundungsdaten. DGPF Tagungsband 19/2010 - Dreiländertagung OVG, DGPF und SGPF, 597-605.

Moussa, W., Fritsch, D.: A Simple Approach to Link 3D Photorealistic Models with Content of Bibliographic Repositories. EuroMed 2010, LNCS 6436, Springer Berlin Heidelberg, 482-491.

Peter, M., Haala, N., Schenk, M., Otto, T.: Indoor Navigation and Modeling Using Photographed Evacuation Plans and MEMS IMU. International Archives of Photogrammetry, Remote Sensing and Spatial Information Sciences, Vol. XXXVIII, Part 4, 6 pages (on CD-ROM).

Raizner, C., Fritsch, D.: Stray Light Analysis of High-Dynamic-Range Cameras Based on Digital Image Processing. Jahrestagung Deutsche Gesellschaft für angewandte Optik, Esslingen, ISSN 1614-8436.

Doctoral Theses

Becker, S.: Automatische Ableitung und Anwendung von Regeln für die Rekonstruktion von Fassaden aus heterogenen Sensordaten. Supervisor: Prof. D. Fritsch, Co-Supervisors: Prof. K. Rothermel, Prof. L. Plümer.

Diploma Theses / Master Theses

Wenzel, K.: Evaluation of dense pointclouds derived from aerial imagery by Semi-Global Matching. Supervisor: Haala, N.

Zhu, H.: Digital Preservation of the Hirsau Abbey by Means of HDS and Close Range Photogrammetry. Supervisor: Fritsch, D.

Lu, Z.: Automatic Map Recognition. Supervisor: Walter, V.

Khosravani, A.M.: Digital Preservation of the Hirsau Abbey by Means of HDS and Low Cost Close Range Photogrammetry. Supervisor: Fritsch, D.

Pattinson, T.: Quantification and Description of Distance Measurement Errors of a Time-of-Flight Camera. Supervisor: Böhm, J.

Liu, S.: Recognition of 3D Lines in Point Clouds from Image Matching. Supervisor: Haala, N.

Moussa, W.: Digital Preservation of the Hirsau Abbey by Means of Static LIDAR and HD Close Range Photogtrammetry. Supervisor: Fritsch, D.

Study Theses

Scheiblauer, B.: Aerotriangulation simulierter Bilddaten des Aufnahmesystems „Stuttgarter Adler". Supervisor: Cramer, M.

Korcz, D.: Performancesteigerung des Volume-Carving-Ansatzes zur Volumenrekonstruktion aus statischen LiDAR Daten. Supervisor: Cefalu, A.

Haußmann, S.: Aerotriangulation eines Bildverbandes des „Stuttgarter Adlers", Supervisor: Cramer, M.

Appenzeller, B.: Virtuelle Stadtmodelle als Landmarken für die visuelle Navigation. Supervisor: Böhm, J.

Otto, T.: Miniaturisiertes Streifenprojektionssystem. Supervisor: Böhm, J.

Schenk, M.: Innenraumnavigation mit einer MEMS-Inertialmesseinheit. Supervisors: Peter, M., Haala, N.

Kusari, A.: Visualisierung von 3D-Gebäuden in unterschiedlichen Detaillierungsstufen und Repräsentationsformen. Supervisor: Walter, V.

Activities in National and International Organizations

Böhm, J.:

Co-Chair ISPRS Working Group V/4 - Image-based and range-based 3D modelling
Mitglied im VDI/VDE GMA Fachausschuss 3.32 Optische 3D-Meßtechnik - Gemeinschaftlicher Ausschuss des VDI und der DGPF

Cramer, M.:

President EuroSDR Technical Commission I - Sensors, primary data acquisition and georeferencing
Co-Chair ISPRS Working Group I/5 - Integrated Systems for Sensor Georeferencing and Navigation

Fritsch, D.:

Member D21 Advisory Board
Member Board of Trustees German University in Cairo (GUC)
Member GUC Academic Committee
Member Apple's University Education Forum (UEF)
Member Advisory Board Finnish Geodetic Institute

Chairman Board of Trustees 'The ISPRS Foundation'
Member Advisory Board ISPRS
Vice-President Research EuroSDR

Haala, N.:
Co-Chair ISPRS WG III/4 - Automatic Image Interpretation for City-Modelling
Vorsitz DGPF Arbeitskreis Sensorik und Plattformen

Walter, V.:
Nationaler Berichterstatter für die ISPRS Kommission IV

Education - Lectures/Exercises/Training/Seminars

Bachelor Geodäsie und Geoinformatik

Introduction into Geodesy and Geoinformatics (Cramer, Fritsch, Sneeuw, Keller, Kleusberg)	4/2/0/0
Geoinformatics I (Fritsch, Walter)	2/2/0/0
Adjustment Theory and Statistical Inference I (Fritsch, Sneeuw)	1/1/0/0

Diplomstudiengang Geodäsie und Geoinformatik

Adjustment Theory and Statistical Inference II (Fritsch, Sneeuw)	2/1/0/0
Advanced Projects in Photogrammetry and GIS (Böhm, Cramer, Haala, Walter)	1/2/0/0
Aerotriangulation and Stereoplotting (Cramer)	2/1/0/0
Close Range Photogrammetry (Fritsch, Böhm)	2/1/0/0
Databases and Geoinformation Systems (Walter)	2/1/0/0
Digital Terrain Models (Haala)	1/1/0/0
Digital Image Processing (Haala)	2/1/0/0
Digital Signal Processing (Fritsch, Böhm)	2/1/0/0
Geodetic Seminar I, II (Fritsch, Sneeuw, Keller, Kleusberg)	0/0/0/4
Geoinformatics II (Walter)	2/1/0/0
Integrated Fieldworks (Fritsch, Sneeuw, Keller, Kleusberg)	0/0/4/0
Introductory Readings to Photogrammetry (Cramer)	2/0/0/0
Image Acquisition and Monoplotting (Cramer)	2/1/0/0
Urban Planning (Dvorak)	1/0/0/0
Pattern Recognition and Image Based Geodata Collection (Haala)	2/1/0/0
Photogrammetry and GIS (Cramer)	2/1/0/0
Animation and Visualisation of Geodata (Haala, Kada)	1/1/0/0
Cartography (Urbanke)	1/0/0/0

Master Course Geoengine

Airborne Data Acquisition (Fritsch, Cramer)	1/1/0/0
Geoinformatics (Fritsch, Walter)	2/1/0/0
Signal Processing (Fritsch, Böhm)	2/1/0/0
Topology and Optimisation (Fritsch, Kada)	2/1/0/0

Master Courses „Infrastructure Planning“ and „Water Resource Management“

Advanced GIS (Walter)	2/0/0/0

Diplomstudiengang Geographie Tübingen

Geoinformatics I (Fritsch, Walter)	2/2/0/0
Geoinformatics II (Walter)	2/1/0/0
Practical Training in GIS (Walter)	0/0/4/0

Diplomstudiengang Luft- und Raumfahrttechnik

Introduction into Photogrammetry (Cramer)	2/0/0/0